Fall 2009

Explorations of hippocampal zinc using zinc-selective fluorescent dyes

Irma Nydegger
University of Iowa

EXPLORATIONS OF HIPPOCAMPAL ZINC USING ZINC-SELECTIVE FLUORESCENT DYES

by

Irma Nydegger

An Abstract

Of a thesis submitted in partial fulfillment
of the requirements for the Doctor of
Philosophy degree in Chemistry
in the Graduate College of
The University of Iowa

December 2009

Thesis Supervisor: Professor Alan R. Kay

ABSTRACT

Zn is a transition metal that fulfills many roles in mammalian cells, from structural support for many proteins, to second messenger and enzymatic cofactors. Specific neuronal terminals in the hippocampus contain higher Zn concentrations than other brain cells, but it is still unclear as to why Zn accumulates there. Since Zn is co-packaged with the neurotransmitter glutamate in synaptic vesicles, one possibility is that it gets released during neurotransmission. To study zinc uptake in the cytoplasm and the possibility of Zn release, we employed different fluorescent Zn indicators. These dyes passively cross the cell membrane and become fluorescent upon zinc binding. We found that the extracellular concentration of zinc and therefore zinc influx into the cell is limited by the presence of phosphate, which induces zinc precipitation by forming insoluble zinc-phosphate salts. Zinc solubility and influx is increased by the application of histidine to the extracellular medium. We also found that exogenously applied zinc in the presence of a zinc ionophore seems to translocate in vesicles and cytoplasmic compartments. Zinc seems to be very tightly buffered as it enters the cytoplasm, since transient increases in fluorescence (as observed during Ca^{2+} influx into the cytoplasm) are not observed. Our data also seems to indicate that zinc is not being freely released in the extracellular space, but is being externalized instead.

Abstract Approved: _____
Thesis Supervisor

_____
Title and Department

_____
Date

EXPLORATIONS OF HIPPOCAMPAL ZINC USING ZINC-SELECTIVE FLUORESCENT DYES

by

Irma Nydegger

A thesis submitted in partial fulfillment
of the requirements for the Doctor of
Philosophy degree in Chemistry
in the Graduate College of
The University of Iowa

December 2009

Thesis Supervisor: Professor Alan R. Kay

Graduate College
The University of Iowa
Iowa City, Iowa

CERTIFICATE OF APPROVAL

_____

PH.D. THESIS

_____

This is to certify that the Ph.D. thesis of

Irma Nydegger

has been approved by the Examining Committee
for the thesis requirement for the Doctor of Philosophy
degree in Chemistry at the December 2009 graduation.

Thesis Committee: _____
Alan R. Kay, Thesis Supervisor

_____
Lei M. Geng

_____
Amnon Kohen

_____
Christopher Cheatum

_____
Garry R. Buettner

To The God of the universe for sustaining me when I couldn't keep going.

Science without religion is lame, religion without science is blind.
Albert Einstein

ACKNOWLEDGMENTS

My wonderful husband who has been so supportive of everything I do and most of all has always managed to find ways to make me laugh. You have been through the highs and the lows and have become by biggest cheerleader. I am so thankful that God brought you into my life. My parents who taught me to believe in myself and never give up no matter how hard things got. I thank you for making the biggest sacrifice anyone could make to give me a better life. Thank you for all your prayers and good wishes and love. Ju them falemnderit shume prinderve te mi, qe e para me dhane jeten. Ju falenderoj qe me dhate besim ne vetvete, per te gjithe ato oret qe me keni ndenjur tek koka, me shume durim dhe shume perkushtim. Ju falenderoj per sakrificen me te madhe qe mund te beje dikush, qe me derguat ne mes te Amerikes per te me dhene nje enderr. Zoti ju bekofte! Ju dua shume!

My advisers Alan and Don who taught me so much. Alan, thank you so much for taking me in as an "orphaned" student. Thank you for opening up a whole new research area to me, for teaching me new things and for showing me how to look at a problem from different angles and exhaust every possibility. I have really enjoyed working in your lab, it made my experience here definitely worthwhile. To Chris Cheatum, for adopting me into your group as another student (almost, but not quite a p-chemist). Thank you for all the political discussions and all the cribbage games (even the ones lost).

To all my friends who were on the sidelines cheering me on. To Jigar and Jen, the ex-cannonites, Timmy, Perry and Mike; Samrat and Mary, Will and Irene. Thank you for all your support and advice. To all, I thank you from the bottom of my heart.

ABSTRACT

Zinc is a transition metal that fulfills many roles in mammalian cells, from structural support for many proteins, to second messenger and enzymatic cofactors. Specific neuronal terminals in the hippocampus contain higher zinc concentrations than other brain cells, but it is still unclear as to why zinc accumulates there. Since zinc is co-packaged with the neurotransmitter glutamate in synaptic vesicles, one possibility is that it gets released during neurotransmission. To study zinc uptake in the cytoplasm and the possibility of zinc release, we employed different fluorescent zinc indicators. These dyes passively cross the cell membrane and become fluorescent upon zinc binding. We found that the extracellular concentration of zinc and therefore zinc influx into the cell is limited by the presence of phosphate, which induces zinc precipitation by forming insoluble zinc-phosphate salts. Zinc solubility and influx is increased by the application of histidine to the extracellular medium. We also found that exogenously applied zinc in the presence of a zinc ionophore seems to translocate in vesicles and cytoplasmic compartments. Zinc seems to be very tightly buffered as it enters the cytoplasm, since transient increases in fluorescence (as observed during Ca^{2+} influx into the cytoplasm) are not observed. Our data also seems to indicate that zinc is not being freely released in the extracellular space, but is being externalized instead.

TABLE OF CONTENTS

LIST OF TABLES

Table

LIST OF FIGURES

Figure

LIST OF ABBREVIATIONS

DEDTC – Diethyldithiocarbamate

DTDP – 2,2'-dithiodipyridyl

EDPA – Ethylenediamine - *N*,*N*′- diacetic - *N*,*N*′- di-β -propionic acid

EDTA – Ethylenediaminetetraacetic acid

FZ-3 – FluoZin-3

FZ-3-AM – FluoZin-3 acetoxymethyl

GSH – Glutathione

KO – Knock-out

MT – Metallothionein

NGF – Nerve growth factor

T – Thionein

TPEN – *N,N,N',N'*-tetrakis(2-pyridylmethyl)ethylenediamine

WT – Wild Type

ZnAF-2 – Zinc aminofluorescein-2

ZnT3 – Zinc transporter 3

ZP1 – ZinPyr 1

CHAPTER I.

INTRODUCTION

Scope of Research

Zinc is a transition element that is found in all cells and is necessary for life (Dyck, 2009; King and Cousins, 2006; Prasad et al., 1963). Zinc provides an important structural and stabilizing role to several hundreds of proteins and is an essential co-factor for many more enzymes (Vallee and Falchuk, 1993). Zinc is also involved in stabilizing DNA, RNA and ribosome structures (Dyck, 2009; MacDonald, 2000). Proteins that have a zinc-binding motif constitute almost half of the proteins required for regulating transcription, (Dyck, 2009; Tupler et al., 2001) whereas genes that encode for proteins that contain zinc-binding sites comprise almost 10% of all genes in the human genome (Cousins et al., 2006; Dyck, 2009; Lander et al., 2001; Venter et al., 2001).

By fulfilling these roles in proteins and enzymes, zinc is involved in the regulation of many processes in the body such as the immune system, DNA synthesis, behavioral response, reproduction, fetal development and membrane stability, bone formation, and wound healing, cell proliferation and normal growth, brain development and oxidative stress to name a few (Barceloux, 1999; Dyck, 2009; Halstead et al., 1972; Oteiza and Mackenzie, 2005; Prasad, 1991).

In the brain, zinc is tightly regulated and exists in two different states. In the first state zinc is tightly bound to proteins as a co-factor aiding in their function and also to regulatory proteins such as metallothioneins. In the second state, zinc is loosely associated with the synaptic vesicles in certain glutamatergic pathways such as in the hippocampus and is termed chelatable zinc.

Protein bound zinc is histochemically invisible, but the so-called chelatable zinc within the vesicles can be easily visualized with histochemical methods (Frederickson, 1989). The first report of a pre-synaptic vesicle containing zinc was over forty years ago

by Finn-Mogens Haug in 1967 (Haug, 1967). Most of the zinc-containing vesicles are glutamatergic and given that glutamate is the most important and most abundant excitatory neurotransmitter in the brain, it has been proposed that zinc might be involved in the neurotransmission process as well. Interestingly, zinc is not only abundant in overwhelmingly glutamatergic pathways, but its distribution in these pathways within the same brain structure also varies. For example, in the hippocampus, zinc is restricted to areas containing synapses such as the dentate gyrus and mossy fibers, however the pyramidal cell body layer and the granule layer seem to strangely lack synaptic zinc (Slomianka, 1992). The protein that is crucial in stocking zinc into synaptic vesicles was first identified by Palmiter's group more than a decade ago (Cole et al., 1999; Palmiter et al., 1996; Wenzel et al., 1997a), however deletion of the gene that encodes for this protein and subsequently, loss of all chelatable zinc in the brain led to no apparent defects in animals (Cole et al., 2001; Lopantsev et al., 2003), except for a slightly higher susceptibility to kainic acid-induced epileptic seizures (Cole et al., 2000). This suggests that chelatable zinc may not important enough, or that the brain somehow compensates for the deletion of ZnT3, or that the real defects are hid so well as to evade the scrutiny of scientists so far. The very existence of chelatable zinc in such high concentration (>300uM) as well as the energetic cost of packaging and maintaining zinc levels in glutamatergic vesicles negates the idea that chelatable zinc is insignificant (Budde et al., 1997; Frederickson, 1989; Frederickson et al., 1983; Xie and Smart, 1991).

If zinc is important in neurotransmission and plays a role in modulating the synaptic response it has to fulfill certain universal conditions established for neurotransmitter molecules. First, it has to be located pre-synaptically; second, it has to be released during synaptic transmission; third, if it is released, it should exert an effect in the post-synaptic cell and last, its action on a post-synaptic cell should be blocked via an antagonist.

Two of these criteria have been widely established. Zinc is located in pre-synaptic

cells and it does influence many post-synaptic receptors. Evidence seems to point out that exogenously applied zinc modulates several major ligand-gated ion channels such as γ-aminobutyric acid (GABA) and glutamate receptors. GABA is the major inhibitory neurotransmitter in the brain and its receptors are divided into two groups: $GABA_A$ and $GABA_B$. Of these two receptors, $GABA_A$ seems to be susceptible to exogenous zinc (Westbrook and Mayer, 1987), while $GABA_B$ is not (Lambert et al., 1992). Since zinc has been shown to block *N*-methyl-D-aspartate receptors (Peters et al., 1987; Westbrook and Mayer, 1987) and $GABA_A$ receptors (Smart and Constanti, 1990; Westbrook and Mayer, 1987) it has been suggested that zinc might play a protective role. In high concentrations however, zinc can become neurotoxic (Duncan et al., 1992).

All of the current work on zinc however, does not provide a definite answer as to what its role is in synaptic transmission, nor is it absolutely clear whether zinc is being released with glutamate during synaptic transmission. The goal of this research is to use zinc-selective fluorescent probes to determine if zinc is being released in the extracellular medium.

Thesis Overview

The aim of this research is to determine whether hippocampal zinc is released during synaptic transmission as well as to evaluate zinc homeostasis and cell regulation using fluorescent probes. We first performed fluorescence experiments with the zinc-selective probe ZnAF-2 and different intracellular and extracellular chelators to monitor the possible zinc release during brain slice stimulations with elevated KCl. The widely accepted view is that zinc is released during stimulation as the synaptic vesicles fuse to the synaptic terminal membrane and is then free to diffuse in the synaptic cleft. This is known as the Zinc-release hypothesis. Our experiments have revealed the possibility that zinc is not being released, but is however externalized during stimulation and subsequent vesicle fusion. We hypothesize instead that zinc is bound within the synaptic vesicle to a

membrane protein or other molecule as a ternary complex. Zinc remains bound even after the vesicles fuse to the membrane and is not released and free to diffuse in the synaptic cleft. We have termed this hypothesis: the zinc externalization. The difficulty in determining that zinc is not fully released in the extracellular medium during synaptic transmission lies in the fact that the extracellular chelators, which are meant to intercept the released zinc, may in fact still strip zinc off even if it is only externalized in the form of a ternary complex with the fluorescence probe and a membrane protein. And finally, we have performed experiments with a different zinc-selective probe FZ3-AM and ZnT3 knock-out mice that are meant to reveal how zinc is buffered as it enters the cytoplasm. These measurements demonstrate how quickly free zinc gets sequestered once it enters the cell and where it localizes (if it stays in the cytoplasm or if it makes its way into synaptic vesicles). The work presented in this thesis provides evidence that questions the Zinc-release hypothesis and lends support to the zinc externalization hypothesis. Evidence put forth in this thesis also supports the fact that free zinc is quickly buffered in the cell by such molecules as Metallothionein (MT) or Glutathione (GSH), however more work needs to be done to fully understand these processes.

CHAPTER II.

THEORETICAL BACKGROUND

Zinc in the Brain

The Hippocampal Anatomy

The hippocampus is a unique component of the mammalian brain, which is organized on quite different principles from the adjacent neocortex. It is located in the medial temporal lobe against the floor of the lateral ventricle. De Garengeot was the first to christen the hippocampus as Cornu Ammonis (Latin for horn of the ram) in 1742, after Amun Kneph, the Egyptian mythological god. This terminology still remains today as part of the notation of the different areas of the hippocampus, CA1 – CA3 (CA standing for cornu ammonis) though it does not describe the whole hippocampal structure any longer. The term hippocampus was introduced by the Italian anatomist Giulio Cesare Aranzi in the 16th century due to its resemblance to the sea-horse. In 1886, Camillo Golgi used his new silver staining technique to reveal the beautifully arranged layers of the hippocampus (2007; Mazzarello, 1999).

The hippocampus is organized in highly laminated areas with two distinct double horseshoe shapes (see figure 1). The hippocampus is part of a larger structure called the hippocampal formation, which is divided into the dentate gyrus, CA1-4, subiculum, presubiculum, parasubiculum and the entorhinal cortex (figure 1). The hippocampus itself is then divided into the dentate gyrus and CA1 – CA4 (Bentivoglio and Swanson, 2001).

The dentate gyrus (DG) is probably the most distinctive area of the hippocampal formation, with a characteristic V or U shape and no subdivisions. The DG receives its primary input from the entorhinal cortex via the perforant pathway. Cells in the dentate gyrus form a separate layer called the granule cell layer. The axons of these cells send out projections that are bundled together in a layer called the mossy fiber pathway and form the hilus with its characteristic V or U shape (O'Keefe and Nadel, 1978). The mossy

fibers form synapses onto cells in area CA3 of the hippocampus, which in turn synapses with cells in the area CA1, called the Schaffer Collateral projection after the Hungarian anatomist Karl Schaffer (1892) who first discovered it. A prominent feature of the areas CA1 and CA3 is the pyramidal cell layer that they form. The cell bodies of this layer are large and pyramid shaped (O'Keefe and Nadel, 1978). Originally classified by Lorente De No, the CA layers were divided into CA1-3, with CA2 having the large pyramidal cell body like CA3, but like CA1 does not receive input from the mossy fibers of the dentate gyrus. CA1 receives inputs from both the CA3 and the entorhinal cortex and projects primarily to the subiculum. The subiculum, parasubiculum and presubiculum are sometimes described together as the subicular complex. These structures have different anatomical features and are thought of as separate cortical areas. The end of the Schaffer collateral inputs from CA3 marks the border between subiculum and CA1. The presubiculum lies next to the subiculum, but its layers have not yet clearly been differentiated. The parasubiculum is next to the presubiculum and it contains a wedge-shaped cell layer that resembles the cells of the presubiculum, but is not as dense (2007). The flow of input is entorhinal cortex, to dentate gyrus, to CA3, to CA1, to the subiculum.

Neural Signaling

To understand in part why it is important that zinc is found in such high concentrations in some glutamatergic synapses, it is important to take a look at the make-up of a synapse and the basis of neural signaling in the brain in general. The cells that constitute the nervous system are divided into nerve cells called neurons and supporting cells called neuroglia. The neuronal cells are divided into the cell body and neurites, which are cellular extensions of the nerve cells. Neurites are divided into dendrites and axons. Information processing in the nerve cells is passed on from dendrite to axon. Neurons contain the same organelles as all cells, but their distribution may be more

specific to certain regions of neurons (2004). Moreover, cells of the nervous system differ in the organization of the proteins that make up the cytoskeleton (2004; O'Donnell et al., 2009; Qian Cai and Sheng, 2009). Even though these proteins such as actin, myosin and tubulin are found in other cells, the specific organization that is found in neurons speaks to the importance of the cytoskeleton to the stability and proper functioning of the neuronal projections and synapses of neuronal cells. These proteins are crucial in the development of axons and dendrites as well as the positioning of the many cellular components including vesicles (2004). The most prominent feature of neurons is their widespread branching, especially the elaborate branching of the dendrites. These dendrites that branch out of the cell body are the points of contact between adjacent neuronal cells. There is a wide distribution of dendrite arborizations depending on the specific function of the neuronal cell. Some cells do not contain any dendrites at all; while others contain such an elaborate branching of dendrites they resemble trees. This feature also determines the number of inputs that a neuronal cell receives. Cells that contain no dendrites receive input from very few cells, while others that contain many dendrites receive input from a large number of other neuronal cells. This input is made through contacts between the axonal projection of the pre-synaptic cell and the dendrites of the post-synaptic cell. This contact is also known as synaptic terminal (2004). The gap between the pre- and post-synaptic cells is called the synaptic cleft and is approximately 20 nm wide. The two cells then communicate by the release of chemicals into the synaptic cleft and their binding to receptors on the post-synaptic cell. The number of inputs that a certain cell receives is anywhere from 1 to 100,000. This indicates that there is a specialization of the function of each nerve cell and the number of inputs each cell receives dictates its function. The basis of signal propagation in a neuronal cell is called an action potential. The action potential is an electrical wave that is transmitted from the point where it is initiated, down the axon and toward the synaptic terminal (2004). The secretory organelles located in the pre-synaptic terminal are called synaptic vesicles.

These spherical entities are about 50 nm in diameter and contain neurotransmitter molecules. These molecules are released in the synaptic cleft during synaptic transmission and modify the response of the post-synaptic cell by binding to specific receptors on the post-synaptic membrane. There is a signal transduction that occurs in the synaptic cleft. An electrical signal is propagated through the axon to the axonal terminal. This signal is then transformed into a chemical signal in the synaptic cleft and then back to an electrical signal in dendrite of the post-synaptic cell. The electrical signal that is propagated in the axon is called an action potential (also called impulse) (2004). So how is an action potential generated?

The Action Potential

Neurons are polarized cells and possess a potential difference across the membrane at its resting state. This potential difference is called the resting membrane potential and its value depends on a particular neuron (ranging anywhere from -40 to -90mV). When the membrane is depolarized (membrane potential becomes more positive on the inside than outside) beyond a certain level called the threshold potential, an action potential is generated (2004). The action potential is made possible by the movement of ions across the neuronal cell membrane. The ions responsible for the establishment of the membrane potential are the K^+ and Na^+ ions. The concentration of K^+ ions is greater on the inside of the membrane (100 mM) than outside (5 mM), whereas the opposite is true for the Na^+ ions (15 mM inside and 150 mM outside). Due to this difference in concentrations as well as the membrane permeability for these ionic species, an electrical signal can be generated (2004).

The action potential is propagated forward from the point of initiation and down the axon terminal. The inward current of Na^+ ions precedes the action potential and depolarizes the membrane ahead of the action potential to the threshold level, causing it to move forward. This is followed by an outward current of K^+ ions, which

hyperpolarizes the membrane (makes the membrane more negative on the inside than outside) and quickly re-establishes the resting potential. The current that propagates through the axon is inversely dependent upon the distance travelled. The increase in distance is achieved by the use of myelination, which is the wrapping of axons with layers and layers of membrane from oligodendrocyte cells (in CNS and Schwann cells in PNS) (2004). Myelination increases membrane resistance by tens to hundreds of times. The voltage gated ion channels that are necessary for action potential generation are located only on certain gaps in the myelin sheath called the Nodes of Ranvier. This confines the current only to these Nodes and the action potential is said to jump from node to node. This is known as saltatory conduction (2004).

Synaptic Transmission

As stated earlier, neurons communicate with each other at synapses via the release of neurotransmitter molecules. Neurotransmitters can be released in the synaptic cleft when the pre-synaptic terminal gets depolarized. Neurons require sufficient stimulus to release neurotransmitter from the pre-synaptic terminal, thus they have to integrate the inputs they receive from other neurons both temporally and spatially (2004).

Most excitatory synapses occur on little protrusions on dendrites that are called dendritic spines. Depolarization of the synaptic terminal membrane is required for synaptic vesicle fusion and neurotransmitter release. These vesicles are docked at release sites at the pre-synaptic terminal, ready to be activated.

The synaptic vesicle pool is divided into 3 main groups: the readily releasable pool, the recycling pool and the reserve pool (figure 2a). The readily releasable pool is made up of synaptic vesicles that are docked at the site of release called the active zone and are immediately available after stimulation (Rizzoli and Betz, 2005). Not all the vesicles in the active zone are part of the readily releasable pool however (Rettig and Neher, 2002; Rizzoli and Betz, 2005). The ready releasable pool is itself divided into the

slowly releasable pool and the rapidly releasable pool (Rettig and Neher, 2002). The readily releasable pool is depleted similarly by using several stimulation methods such as 5-15 shocks of high-frequency electrical stimulation, 1s of hypertonic shock, or a few ms of depolarization (Rizzoli and Betz, 2005). The recycling pool is defined as the synaptic vesicle pool that release under moderate stimulation (Rizzoli and Betz, 2005). This pool is accessed by stimulation with physiological frequencies and it is continuously refilled with vesicles that have released and are refilled with neurotransmitter. This pool makes up 5-20% of all synaptic vesicles (Rizzoli and Betz, 2005). The vesicles in the reserve pool are released only during periods of intense stimulation. They make up 80-90% of all synaptic vesicles. Physiological activity is not sufficient to cause the release of the reserve pool. It has been suggested that this pool is mobilized only when the reserve pool is exhausted (Rizzoli and Betz, 2005). The activation of the synaptic vesicle pool is achieved through Ca^{2+} influx into the terminal during cell depolarization (2004). The potential change activates voltage gated Ca^{2+} channels, which allow Ca^{2+} ions to pour in due to the large concentration gradient (about 100 nM inside and 2 mM outside). Synaptic vesicles undergo exocytosis and fuse to the cell membrane in a Ca^{2+}-dependent process, allowing for neurotransmitter release. Vesicles can undergo two types of exocytosis: complete fusion at the synaptic membrane (also called full fusion), or a partial fusion called “kiss and run” (figure 2b) (He and Wu, 2007). Heuser and Reese first showed full vesicular fusion over 30 years ago, by observing the full collapse of the vesicle at the synaptic membrane and subsequent endocytosis and recycling of the vesicle (Heuser and Reese, 1973). In a series of papers, Ceccarelli et al. provided evidence of the “kiss and run” vesicle fusion (Ceccarelli et al., 1972, 1973), where the vesicle forms a fusion pore (Breckenridge and Almers, 1987; Fesce et al., 1994; Zimmerberg et al., 1987) and recycles rapidly via endocytosis without complete collapse at the synaptic membrane. The two modes of fusion yield different neurotransmitter release and the cell may use both to regulate synaptic strength and plasticity (He and Wu, 2007).

The proteins that are involved in the fusion of vesicles with the membrane are very specific and their activity is tightly regulated. One type of protein that is required is called SNARE (Snap Receptor protein) and is found in both the vesicle (V-SNARE) and the target membrane (T-SNARE). This pair interacts very specifically to bring the membranes together and prepare them for the fusion process. Another protein called Synaptotagmin regulates the interaction of V- and T-SNAREs and blocks the fusion of the vesicle with the membrane. In the presence of Ca^{2+}, synaptotagmin undergoes a conformational change and the fusion process is free to proceed (2004).

Once the vesicles fuse and the neurotransmitter is released, it diffuses across the synaptic cleft and binds to specific receptors in the post-synaptic cell, causing a conformational change and allowing a flux of Na^{+} ions and subsequent membrane depolarization in the post-synaptic cell. The action potential has then been successfully transmitter from one cell to the next (2004).

Zinc in the Hippocampus

Zinc in the hippocampus was discovered more than 5 decades ago via a histochemical stain that first rendered it visible in the mossy fiber pathway (Maske, 1955). Subsequent techniques such as Timm's stain were developed to improve the visualization of the metal in hippocampal synaptic terminals (Kay and Toth, 2008). Timm's stain uses silver sulfide to precipitate zinc as an insoluble salt and then silver is deposited to intensify the staining (Cassell and Brown, 1984; Haug, 1967; Timm, 1958). This form of zinc is called "free" or "chelatable" zinc as opposed to the zinc that is tightly bound to proteins and enzymes as a structural support, or as a co-factor (Kay et al., 2006; Kay and Toth, 2006). Zinc is found in glutamatergic synapses (synapses containing glutamate as their main neurotransmitter) in the brain (Frederickson et al., 1990; Kay and Toth, 2008), however only a subset of about 50% of glutamatergic synapses contains zinc. This distribution is also true for the hippocampus that while the

mossy fiber pathway contains high concentrations of chelatable zinc (>300μM); other areas seem to lack it. This remains a central issue in determining the role of zinc at these synapses. Glutamate is the main excitatory neurotransmitter in the brain, therefore due to the co-packaging of zinc with glutamate in these vesicles, it has been postulated that zinc may be involved in glutamate neurotransmission such as glutamate transport, packaging and even modulating its response as a neurotransmitter (Frederickson et al., 1990).

Zinc in Synaptic Vesicles

While about 80% of zinc in the brain is bound to enzymes and proteins and fulfills roles such as structural support or co-factor, the rest of the zinc is sequestered within synaptic vesicles (Frederickson, 1989). While this zinc is certainly not completely free, it is not as tightly bound as the zinc that is part of proteins or enzymes. This zinc is most likely coordinated to certain transmembrane molecules or proteins in the synaptic vesicle. Vesicular zinc is mostly found in neurons that use glutamate, glycine or GABA as their main neurotransmitter (Nakashima and Dyck, 2009). Zinc-containing glycinergic neurons are mainly located in the spinal cord, while GABAergic neurons that contain zinc in their synapses are found mainly in the cerebellum and spinal cord (Birinyi et al., 2001; Wang et al., 2002; Wang et al., 2001). The largest population of vesicular zinc is found in glutamatergic neurons, however not all glutamatergic neurons are rich in synaptic zinc (Beaulieu et al., 1992; Slomianka, 1992). These zinc-rich neurons are found mainly in cortex, hippocampus, amygdala and the olfactory bulb (Dyck, 2009; Frederickson and Moncrieff, 1994; Ichinohe and Rockland, 2005; Perez-Clausell, 1996). Interestingly, vesicular zinc distribution within a specific brain structure may change as well. For example, in the hippocampus vesicular zinc is consigned to the synaptic terminal layer such as the mossy fiber, but is largely absent from the cell body layer such as pyramidal and granule cell layers. The same is true in the cortex, where layers I – III and V – VI are rich in synaptic zinc, but layer VI contains little zinc (Dyck et al., 1993).

Free vs. Bound Zinc

As mentioned earlier, most of the zinc found in the brain is bound to proteins and enzymes and only about 20% is in a loosely bound state. Intracellular concentrations of free zinc are low (estimated to be in the pM to nM range) (Bird et al., 2003; Fierke and Thompson, 2001; Green and Berg, 1990; Michael et al., 1992) suggesting that it is tightly buffered in the cytoplasm. In addition to proteins such as alcohol dehydrogenase and Cu/Zn superoxide dismutase, which use zinc to properly function, there are other proteins or small molecules that regulate free zinc concentration. Such molecules are typically rich in cysteine or histidine residues and include metallothionein/thionein (MT/T) pair and glutathione. Other low affinity zinc binding sites exist that include lipids, DNA or proteins and small molecules such as citrate also play a regulatory role for zinc (Eide, 2006). MT is one of the main regulatory proteins for intracellular zinc. MT was isolated over 5 decades ago from equine kidney cortex (Margoshes and Vallee, 1957). MT has a dumbbell shape and binds up to seven zinc ions in two distinct zinc-cysteine clusters of the form Zn_3Cys_9 and Zn_4Cys_{11} (Maret, 2003). These 20 Cys residues are highly conserved and essential to the structure and function of MT (Maret, 2009). Each zinc ion is tetrahedrally coordinated with sulfur ions, however the zinc binding affinity of the different sites varies with one being weak, two intermediate and four high affinity (Krezel and Maret, 2007). MT was first thought to play the role of zinc chaperone to provide zinc for the hundreds of proteins and enzymes that utilize it for structural and/or enzymatic function, however the number of these proteins that require zinc would be too large to be supplied only by MT as a chaperone. MT however, is a trafficking protein and is found to translocate to the inner membrane of the mitochondria and the nucleus, which do not have any zinc transporter proteins that are identified (Tsujikawa et al., 1991; Ye et al., 2001). It is not yet clear how or if MT interacts with zinc transporters to transfer zinc in intracellular compartments. If this interaction existed it could explain how the cell, especially a neuronal cell could stock intracellular compartments such as synaptic

vesicles with large amounts of “chelatable” or “labile” zinc, while maintaining a very low intracellular free zinc concentration so as not to interfere with other metal homeostasis or disrupt the function of hundreds of zinc proteins.

Zinc Homeostasis

Zinc is a transition element that is found in all cells and is necessary for life (Dyck, 2009; King and Cousins, 2006; Prasad et al., 1963). In adults, lack of zinc can cause several disorders such as memory loss, susceptibility to stress and lethargy (Sandstead, 1984). Zinc provides an important structural and stabilizing role to several hundreds of proteins and is an essential co-factor for many more enzymes (Vallee and Falchuk, 1993). Zinc is also involved in stabilizing DNA, RNA and ribosome structures (Dyck, 2009; MacDonald, 2000). Proteins that have a zinc-binding motif constitute almost half of the proteins required for regulating transcription, (Dyck, 2009; Tupler et al., 2001) whereas genes that encode for proteins that contain zinc-binding sites comprise almost 10% of all genes in the human genome (Cousins et al., 2006; Dyck, 2009; Lander et al., 2001; Venter et al., 2001).

By fulfilling these roles in proteins and enzymes, zinc is involved in the regulation of many processes in the body such as the immune system, DNA synthesis, behavioral response, reproduction, fetal development and membrane stability, bone formation and wound healing, cell proliferation and normal growth, brain development and oxidative stress to name a few (Barceloux, 1999; Colvin et al., 2003; Dyck, 2009; Halstead et al., 1972; King and Cousins, 2006; Oteiza and Mackenzie, 2005; Prasad, 1991).

Even though it has been established that zinc plays an important role in many processes, zinc homeostasis and regulation both intracellularly and extracellularly still remains poorly understood. Findings such as zinc modulation of protein kinase C signaling pathways (Korichneva et al., 2002) and zinc inhibition of GABAergic

neurotransmission (Hosie et al., 2003a) seem to indicate that the concentration of zinc, whether intracellular or extracellular could be important in cell signaling activity. In the brain, zinc is important for early development, however does not seem to diminish with aging (Frederickson, 1989). In cultured mammalian cells the zinc quota (Outten and O'Halloran, 2001), which is defined as the total zinc content required for optimal growth of the cell, is estimated to be approximately 10^8 zinc atoms per cell, whereas in yeast and bacteria this number is lower (10^7 and 10^5 respectively) (MacDiarmid et al., 2000; Outten and O'Halloran, 2001; Palmiter and Findley, 1995a; Suhy et al., 1999). These concentrations are not uniform in all mammalian cells as some neurons and prostate cells tend to accumulate high concentrations of zinc as compared with other types of cells (Costello and Franklin, 1998; Frederickson et al., 2000). Zinc concentration in the extracellular space in estimated to be in the nanomolar range (Takeda, 2000). The zinc concentration in the cytoplasm of a typical neuronal cell is estimated to be 590μM (Tarohda et al., 2004), with most of the zinc sequestered by metal-binding proteins such as MT, or zinc-finger proteins, or other molecules such as GSH (Burdette and Lippard, 2003; Maret, 2003; Palmiter, 1998). The intracellular concentration of free zinc is estimated to be between 10^{-5} to 10^{-12}M (Abebodun and Post, 1995; Canzoniero and Sensi, 1997; Kleineke and Brand, 1997; Palmiter and Findley, 1995a; Romero-Isart and Vasak, 2002; Sensi et al., 1997; Simons, 1991; Thompson et al., 2002; Van Zile et al., 2000), however it has been suggested that the true concentration of free zinc in the cytosol may be much lower (Finney and O'Halloran, 2003). The reason for the large range of concentrations could be the zinc contamination during sample preparation due to proteolysis of organelles or other processes such as oxidation, or the fact that large concentrations of fluorescent dyes are used to measure small concentrations of zinc (Dineley et al., 2002; Eide, 2006). As a result, the true concentration of intracellular free zinc remains elusive, however it could be argued that free zinc could be as low as nM to pM range following the metal binding affinities of many zinc metalloproteins, which fall

in the same range (Bird et al., 2003; Fierke and Thompson, 2001; Green and Berg, 1990; Michael et al., 1992). This low concentration is remarkable as compared to the total zinc concentration in the cell (1 nM free zinc is equivalent to less then 0.001% of the total zinc concentration) (Eide, 2006). The low intracellular free zinc concentration points to the tight balance and control between zinc transport, efflux and influx and zinc exchange from transport proteins to newly synthesized metalloproteins or enzymes (Eide, 2006).

Zinc Transporters

Several proteins have been identified that act as zinc transporters, some remove zinc from the cytoplasm into different intracellular compartments or expel it outside the cell and others allow zinc to be transported into the cytoplasm when intracellular zinc levels fall. Prior to the identification of the first zinc transporter named ZnT1 in 1995 (Palmiter and Findley, 1995a), zinc was thought to be co-transported in one of three different ways: as an anionic complex, as an amino acid chelate (typically via histidine or cysteine), or the transferring receptor route (Reyes, 1995; Ripa and R., 1995). Two different protein families have now been identified as transporters for zinc. The ZnT protein family (also known as solute-linked carrier 30 or SLC30A) lowers zinc concentrations in the cytoplasm by transporting zinc extracellularly or to other intracellular compartments, including vesicles. The Zip family of proteins (also known as Zrt- and Irt-proteins or SLC39A) are involved in zinc uptake from the extracellular space, or from intracellular stores into the cytoplasm (Eide, 2004; Liuzzi et al., 2001; Palmiter and Huang, 2004). The ZnT family consists of 10 proteins, ZnT1-10. The transporter activity of the ZnT1, 2, 4-8 transporters has been confirmed through cell survival placed in high zinc content, or through other routes such as zinc uptake and/or accumulation in mutated cells, yeast strains and Xenopus oocytes (Chimienti et al., 2004; Cragg et al., 2002; Huang and Gitschier, 1997; Huang et al., 2002; Kambe et al., 2002; Kirschke and Huang, 2003a; Palmiter et al., 1996; Palmiter and Findley, 1995b). ZnT3 activity was

confirmed through a knockout mouse by the Plamiter lab (Cole et al., 1999; Palmiter et al., 1996; Wenzel et al., 1997b). The zinc transport mechanism of the ZnT family of proteins is not well understood, however zinc efflux and intracellular store deposition occur against a concentration gradient, so it is likely that they use an active transport mechanism. Homologous proteins have been found to exchange zinc for H^+ or K^+(Chao and Fu, 2004; Guffanti et al., 2002). If these homologous proteins are reconstituted in proteo-liposomes, neither a proton gradient nor ATP is required for zinc transport (Bloß et al., 2002). Human ZnT proteins contain significant sequence homology and most of these proteins are predicted to have 6 transmembrane domains (except ZnT5, which contains 12 domains). Both the N and C termini of these proteins face the cytoplasm and most of the proteins also contain a long intracellular loop that include a different number of histidine residues, which are believed to be zinc ion-binding domains (Murgia et al., 1999; Seve et al., 2004). Some of the ZnT proteins form homo- or hetero-oligomers and various motifs in their sequence indicate the possibility of protein-protein interactions (Murgia et al., 1999; Sim and Chow, 1999), therefore ZnT proteins may be involved in the insertion of zinc into enzymes through the transport of zinc into the Golgi apparatus (Suzuki et al., 2005).

The Zip family of proteins on the other hand, consists of 14 members. The zinc transport activity for the Zip1-8 and 14 members has been demonstrated by measuring the uptake of ^{65}Zn or via zinc-selective fluorescent probes such as Zinquin, Newport Green and FZ-3-AM (Begum et al., 2002; Dufner-Beattie et al., 2003a; Dufner-Beattie et al., 2003b; Gaither and Eide, 2000, 2001a, b; Huang et al., 2005; Liuzzi et al., 2005; Taylor et al., 2005; Wang et al., 2004). Similar to ZnT protein family, the mechanism of zinc transport for the Zip family of proteins is not well understood, but it could be facilitated through a concentration gradient and induced by HCO_3^- (Gaither and Eide, 2000, 2001a, b). The Zip family is divided into four sub-groups: Zip I, Zip II, gufA and LZT (Taylor and Nicholson, 2003). Zip1-3 belong to the Zip II subgroup, Zip9 is part of

the Zip I subgroup, Zip 11 belongs to gufA and Zip4-8, Zip10 and Zip12-14 belong to the LZT subgroup. The first Zip family member to be discovered was Zip6 (also known as LIV-1) and is the protein after which the LZT subgroup is named (Taylor, 2000). Zip6 has only 6 transmembrane domains, whereas most of the other proteins in the Zip family are predicted to contain 8 domains. The zinc pore could be formed by two of these transmembrane domains, IV and V, since they seem to be conserved throughout the Zip family (Gaither and Eide, 2001a; Rogers et al., 2000). Contrary to the ZnT family of proteins, the Zip family is predicted to have both N and C termini that are extracellular, but the intracellular loop rich in histidine residues is conserved in both (Taylor and Nicholson, 2003). Most of the Zip proteins have been located at the plasma membrane, with the exception of Zip7, which was located at the Golgi apparatus (Huang et al., 2005; Kirschke and Huang, 2003b), however the location of these proteins might change with physiological zinc conditions and availability.

ZnT3 Transporter Protein

ZnT3 is a member of the ZnT family of zinc transporters that are responsible for buffering zinc in the cytoplasm by expelling it outside the cell or by transporting it into cellular compartments. ZnT3 mRNA levels are highest is the brain and testis although no ZnT3 protein is expressed in testis (Palmiter et al., 1996). ZnT3 was first identified by Palmiter's group more than a decade ago and is the protein that stocks and maintains the high concentration of loosely bound zinc also known as chelatable zinc found in certain glutamatergic pathways in the brain (Wenzel et al., 1997b). The amount of ZnT3 that is found in areas of the brain that contain high concentrations of zinc, corresponds to the amount of chelatable zinc that can be visualized by using histochemical methods of fluorescence imaging (Cole et al., 1999; Wenzel et al., 1997b). ZnT3 seems to require the AP3 chaperone complex to be transported from endosomes to synaptic vesicles since mutation of the AP3δ gene in the mocha mouse leads to zinc depletion in synaptic

vesicles and other storage compartments such as melanosomes and platelets (Kantheti et al., 1998). ZnT3 mRNA reaches detectable levels just a few days before birth and full adult levels 3 weeks after birth, however factors regulating ZnT3 gene expression are unknown (Cole et al., 1999). Mice that are heterozygous for ZnT3 have half of the amount of zinc that wild type mice contain in their synaptic vesicles, whereas complete ZnT3 knock-out mice lack all of their vesicular zinc (Cole et al., 1999). Both heterozygous and complete knock-out mice appear normal, have no behavioral or spatial learning disabilities, no memory problems and are able to reproduce normally (Cole et al., 2001; Cole et al., 1999). ZnT3 knock-out mice seem to be more susceptible to kainic acid-induced epileptic seizures, but are not affected by other seizure-inducing agents such as flurothyl, bicuculline, or pentylenetetrazol (Cole et al., 2000). The lack of vesicular zinc does not inhibit the accumulation of zinc in the post-synaptic cell and the subsequent neuronal damage (Cole et al., 2000; Lee et al., 2000), however there seems to be no difference from electrical recordings of knock-out vs. control mice (Lopantsev et al., 2003). Synaptic zinc also is implicated in the formation of amyloid peptide aggregates in Alzheimer's disease (Cherny et al., 2001). The formation of amyloid plaques is significantly reduced by the disruption of the ZnT3 allele in a transgenic mouse that expresses a mutant human amyloid precursor protein, implicating vesicular zinc in the formation of amyloid aggregates (Lee et al., 2002).

Zinc-selective Fluorescent Dyes

Fluorimetric probes for metal sensing were first synthesized by the Tsien lab (Grynkiewicz et al., 1985) for the detection of Ca^{2+} levels. These probes are designed to couple a fluorescent molecule to a chelator moiety. The chelator part of the probe binds the metal and causes the molecule to become fluorescent. These Ca^{2+} indicators (i.e. fura-2) have a higher affinity for transition metals such as zinc (Gee et al., 2002b) and produce a shift in fluorescence emission upon zinc binding. The problem with the use of Ca^{2+}

fluorescence indicators for zinc measurements is their sensitivity to Ca^{2+}, which exists in much higher concentrations as compared to zinc (Canzoniero and Sensi, 1997). A new generation of zinc fluorescent probes has emerged to correct for Ca^{2+} and Mg^{2+} interference. These probes are tailored to be selective for zinc, although other metals might bind, but in a much smaller quantity.

FluoZin-3 Properties, Binding and Chemistry

FluoZin-3 (FZ-3) is a visible wavelength, zinc-selective, tetra-anionic fluorescent dye that was synthesized as an improvement on previous fluorescent dyes that either needed UV excitation or contained aliphatic tertiary amines that are protonated at physiological pH (Gee et al., 2002a). FZ-3 structure lacks one of the N-acetic acid moieties that are found in the Ca^{2+} probes fluo-3 and fluo-4, lowering its affinity for Ca^{2+} while maintaining the zinc affinity (Gee et al., 2002a). FZ-3 quantum yield in the absence of zinc (chelated by TPEN) was reported to be insignificant, but increases several hundred times in the presence of 5μM zinc, to a value of 0.43 (figure 3). Titration of the dye with increasing zinc concentrations gave a K_d of 15 nM. FZ-3 fluorescence is stable in the pH range of 6-9, but decreases sharply if pH is lowered below 6 (figure 3). FZ-3 fluorescence is not affected by other divalent cations (table in figure 3) (Gee et al., 2002a). The ability of FZ-3 to respond to zinc in the presence of relevant divalent cations at physiological conditions such as Ca^{2+} and Mg^{2+} was under some dispute, but data from our lab indicates that FZ-3 fluorescence is not perturbed by physiological concentrations of Ca^{2+} and Mg^{2+} (2 mM) (Zhao et al., 2008). In fact, even in the presence of Ca^{2+} concentrations as high as 10 mM, FZ-3 was able to detect increases in zinc concentrations as low as 100 pM (Zhao et al., 2008). FZ-3 is a membrane impermeable fluorescent dye and has been used in many biological applications such as detecting zinc release from pancreatic β cells (Gee et al., 2002a) as well as measuring the affinity of

metallothionein binding sites for zinc and visualizing externalized zinc in hippocampal slices (Kay, 2003) to name a few.

ZnAF-2 Properties, Binding and Chemistry

ZnAF-2 (Zn-Aminofluorescein) was synthesized as an improvement on previous zinc-selective fluorescent dyes, ACF-1 and ACF-2. These dyes were excitable with visible light, which is suitable for biological studies, however they had small quantum yields and slow zinc-complex formation rates (up to 100 min) (Hirano et al., 2000). In ZnAF-2 fluorescein replaced 6-hydroxy-9-phenylfluorone as a fluorophore due to its high quantum yield and *N,N,N',N'*-tetrakis(2-pyridylmethyl)ethylenediamine or TPEN as the zinc binding moiety (Hirano et al., 2000). ZnAF2 in the absence of zinc exhibits almost no fluorescence at pH 7.5. Fluorescence intensity increases approximately 51 fold upon zinc addition to the apo form of the dye (Hirano et al., 2000). ZnAF-2 fluorescence intensity does not seem to change much above pH 7.5, however increases sharply from pH 5.5 to pH 7.4 (see figure 4). The excitation (492 nm) and emission (514 nm) do not shift with the addition of zinc (see table 1 in figure 4) (Hirano et al., 2000). The dissociation constant was determined through zinc and buffered solutions and was found to be 2.7 nM. The detection limit was also found to be in the sub nM range, allowing for the selectivity needed in biological applications (Hirano et al., 2000). When ZnAF-2 fluorescence in the presence of divalent cations is compared to that of zinc, it was found that ZnAF-2 is highly selective for zinc (see table 2 in figure 4). Cadmium was the only divalent cation that increased ZnAF-2 fluorescence to 1/3 of the fluorescence in the presence of zinc and could potentially interfere with zinc measurements (Hirano et al., 2000). This interference should not pose a problem, since cadmium is not a native cation that is found in mammalian cells. ZnAF-2 fluorescence was not affected in the presence of Fe^{2+} and Fe^{3+} and was quenched in the presence of Cu^{2+} (Hirano et al., 2000). Other cations that are found in high concentrations in cells, such as Na^{+} and K^{+} did not affect

the dye fluorescence either in the absence or in the presence of zinc (Hirano et al., 2000). It was originally reported that ZnAF-2 was not membrane permeable and an acetoxymethyl form of the dye (ZnAF-2 DA) was synthesized for use in biological systems (Hirano et al., 2000). Previous work in our lab, however determined that ZnAF-2 is indeed able to cross membranes and stain the zinc rich synaptic vesicles in hippocampal slices (Kay and Toth, 2006). This discrepancy points the importance of determining the membrane permeability of the zinc-selective dye, as the location of the dye can affect the interpretation of the results (Kay and Toth, 2006).

Zinpyr 1, Properties, Binding and Chemistry

ZinPyr 1 (ZP1 – for structure see figure 5) is another zinc-selective fluorescent probe that was synthesized to improve upon the desired properties of a fluorescent dye that is used as a metal sensor such as ion selectivity, excitation and emission that lie outside the UV and autofluorescence of tissue and have high quantum yields (Burdette et al., 2001). ZP1 is a fluorescein-derivative dye thus exhibits a quantum yield of 0.87 in the presence of 25μM zinc (and 0.38 in the absence of zinc). Zinc binding causes the ZP1 excitation wavelength to shift from 515 nm ($\varepsilon = 79.5 \times 10^3\ M^{-1}\ cm^{-1}$) to 507 nm ($\varepsilon = 84.0 \times 10^3\ M^{-1}\ cm^{-1}$) (Burdette et al., 2001). Ca^{2+} and Mg^{2+} do not influence ZP1 fluorescence even at concentrations as high as 5 mM and transition metals such as Cu^{+}, Cu^{2+}, Ni^{2+}, Co^{2+}, Mn^{2+} and Fe^{2+} quench ZP1 fluorescence (see figure 5) (Burdette et al., 2001). ZP1 fluorescence drops to 80% from pH 5.5 to pH 7.4, but is fairly constant between 5.5 and 6.5 (see figure 5). At pH 7, the K_d of the Zn-ZP1 complex is 0.7 nM. In biological experiments to characterize the loading of ZP1 in Cos-7 cells, ZP1 was found to localize in acidic compartments, which seems to be a challenge of ZinPyr dyes (Burdette et al., 2001). The dye is suited to monitoring the changes in zinc fluorescence even though initial high background fluorescence that is observed from the apo form of the dye would present a difficulty in quantifying free zinc concentrations (Burdette et al., 2001).

Zinc Chelators

The use of chelators in biological experiments is of utmost importance. Chelators have played an important role in advancing our understanding of the role of metals in the cell. Typically, chelators contain N, O or S atoms in their structure that provide a coordination site for the binding of metals. A good transition metal chelator needs to be insensitive to Ca^{2+} and Mg^{2+}, since these ions exist in much larger concentrations in physiological conditions than other metals such as zinc for example. Another important feature of a chelator used in biological applications is its ability to cross membranes. The membrane permeability of a chelator needs to be well established before an experiment is performed, since it would affect the interpretation of the data.

Membrane Impermeable Chelators

Ethylenediaminetetraacetic acid (EDTA) is the most widely used metal chelating agent in biological applications. At pH 7.4, all the carboxylic groups in EDTA are deprotonated, therefore it is a membrane impermeable chelator (Kay and Toth, 2008; Skoog et al., 2000). EDTA when used as CaEDTA, can fulfill the role of a membrane impermeable chelator since it has a high affinity for zinc (K_d=3.1x10^{-17} (Skoog et al., 2000)) and does not affect physiological levels of Ca^{2+} and Mg^{2+} (Kay 2006). EDTA has a much higher affinity for zinc than it does for Ca^{2+} and Mg^{2+} ($K_{d\,Ca2+}$=2x10^{-11} and $K_{d\,Mg2+}$=2x10^{-9} (Skoog et al., 2000)) (Kay and Toth, 2008). In the presence of physiological concentrations of Ca^{2+} (2-3 mM), EDTA is saturated with Ca^{2+} and zinc has to displace it first before it binds to EDTA, causing the rate of zinc chelation to be slow (Kay, 2003; Paoletti et al., 2009b), even though EDTA has been shown to successfully bind extracellular zinc (Molnar and Nadler, 2001b; Ruiz et al., 2004; Vogt et al., 2000).

EDPA (ethylenediamine - *N*,*N*′- diacetic - *N*,*N*′- di-β -propionic acid) is another membrane impermeable chelator that has a lower affinity for Ca^{2+} and Mg^{2+} than does EDTA, therefore it can bind zinc faster (Kay, 2003). EDPA has not been as widely used

as EDTA, but it is better suited to intercept zinc in the extracellular space if it is released since it binds zinc faster.

Histidine (his), besides being one of the 20 essential amino acids, can also serve as a membrane impermeable chelator. His forms both mono and bis-histidine complexes with zinc (Martell and Hancock, 1996; Sivarama Sastry et al., 1960) and has been proposed to augment zinc transport. His has been found to facilitate zinc transport in erythrocytes (Aiken et al., 1992) and in the intestines of rats (Wapnir et al., 1983), trout (Glover and Hogstrand, 2002) and lobsters (Conrad and Ahearn, 2007), however data in our lab has suggested that his only increases zinc solubility in the extracellular space instead of being co-transported with zinc (see chapter 4). Extracellular application of his has also been found to increase nickel tolerance and supply in the non-metal accumulating plant of the genus *Alyssum* (Kramer et al., 1996).

Membrane Permeable Chelators

DEDTC (diethyldithiocarbamate) is a membrane permeable chelator that diffuses through membranes and can chelate zinc from any intracellular compartment and even from proteins (Danscher et al., 1975; Kay and Toth, 2008). DEDTC has been successfully shown to chelate vesicular zinc in numerous studies (Daumas et al., 2004; Frederickson et al., 1990; Lassalle et al., 2000; Lu et al., 2000; Takeda, 2000).

TPEN (*N,N,N',N'*-tetrakis(2-pyridylmethyl)ethylenediamine) is another membrane permeable chelator that is used widely in biological experiments. TPEN is bulkier than DEDTC, but has a higher affinity for zinc (K_d=4x10^{-16} (Canzoniero et al., 2003)), thus it binds it more strongly. Due to the strong affinity for zinc, TPEN is able to strip zinc from some of its protein binding sites, interfering with normal zinc homeostasis.

Zinc Ionophores

Typically, zinc (or any other endogenous metal ions) is transported via specific ion transporters that use pH gradients, ATP, or any other mechanism to allow zinc trafficking in and out of the cell. An ionophore is a molecule that chelates zinc and acts as a shuttle by allowing it to pass through the cell membrane, circumventing zinc transporters.

Pyrithione (pyr) is an ionophore that chelates zinc (K_d=1x10^{-6} (Canzoniero et al., 2003)) and shuttles it across both cell and synaptic membranes (Kay 2008). If zinc and pyr are co-applied extracellularly, pyr will allow zinc to cross membranes and move into the cytoplasm as well as into synaptic vesicles. If pyr is applied alone, it will allow zinc to diffuse out of intracellular storage and into the cytoplasm and possible extracellularly as well (Forbes et al., 1989).

Clioquinol (iodochlorhydroxy- quin, 5-chloro-7-iodo-8-hydroxyquinoline – CQ) is a Cu(II) and Zn(II) chelator that has been used with some success in Alzheimer's disease treatment. CQ has been shown to inhibit accumulation of β-amyloid plaques in transgenic mice (Cherny et al., 2001) via zinc chelation. CQ can be used as an intracellular zinc ionophore, because it can chelate loosely bound zinc, but not zinc that is bound in proteins or enzymes since it has a lower affinity (K_d=1x10^{-7} (Cherny et al., 2001; Nitzan et al., 2003)) for zinc than other membrane permeable chelators such as TPEN.

The work in this thesis covers several topics such as the interaction of zinc with phosphate under physiological conditions, zinc buffering and trafficking in the hippocampus and determining whether zinc is released or externalized during synaptic transmission. The experimental methods for all experiments (except for chapter 7) are included in chapter 3. Chapter 4 discusses the interaction between zinc and phosphate in the extracellular medium. We found that the extracellular concentration of zinc and therefore zinc influx into the cell is limited by the presence of phosphate, which induces

zinc precipitation by forming insoluble zinc-phosphate salts. Zinc solubility and influx is increased by the application of histidine to the extracellular medium. Histidine is not co-transported with zinc, but facilitates its cellular influx by increasing zinc solubility and as a consequence the extracellular free zinc concentration. Chapter 5 discusses zinc buffering in hippocampal slices. We found that exogenously applied zinc in the presence of a zinc ionophore seems to translocate in vesicles and cytoplasmic compartments. Zinc seems to be very tightly buffered as it enters the cytoplasm, since transient increases in fluorescence (as observed during Ca^{2+} influx into the cytoplasm) are not observed. Chapter 6 discusses the externalization of zinc during stimulation. We found that contrary to the zinc release hypothesis, zinc is not released in the extracellular space, as the fluorescence signal does not decrease with continued washing, as would be the case if the zinc-dye complex were released. We hypothesize that zinc is being externalized instead as part of a ternary complex with a molecule/protein in the synaptic membrane. Chapter 7 describes the influence of nerve growth factor application time on PC12 cell exocytic release. Nerve growth factor (NGF) treatment causes PC12 cells to undergo differentiation and grow neurites. PC12 cells can be stimulated with elevated KCl isotonic solution and release catecholamines. We found that untreated cells undergo massive release upon KCl stimulation, while in treated cells the release lessens. Also, the longer the NGF treatment time, the more localized the release becomes. This work was done under Dr. Donald M. Cannon Jr.

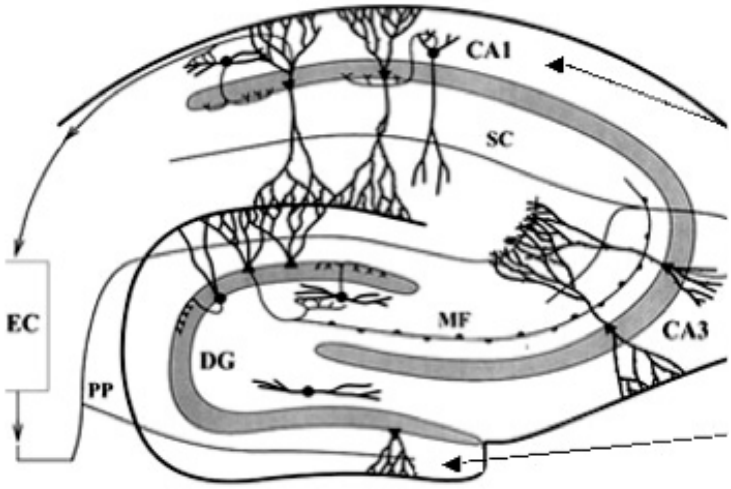

Figure 1. A simplified diagram of the hippocampus

Note: DG stands for dentate gyrus, MF for mossy fibers, PP for perforant path, SC for Schaeffer collateral pathway, CA1 and CA3 for cornu ammonis 1 and 3. http://krasnow.gmu.edu/L-Neuron/ascoli/sfn98/

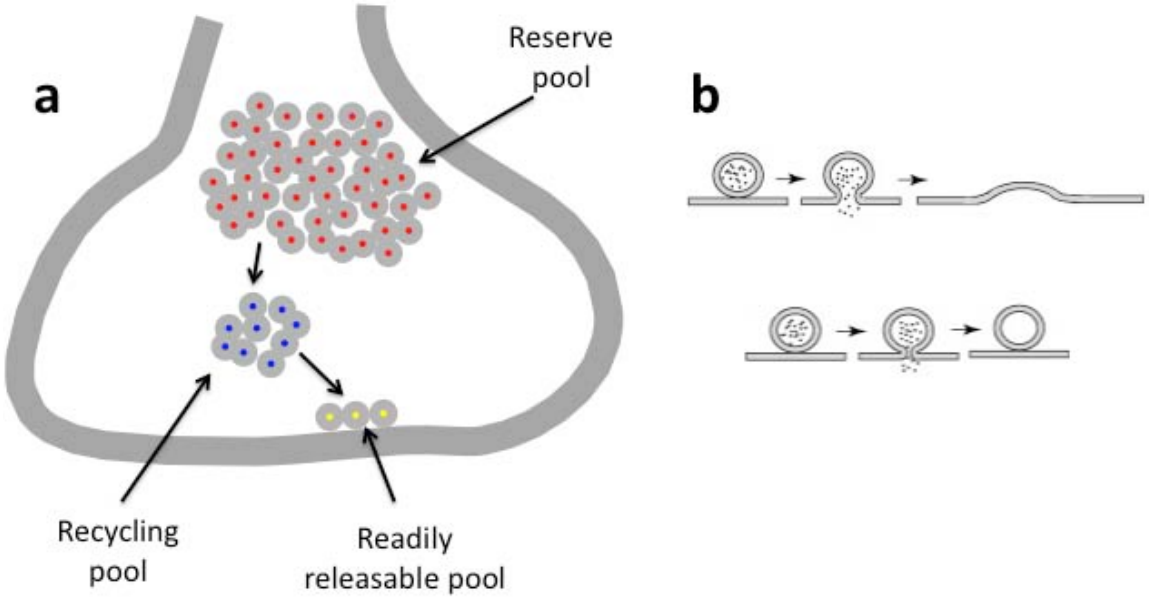

Figure 2. Description of the synaptic vesicle pools and vesicle fusion

---

Note: The three pools of synaptic vesicles are illustrated in figure 2a. Figure 2b (He and Wu, 2007) shows a full collapse of a vesicle at the synaptic terminal membrane (top) and a “kiss and run” fusion (bottom).

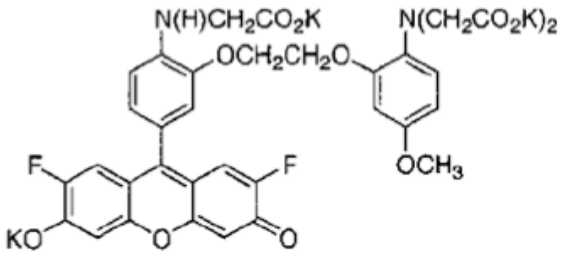

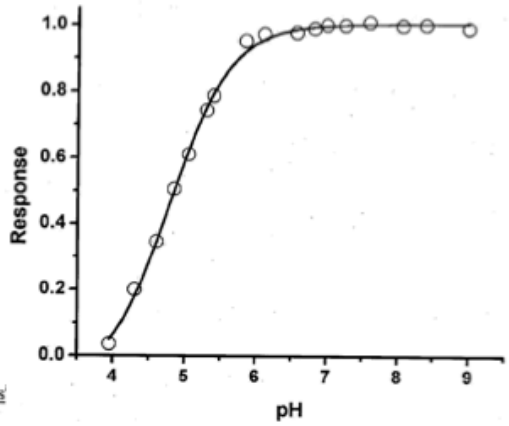

Table T1. Tabulated Fluorimetric Sensitivity of FluoZin-3 (9) to Various Ions[a]

Ion	Fluorescence[b]
TPEN (100 μM)	0
EGTA (10 mM)	0
Ca^{2+} (100 μM)	49
Mg^{2+} (10 mM)	44
Cu^{2+} (100 μM)	1
Fe^{2+} (100 μM)	78
Cd^{2+} (100 μM)	36
Hg^{2+} (100 μM)	86
Ni^{2+} (100 μM)	8
Co^{2+} (100 μM)	9
Ba^{2+} (100 μM)	22
Pb^{2+} (100 μM)	3
Mn^{2+} (100 μM)	48
Tb^{3+} (100 μM)	0
La^{3+} (100 μM)	42

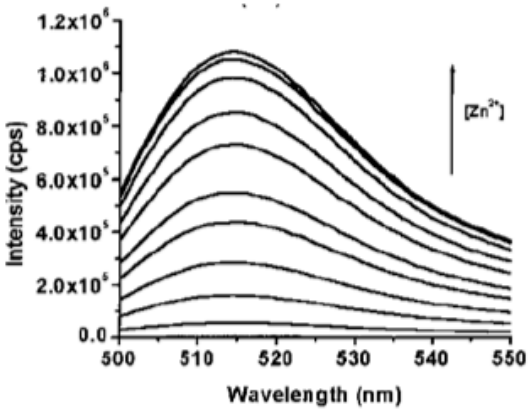

Figure 3. FluoZin-3 characteristics

Note: FluoZin-3 structure, response to pH, sensitivity to other cations and fluorescence response to zinc (Gee et al., 2002a).

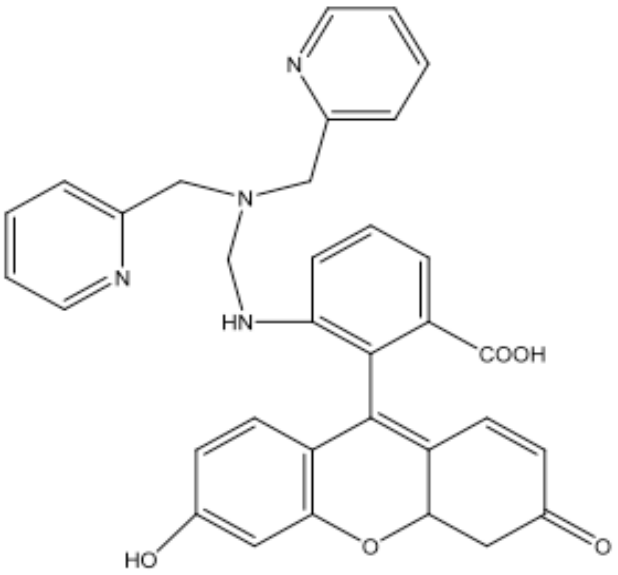

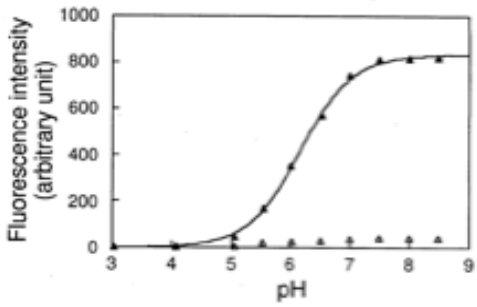

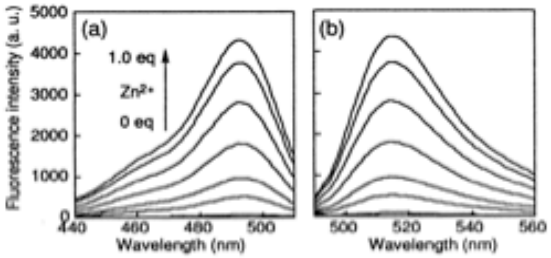

Table 1. Chemical Properties of ZnAFs with and without Zn^{2+}

	free		Zn^{2+}		
compd	ϵ^b	Φ^c	ϵ^b	Φ^c	Kd (M)
ZnAF-2	7.8×10^4 (490)	0.023	7.6×10^4 (492)	0.36	2.7×10^{-9}

Table 2. Selectivity of ZnAF-2 toward Other Cations

compd	free	Zn^{2+} [b]	Cd^{2+} [b]	Co^{2+} [b]	Ni^{2+} [b]	Ca^{2+} [c]	Mg^{2+} [c]
ZnAF-2	80	4105	1462	173	741	89	116

Figure 4. ZnAF-2 characteristics

Note: ZnAF-2 structure, response to pH, fluorescence response to zinc, chemical properties in the presence and absence of zinc and sensitivity to other cations (Hirano et al., 2000).

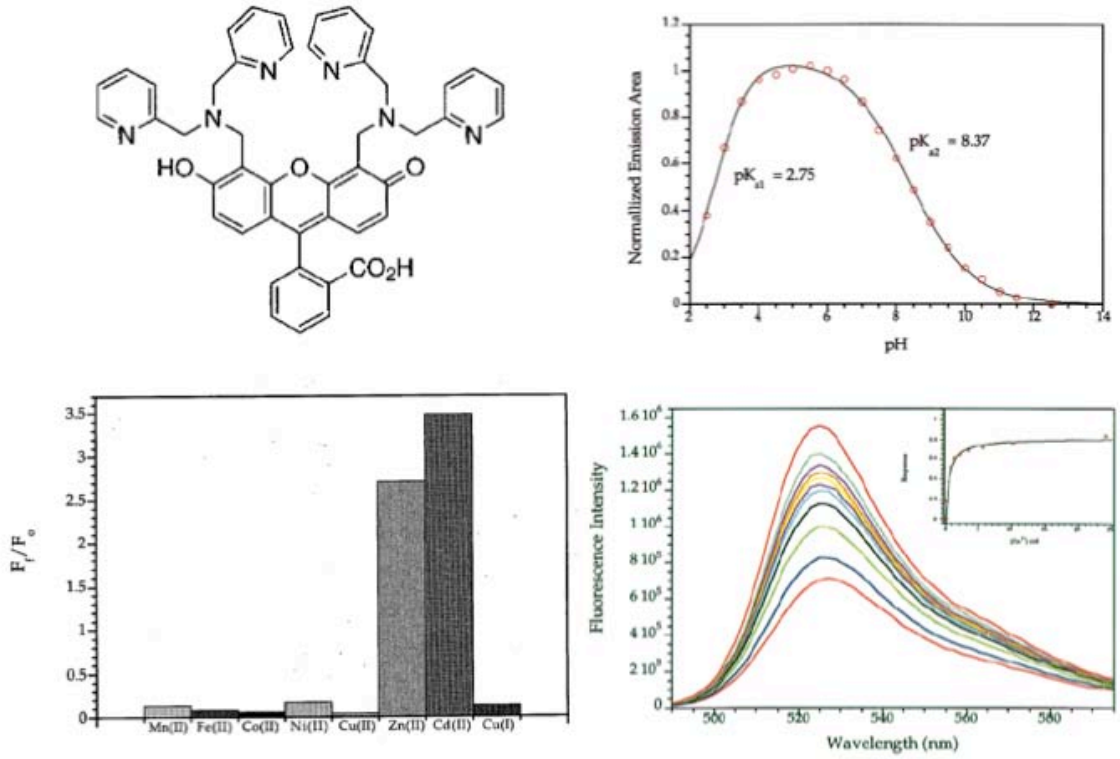

Figure 5. ZinPyr 1 characteristics

Note: ZP1 structure, response to pH, sensitivity to other cations and fluorescence response to zinc (Burdette et al., 2001).

CHAPTER III.

EXPERIMENTAL METHODS

Mouse Colony Establishment and Brain Slice Protocol

All animal procedures were in accordance with NIH and University of Iowa guidelines. The ZnT3 Knock Out (KO) and Wild Type (WT) mice were generously donated from Katalin Tóth's lab in Toronto, Canada. The mice are allowed to breed and pups between 14-21 days old are used for experiments. Mice have a 21-day gestation period and another 21-day birth to wean period. A new litter is ready for experiments about every 30 days.

Sprague-Dawley rats (21-60 day old, male) or Wild Type or KO Bl6 mice (14-21 days old male) are decapitated and the brain removed and placed in ice-cold isotonic solution (see saline composition section). The hippocampus is then dissected and prepared for sectioning. We have used two different methods of hippocampus slicing, the McIlwain chopper and the Vibrotome VF-200. The hippocampus is sliced to 400 or 500 μm thickness and then placed in room temperature saline solution. The solution is continuously bubbled with 95% O_2 and 5% CO_2 (carbogen) to maintain slice viability. The O_2 levels have to be elevated due to fast deterioration of the slice under lower O_2 levels.

We have performed some experiments on the necessity of using ice-cold solution for cutting and varying the time the slices are allowed to recover. After the recovery time is completed the slices are stained with a zinc-selective dye for another hour, while the slices are kept bubbled with carbogen. All dyes are prepared from stock solutions in normal saline and then aliquotted and individually frozen to minimize freeze-thaw cycles. Some dyes (FZ-3-AM, Calcein AM) are prepared with 0.5% DMSO and 0.04% w/v pluronic. Some of the dyes require washing, so the dye solution is removed and replaced with fresh saline solution. This process is repeated twice with fifteen-minute intervals.

Saline Solution Composition

All solutions are prepared fresh every day. Solutions contain a mixture of ions and glucose for nutrition. The solution composition that we use has been modified from Sakmann's solution (Hamill et al., 1981) and contains in mM: 125 NaCl, 2.5 KCl, 2 $CaCl_2$, 1.3 $MgSO_4$, 25 $NaHCO_3$, 1.25 NaH_2PO_4, and 10 or 25 glucose. For the Vibratome VF-200 slice preparation, a slightly different saline composition for cutting the slices is used. The Vibratome VF-200 cutting solution contains in mM: 2.5 KCl, 2 $CaCl_2$, 1.3 $MgSO_4$, 25 $NaHCO_3$, 1.25 NaH_2PO_4, 10 glucose and 250 glycerol. The replacement of NaCl with glycerol has been shown to protect neurons from death, by eliminating the high chloride ion concentration in the extracellular medium. A high chloride concentration can facilitate neurotoxicity via passive diffusion of chloride ions into the cell causing cell swelling and lysis (Ye et al., 2006). The composition of phosphate free saline is (in mM): 125 NaCl, 2.5 KCl, 2 $CaCl_2$, 1.3 $MgSO_4$, 26 $NaHCO_3$ and 10 or 25 glucose. To avoid zinc contamination, high purity reagents are used, while avoiding metals, glass, and plastics that can leach zinc into solutions (Kay, 2004).

Imaging Brain Slices

The slices are stabilized and held stationary with a U-shaped stainless steel piece cross strung with nylon fibers in a temperature-controlled chamber. Solutions are provided by a gravity feed system controlled by either a VC-6 six-channel valve controller or a peristaltic pump. The flow from the gravity feed system is controlled by the height where the system is placed, while the flow from the peristaltic pump is set automatically (typically 2mL/min). Images are acquired on an Olympus Optical BX50WI upright microscope. Illumination is provided by a monochromator set at 480 nm, passed through a dichroic and then through a filter onto the faceplate of a Princeton Instruments cooled CCD camera. Data are acquired by the MetaFluor program and images are analyzed using MetaFluor, ImageJ (NIH) and Microsoft Excel. Data is graphed with the

graphing program Origin. Images are adjusted for the CCD dark current. No black-level adjustment is applied. The fluorescence intensity for chapter four images is expressed as $\% \Delta F/F_o = \% (F-F_o)/F_o$, where F is the fluorescence intensity and F_o the fluorescence intensity at time zero. The fluorescence intensity for images in chapter five and six is expressed as $\% (F - F_{d.c.})/(F_0 - F_{d.c.})$, where F is the fluorescence intensity at time t, F_0, the fluorescence intensity at time zero and $F_{d.c.}$ is the fluorescence intensity from the dark current. Whenever the fluorescence intensity of the hilus is compared to that of the cell bodies, all the data are normalized to the initial fluorescence value of the hilus. All data are expressed as mean ± SEM.

Dye Injection Protocol

In some of the experiments the fluorescent dye is injected into the slice rather than the slice being bathed in dye solution. The injection is carried out via borosilicate glass pipettes (od/id 1.5/0.8) that are pulled through a Sutter P97 puller, program 2 (heat 615, pull 0, velocity 45 and time 200). This program gives a tip of about 3-5 um as measured through a calibrated microforge. The pipette is filled with a working dye solution and positioned through a micromanipulator. Solution is delivered through a picospritzer externally programmed (through Master-8) to deliver pulses of 500msec duration every 1s interval at a pressure of 8psi. The dye is injected into the hippocampal slice for an hour and then an image sequence is collected.

Electrophysiology Recordings of Synaptic Responses

Bipolar tungsten stimulating electrodes (~4 MW), coupled to a stimulus isolation unit are placed in the upper half of the stratum radiatum (CA1) and the field potentials are recorded with glass electrodes (2-5 MW) coupled to an Axoclamp-2B, connected to a low-noise amplifier to a Digidata 1322A A/D using Clampex 9.2 software. The current is adjusted to give a response approximately 60% of the maximal amplitude. Slices that do not produce a maximum fEPSP amplitude of >1 mV are discarded. The fEPSP slopes are

analyzed with the Clampfit software and Microsoft Excel. The data are then graphed through Origin. fEPSPs are stimulated with a pulse of 60 μs duration or a train of 500 pulses of 100Hz.

Light Scattering

The 90° light scattering (excitation 480 nm, emission 484 nm) or fluorescence emission (excitation 484 nm, emission 520 nm) is determined in a Hitachi F-4500 spectrofluorimeter in a rapidly stirred methacrylate cuvette whose temperature is controlled by a circulating water bath (32 ^{o}C). The solution is continuously bubbled with 95% O_2-5% CO_2.

ICP-OES

To measure the amount of zinc precipitated for chapter four experiments, solutions are prepared with different concentrations of zinc, centrifuged at 15,500 g for 30 minutes at 32 °C and the zinc concentration of the supernatant is then determined on Varian 720 ICP Optical Emission Spectrometer. Yttrium is used as an internal standard. Standard curves are constructed using zinc solutions of 10, 30 and 50 μM. The following lines are used to establish calibration curves and calculate the zinc concentration: 202.548, 206.200, 213.857 nm; internal standard: Y line 371.021 nm.

Particle size distributions are measured on a Malvern instruments Zetasizer, Nano series. The following parameters are applied to our experiments: reflective index for $Zn_3(PO_4)_2.H_2O_4$ is 1.594 and absorption is 0.1.

Elemental Analysis of Precipitates

The EDS analysis is performed on a Hitachi S-3400N variable pressure SEM equipped with a Bruker AXS Quantax x-ray microanalysis system. Quantitation is determined with standard-less analysis using the peak to background ZAF method. These experiments were performed in the Center for Microscopy.

Calculation of Precipitate Formation

Precipitate formation is calculated using the program MINTEQA2 (Allison, 2003). The NIST database of formation constants is used and all calculations are performed under 5% CO_2 at 32 °C.

CHAPTER IV.

INTERPLAY BETWEEN PHOSPHATE AND ZINC

Introduction

An essential step in the process of unraveling the mechanisms of action potential generation, synaptic transmission and muscular contraction was identifying the nature of the ionic species necessary for the operation of excitable cells (Burton, 1975). This began with Ringer's demonstration (Ringer, 1883) that extracellular calcium was necessary for cardiac contraction and set in motion the process of formulating media used to sustain cells in vitro. An important step was Krebs and Henseleit's (1932) realization that the constituents of normal plasma would be a good starting point for formulating physiological salines. Building on these foundations McIlwain developed the in-vivo brain slice preparation, one that has been enormously influential in the progress of neuroscience (Li and McIlwain, 1957).

Inorganic phosphate (Pi, orthophosphate) is an essential ion in living organisms playing indispensable roles in ATP synthesis and bone mineralization, among other processes. Pi exists in two predominant forms at physiological pH; $HPO_4^{2-}$and $H_2PO_4^-$ at a ~4:1 ratio. Intracellular Pi is sustained at a concentration of about 2 mM in most mammals and is a key determinant of the free energy available from ATP hydrolysis (Erecinska and Silver, 1989). Plasma Pi levels vary considerably in different vertebrates (Furman et al., 1997). In human plasma, the normal Pi level is ~ 1.1 mM but fluctuates more widely than calcium, and exhibits circadian variations. The concentration of Pi in the CSF of mammals is ~ 0.4 mM however little is known about the concentration in the interstitial space.

Little information is available on the mechanism of Pi uptake into cells of the CNS. A protein initially identified as a Pi transporter (Frederickson and Moncrieff, 1994) was subsequently shown to carry glutamate into synaptic vesicles (Bellocchio et al.,

2000; Takamori et al., 2000) and its Pi transporting capabilities are uncertain. Pi transport has been well characterized in the kidneys where it is transported by members of the Slc34 (Murer et al., 2004) and Slc20 (Collins et al., 2004) families for monovalent and divalent species respectively, in sodium-dependent processes.

There are abundant opportunities for solid minerals to form from the complex mixtures of ions in and around cells, particularly between metals and polyanions like Pi. In a solution with known concentrations of ions it is possible to predict the formation of precipitates from the solubility products (K_{sp}) for the various ion combinations. As a thermodynamic parameter, the K_{sp}s however gives no indication of how fast the precipitate takes to form. One common form hydroxyapatite ($Ca_{10}(PO_4)_6(OH)_2$) takes a long time, others like hopeite ($Zn_3(PO_4)_2{:}4H_2O$) form within a few milliseconds.

Zinc is found at a high concentration in certain glutamatergic vesicles within the mammalian forebrain and it has been proposed to be released and act as a neuromodulator (Paoletti et al., 2009a; Smart et al., 2004). There is a potential chemical impediment to the free release of zinc ions, namely, that zinc-phosphate has a very low solubility product ($9.1x10^{-36}\ M^5$), which limits the concentration of free zinc ions in a solution with a high concentration of Pi. In this communication we show that in brain slices the extracellular free zinc concentration is indeed limited by precipitation. Moreover, we demonstrate that this limitation can be overcome by the provision of amino acids like histidine that increases the solubility of the metal.

Results

Phosphate Induces Zinc Precipitation in Normal Saline

Most normal saline formulations typically include inorganic phosphate, which limits the availability of free zinc ions through the formation of zinc-phosphate precipitates. Thus the provision of zinc in the extracellular space at concentrations above a few micromolars poses something of a problem especially for the zinc release

hypothesis. Slices can be sustained in phosphate free solutions and appear to exhibit normal synaptic responses and cellular activity, however, the effects of withholding phosphate are as yet unknown. To increase the solubility of zinc while preserving Pi we added histidine to normal saline. Histidine forms both mono and bis-histidine complexes with zinc (Martell and Hancock, 1996) but does not act as a neurotransmitter so it would not interfere with normal physiological function of the hippocampus slices (Godfraind et al., 1973).

To detect the formation of precipitate in physiological solutions we performed spectrofluorimeter 90° light scattering experiments. In PFS (phosphate free saline) the addition of zinc up to a concentration of 330μM led to no discernable precipitate formation, which is consistent with the high solubility of the zinc-bicarbonate complex. In normal saline, however, additions of zinc above about ~10μM led to the formation of a precipitate (figure – 6). The addition of EDTA in the cuvette led to a decrease in light scattering as the chelator appropriates zinc from the precipitate formed (black line – figure 6). In histidine containing normal saline the solubility of zinc was increased and formation of precipitate was delayed until higher zinc concentrations were added (red line – figure 6). Histidine also led to the dissolution of precipitate when added after zinc had already precipitated out of solution (figure – 7). Once again when EDTA was added the precipitate was dissolved by zinc chelation (figure – 7).

Modeling Zinc Precipitation Response Curves with MINTEQA2

The geochemical modeling program MINTEQA2 was used to calculate the concentration of soluble zinc species in different saline formulations (Allison, 2003). The program takes into account all possible species that might form in a mixture and uses empirical thermodynamic parameters to calculate the equilibrium concentration of species, including any that might precipitate out of solution. The soluble zinc species

considered are are Zn^{2+}, $ZnOH^{+}$, $Zn(OH)_2$, $Zn(OH)_3^{-}$, $Zn(OH)_4^{2-}$, $ZnCl^{+}$, $ZnCl_2$, $ZnCl_3^{-}$, $ZnCl_4^{2-}$, $ZnOHCl$, $ZnSO_4$, $Zn(SO_4)_2^{2-}$, $ZnCO_3$, $ZnHCO_3^{+}$. Fifty insoluble species were considered in the calculation and the only one that precipitated was $Zn_3(PO_4)_2 : 4H_2O$. Figure 7 shows estimates of the soluble zinc concentration in normal saline as a function of the added zinc concentration. In histidine-free saline the soluble zinc concentration could not exceed ~4 μM (black line). The addition of progressively higher concentrations of histidine led to an increase in the concentration of soluble zinc species. For example with 100 μM zinc and 200 μM histidine, there was 24.4 μM of $Zn.His$, 17.8 μM of $Zn.His_2$ and 2.84 μM of all the other soluble zinc species. Since there is some uncertainty about the extracellular Pi concentration we calculated the solubility of zinc at different Pi concentrations and this is plotted in figure 8. Zinc solubility declines drastically in Pi concentrations above 1.5 mM and the free zinc concentration does not exceed 10 μM even when the total zinc concentration that is added is as high as 1000 μM.

To test the calculated values from the modeling program we assessed the solubility of zinc in normal saline using ICP-OES (inductively coupled plasma optical emission spectroscopy) with different zinc concentrations. The solutions were centrifuged to remove any precipitate and the supernatant was analyzed by ICP-OES. The results are shown in figure 8 and there is an excellent correspondence between the solubility measured by ICP-OES (open symbols) and that estimated by MINTEQA2 (closed symbols).

In human CSF the total amino acid concentration is ~ 700 μM (~ 500 μM glutamine) and the histidine concentration ~ 12 μM (Davson et al., 1993; Wishart et al., 2008). Glutamine leads to little if any increase in the solubility of zinc compared to that in normal saline alone (figure 10). In normal saline with 100 μM zinc and 500 μM glutamine, the free zinc concentration as determined by ICP-OES was 4.4 ± 0.2 (n=5), (5.9 μM from MINTEQA2 – figure 10) and was not influenced by the addition of more

zinc. Citrate can chelate zinc and is found at a concentration of 200-400 μM in CSF. In normal saline that contains 400 μM citrate the addition of 100 μM zinc only leads to a free zinc concentration of 13.9 μM (MINTEQA2 calculation – figure 11). In MINTEQA2 calculations, the addition of progressively higher amounts of zinc to a mixture of amino acids such as glutamine (500 μM), histidine (15 μM) and serine (50 μM) and other molecules such as citrate (220 μM) led to no appreciable increase in zinc solubility (figure 12). Light scattering experiments of increasing zinc concentration additions to the same type of mixture supported the MINTEQA2 calculations (figure – 13).

The precipitate composition formed after the addition of zinc to normal saline was determined by EDS (Energy dispersive X-ray spectroscopy, figure – 14). Atomic percentages were 60.9 ± 4 O, 15.9 ± 0.7 P, 4.6 ± 0.3 Ca and 18.7 ± 0.5 Zn (n=4, from two different samples), with trace amounts of K^+ and Mg^{2+}. The analysis of the precipitate was consistent with an amorphous compound composed largely of $Zn_3(PO_4)_2 \bullet 4H_2O$ (Hopeite) and $CaZn_2(PO_4)_2 \bullet 2(H_2O)$ (Scholzite).

The size distribution of the precipitate in normal saline was assessed by light scattering and found to be polydisperse. The mean particle size of the precipitate formed one minute after zinc addition was 688 nm and the minimum particle size ~200 nm. This is consistent with SEM images of the precipitate (figure – 14).

Pi Reduces Zinc Influx into Brain Slices

To assess the availability of zinc in neuronal tissue we used zinc transport into rat brain slices loaded with the acetoxymethyl (AM) ester form of the zinc-sensitive fluorescent indicator FluoZin-3 (Gee et al., 2002a). In such slices the fluorescence was elevated slightly above the tissue autofluorescence, suggesting that there is some chelatable zinc within cells. Application of the membrane impermeant chelator Ca-EDTA did not lead to a substantial reduction in the signal, whereas the membrane permeable chelators diethyldithiocarbamate (DEDTC) or N,N,N',N'-Tetrakis-(2-pyridylmethyl) -

Ethylenediamine (TPEN) induced a decrease in fluorescence, consistent with the intracellular location of the zinc-indicator complex. FluoZin-3 exhibits little response to calcium or magnesium, even in the millimolar range, and any elevations of fluorescence intensity are only likely to arise from the formation of a zinc-FluoZin-3 complex (Zhao et al., 2009).

Numerous scattered puncta were visible when viewing the parenchyma of FluoZin-3 loaded neocortical slices with little evidence of nuclear staining. Staining was most evident on the outer most aspect of the slices extending ~20 μm into the slice. From the fluorescent images it seems that FluoZin-3 enters synaptic vesicles rendering the endogenous zinc visible, which is consistent with the known ability of AM derivatives to load intracellular membranes (Thomas et al., 2000). To test this hippocampal slices were labeled with FluoZin-3 AM, which led to a faint but clear demarcation of areas that are highlighted by the Timm's stain, namely the hilus and stratum lucidum, showing that FluoZin-3 enters zinc-rich synaptic vesicles (figure – 15).

In normal saline the application of 100 μM zinc led to a small elevation of fluorescence in FluoZin-3 AM loaded neocortical slices, consistent with the precipitation of zinc by phosphate (black curve in figure – 16). The co-application of histidine (200 μM) with 100 μM zinc boosted the metal influx (red or green curve figure – 16). Histidine by itself in normal saline did not increase the fluorescence intensity, which suggests that it does not appropriate enough zinc in the saline or slice to induce any metal influx. In contrast, the addition of 100 μM zinc in PFS induced a substantial metal influx that was not augmented by histidine (figure – 17).

There is some evidence from experiments on intestine that zinc and histidine are co-transported into cells. To test this hypothesis we co-applied either L or D-histidine with zinc. There was little difference between the augmentation of zinc transport by L or D histidine (red and green curve in figure – 16). This suggests that the amino acid is probably not interacting with a stereospecific transporter. Both L and D alanine, which

form weaker complexes with zinc than histidine also, augmented the zinc transport (blue curve in figure – 16). Our results suggest that histidine is simply increasing the solubility of zinc in solution, rather than acting as a specific carrier.

To determine if the outcome of our experiments resulted from an edge artifact, because the probe only labeled the outer most aspect of the slice, we performed experiments where FluoZin-3-AM was injected into the depths of hippocampal slices (figure – 18). The dye was injected so that both the hilus and the cell bodies could be stained and imaged. Under these conditions similar results were obtained to those shown in figure 17.

We also investigated the solubility and transport of cadmium because it has similar properties to zinc and appears to be able to translocate into some cells through zinc transporters (Clapp et al., 2006). Cadmium also increases the fluorescence of FluoZin-3, though only to ~30% of the level of zinc (Zhao et al., 2009). Unlike zinc, cadmium is not precipitated by Pi in normal saline; we found this both empirically and in theoretical calculations. Application of cadmium to slices first led to a decline and then to an increase in fluorescence (figure – 19). Histidine, however, did not increase the rate of cadmium transport, consistent with the solubility of cadmium in normal saline. The latency of the fluorescence increase induced by cadmium application was longer than that in zinc applications (~2 vs ~1 min) (figure – 19). This suggests that either the rate of cadmium transport is considerably slower than zinc or that cadmium displaces zinc from endogenous chelators like metallothionein inducing an increase in fluorescence.

Effect of Phosphate Free Saline on Synaptic Transmission

To determine the effect of removing Pi from normal saline on synaptic transmission we measured the field potentials evoked by stimulation of the Schaffer collaterals in the stratum radiatum of region CA1 of rat hippocampal slices. Over a period of 6 hours there was no decrease in the slope of the field EPSP (figure – 20). We also

studied the effect the removal and re-application of Pi would have on field EPSP of CA1 neurons of younger (14 – 21 days old) and older animals (over 30 days old). The complete removal of Pi for the duration of the experiment or the removal and reapplication of Pi after about 1 h in older animals is not different than control (figure – 21). This suggests that the removal of Pi from the extracellular medium does not affect the normal physiological activity of the hippocampal neurons. The outcome of the experiment was the same for younger animals as well (figure – 22). When the effect of complete Pi removal in young and old animals is compared (figure 23), the slope of the field EPSP in younger animals seems to decrease with time while in older animals it seems to be constant, suggesting that the prolonged lack of Pi in the extracellular medium of hippocampal slices from young animals causes a slight decline in synaptic activity.

Discussion

We have shown here that in brain slices the presence of phosphate in physiological saline limits the concentration that soluble zinc can reach after metal application by the formation of zinc phosphate precipitates. In addition evidence presented shows that amino acids like histidine can increase zinc solubility in the presence of Pi, but they do not play a direct role in the transport of zinc. These results have clear implications for experiments involving the exogenous addition of zinc to brain slices. For example, it accounts for Molnar and Nadler's (Molnar and Nadler) observation that the presence of phosphate inhibited the action of exogenous zinc on GABA receptors. Our results also have perhaps less obvious implications for zinc release and uptake in vivo that we will discuss below. Moreover, our experiments have cast a spotlight on a rather under appreciated yet ubiquitious anion, Pi.

It is widely believed that synaptic zinc acts as a neuromodulator, being released during exocytosis and then diffuses into the synaptic cleft. In contrast our group has provided evidence which conflicts with this idea and instead we have suggested that

rather than being released, zinc is presented to the extracellular space while bound to exocytosed vesicular proteins. We have termed this scenario 'externalization' in contrast to simple release. The presence of extracellular zinc poses a problem for the zinc release hypothesis, as precipitates could form if large amounts of zinc are released. Whether they do form will depend on the concentration of zinc chelators, small ligands, macromolecules, Pi, zinc and pH. We cannot, however, exclude the existence of zinc chelators more powerful than those so far identified.

The concentration of glutamate within vesicles is estimated to be ~ 300 mM, but after exocytosis it declines very rapidly as the molecule diffuses away within the synaptic cleft. Glutamate has a low affinity for zinc nevertheless at high concentrations it can solubilize zinc. For example, at a zinc concentration of 100 μM in normal saline if the glutamate concentration is above ~30 mM no precipitate forms, however below this concentration progressive amounts of precipitate form with half the zinc being precipitated with ~14 mM glutamate (MINTEQA2 calculations).

Histidine has been proposed to augment the transport of zinc by forming a 2:1 complex (Sivarama Sastry et al., 1960) that is either transported as a unit or hands zinc off to a transporter. Histidine has been found to facilitate zinc transport in erythrocytes (Aiken et al., 1992) and in the intestines of rats (Wapnir et al., 1983), trout (Glover and Hogstrand, 2002) and lobsters (Conrad and Ahearn, 2007). However, our results suggest that in brain slices histidine simply increases the solubility of zinc and does not serve to facilitate the transport of zinc.

Our finding that histidine does not augment zinc transport in PFS suggests that under these conditions there is little phosphate in the extracellular space of brain slices. Similarly, because histidine increases zinc transport in normal saline, this indicates that the amino acid concentration is rather low in slices. In human CSF the total amino acid concentration is ~700 μM (~500 μM glutamine) and the histidine concentration ~12 μM

(Davson et al., 1993; Wishart et al., 2008). This concentration of histidine is too low to increase the solubility of zinc in the presence of Pi.

However the fact that in normal saline histidine augments zinc transport does not imply that there are no amino acids in the extracellular space. It could be that the zinc-phosphate particles do not penetrate through the extracellular space, and too little amino acid is likely to leach out to solubilize it. It is likely that the amino acid levels in the extracellular space of brain slices are diminished as they diffuse into the bathing solution. However, there is evidence that extracellular glutamate and perhaps glycine levels remain elevated in slices (Sah et al., 1989).

It does not seem to have been widely appreciated that Pi is an essential component of the extracellular medium that goes beyond its role in pH regulation. If Pi is removed from saline bathing neocortical cells the intracellular ATP and Pi levels remain stable for 30 min but both decline to ~60% of control levels after an hour (Glinn et al., 1997). Furthermore, synaptosomes derived from chronically phosphate deprived rats show an increase in cytosolic calcium and a decrease in ATP (Massry et al., 1991).

Controlled precipitation plays an important role in skeleton formation and other biomineralization processes (Dorozhkin and Epple, 2002). On the other hand the uncontrolled formation of insoluble aggregates plays a prominent role in the pathogenesis of atherosclerosis (Giachelli et al., 2001) and may do so in a number of neuropathologies, including Alzheimer's disease, Huntington's disease and ALS. We would like to suggest that the formation of inorganic precipitates could serve as a nucleus for the accretion of molecules and ions. However, if one is to implicate precipitation in a neuropathology it is important to exclude aggregates that arise during the analysis. In this regard it is instructive to consider the case of entities termed 'nanobacteria' that on closer examination turned out to be calcium carbonate particles (Martel and Young, 2008).

Aggregates of material with a predominantly inorganic basis have been described in a number of neuropathologies that have for the most part been ascribed to the

precipitation of calcium. The development of calcifications within the brain has been noted in the case of ischemia and exitotoxicity (Mahy et al., 1999); no zinc was found in this case (N. Mahy personal communication). Calcifications have also been described in the case of Fahr's syndrome in the basal ganglia (Bouras et al., 1996), spasmodic dysphonia (Simonyan et al., 2008) and in Urbach-Wiethe disease in the amygdala (Thornton et al., 2008); some zinc is found in the case of Fahr's syndrome. It is also worth noting that excess intracellular Pi may lead to the precipitation of calcium as it does in the case of skeletal muscle sarcoplasmic reticulum limiting calcium mobilization (Dutka et al., 2005).

Though Pi is usually incorporated in solutions used for sustaining brain slices, there are cases where its omission is seemingly without effect (Miles, 1990), but this has not been studied systematically. In cultured neurons, many investigators leave out phosphate from the minimal solutions used to perform physiological experiments but preserve it in the media used to culture the cells.

The saline formulations used currently for sustaining brain slices are based on the concentrations of ions in plasma. The plasma concentration of Pi is around 1.1 mM in humans and tends to be higher in other animals. In rats the plasma Pi concentration is 3.2±0.1 mM and in CSF 0.47±0.01 mM (Mulroney et al., 2004). The latter is close to the concentration in humans and it is likely but not certain that the extracellular concentration is similar. Most mammalian slice normal saline formulations have Pi at a concentration of around 1 mM; to mimic CSF more closely it may be worthwhile shifting to a concentration of ~0.5 mM.

It is worth considering whether Pi might play roles other than that of the substrate for ATP synthesis. For example might it act as an allosteric regulator of ion channels and transporters? Moreover, the outward directed Pi gradient could be employed in carrier-mediated mechanisms to transport ions, although none have thus far been identified.

There is a pressing need for experiments to determine the range of concentrations of Pi in the extracellular space and to determine the effect of changes in Pi on neuronal and synaptic activity. NMR measurements in the intact brain can distinguish between extra and intracellular Pi and may provide a means for assessing the extracellular Pi concentration (Gilboe, 1998).

To the best of our knowledge there have been no systematic studies of the effect of phosphate free normal saline on synaptic transmission. We found that phosphate removal for up to 6 hours had no effect on transmission at the Schaffer collateral CA1 synapse. This suggests that intact neuronal tissue either has considerable reserves of Pi or that it is endowed with an exceptional capacity to reclaim Pi that passes into the extracellular space. Until it becomes feasible to measure extracellular Pi, it is not possible to say whether or not Pi levels are sustained in slices held in PFS.

It is clear that the role of Pi extends beyond that of a pH-buffering agent. There is little information on the mechanisms to control the intra and extracellular Pi levels, which could have a profound impact on the precipitation of metals. Moreover, the level of amino acids, like histidine could play an important role in formation of metal-phosphate precipitates.

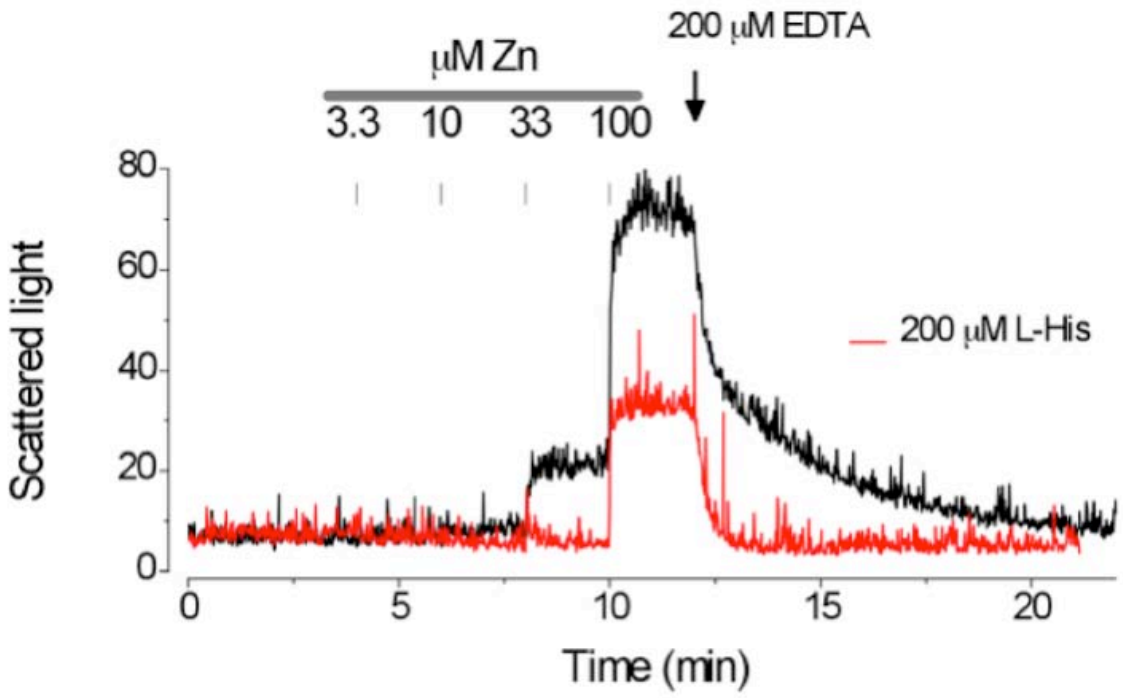

Figure 6. Zinc-phosphate precipitate in the presence and absence of Histidine

---

Note: Scattered light experiment. Addition of increasing concentrations of zinc to normal saline in the presence (red line) and absence (black line) of Histidine. EDTA was added to the cuvette in both cases to determine that zinc was part of the precipitate formed.

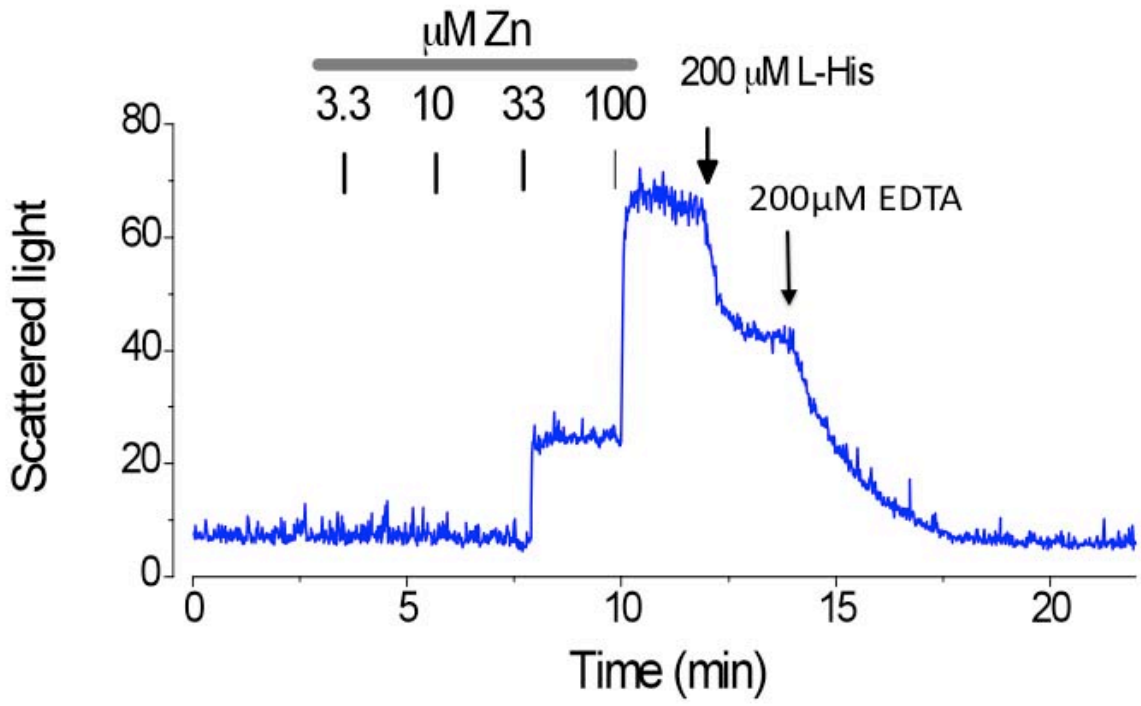

Figure 7. Dissolution of zinc-phosphate precipitate with Histidine addition

---

Note: Scattered light experiment. Addition of increasing concentrations of zinc to normal saline leads to precipitate formation. Addition of 200 μM Histidine leads to some dissolution of the existing precipitate showing that Histidine can appropriate some of the zinc from the precipitate. Addition of EDTA completely strips zinc from the precipitate formed, thus dissolving whatever is left of the complex.

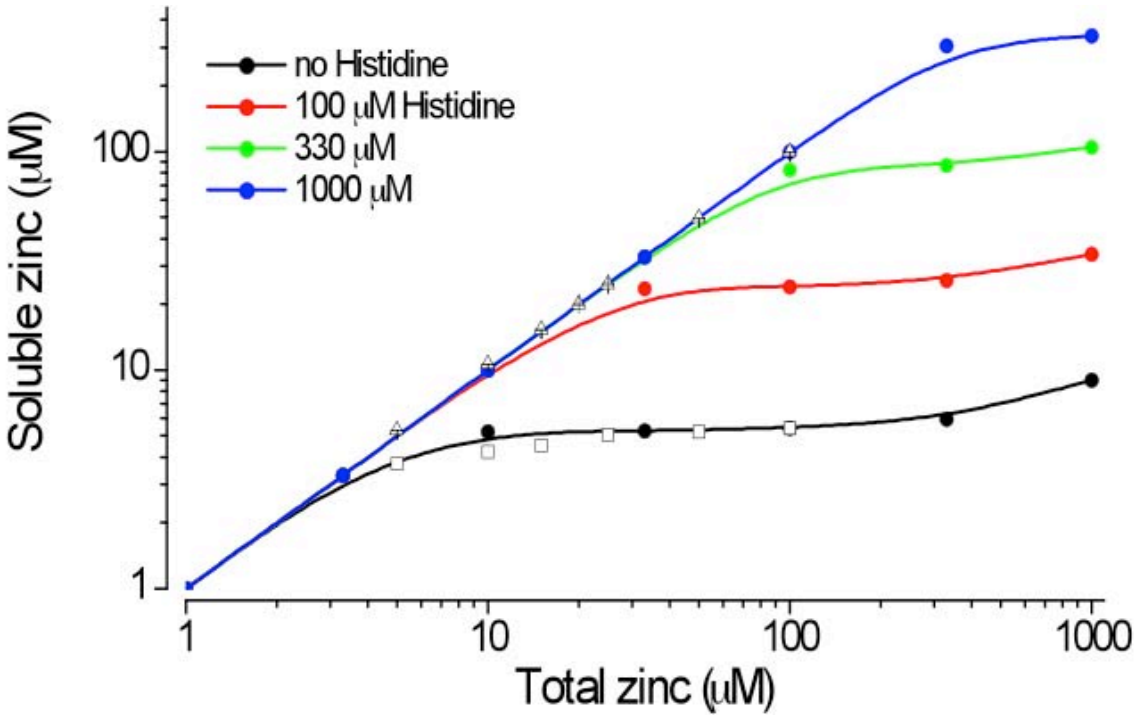

Figure 8. Correlation of MINTEQA2 calculations and OES experiments

---

Note: Graphs represent the amount of soluble zinc vs. total amount of zinc added to normal saline without (black curve) and with progressively higher amounts of Histidine. In the absence of histidine (black curve filled circles) the amount of free zinc in solution does not exceed a few micromolar even when the total amount of zinc added is 1000 μM. The MINTEQA2 results are represented by filled circles, whereas OES data is given by the open symbols. There seems to be good correlation between the calculated and the measured values.

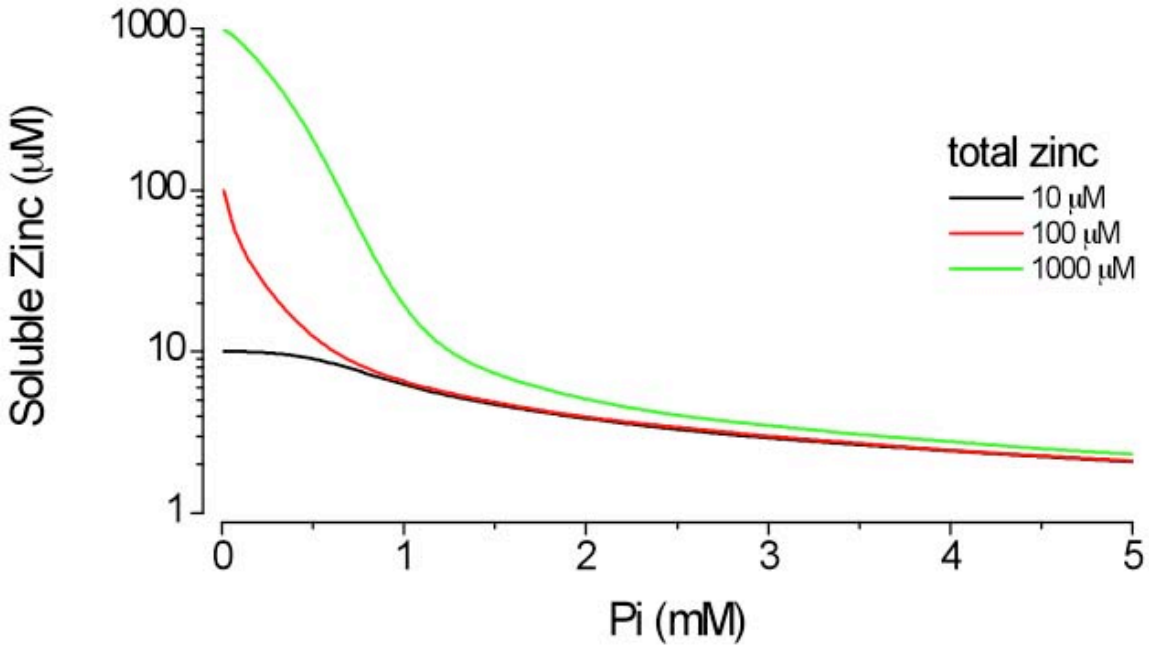

Figure 9. Amount of soluble zinc as a function of phosphate concentration

---

Note: The amount of zinc soluble in the normal concentration of Pi used in saline formulations (1.3 mM) is very little even when the total zinc added is 1 mM.

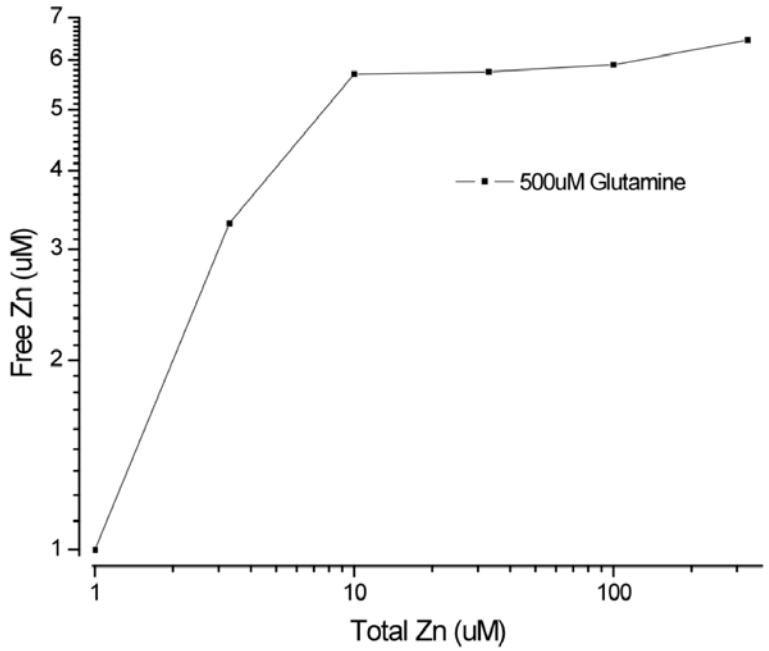

Figure 10. Effect of glutamine on zinc solubility

Note: The amount of soluble zinc as a function of total zinc added to normal saline containing 500 μM Glutamine.

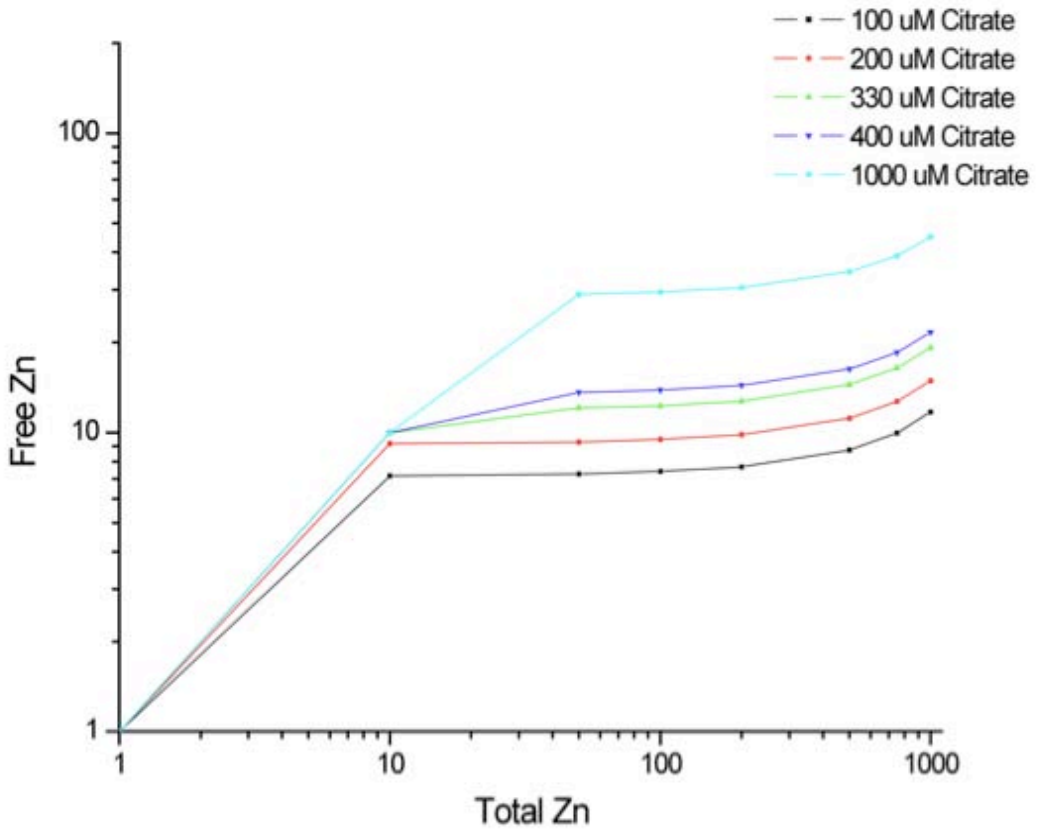

Figure 11. Effect of citrate on zinc solubility

Note: The amount of soluble zinc as a function of total zinc concentration added to normal saline that contains increasing amounts of citrate.

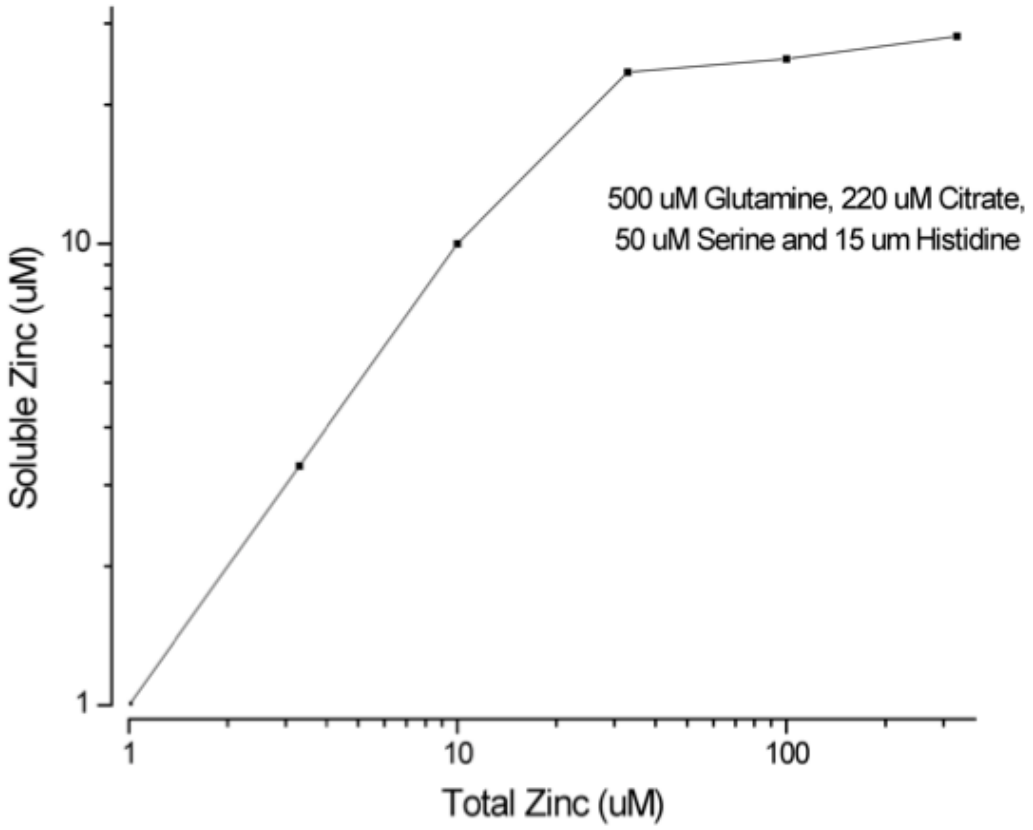

Figure 12. Combined effect of glutamine, histidine and citrate on zinc solubility

---

Note: Soluble zinc as a function of total zinc added to normal saline containing 500 μM Glutamine, 220 μM Citrate, 50 μM and 15 μM Histidine.

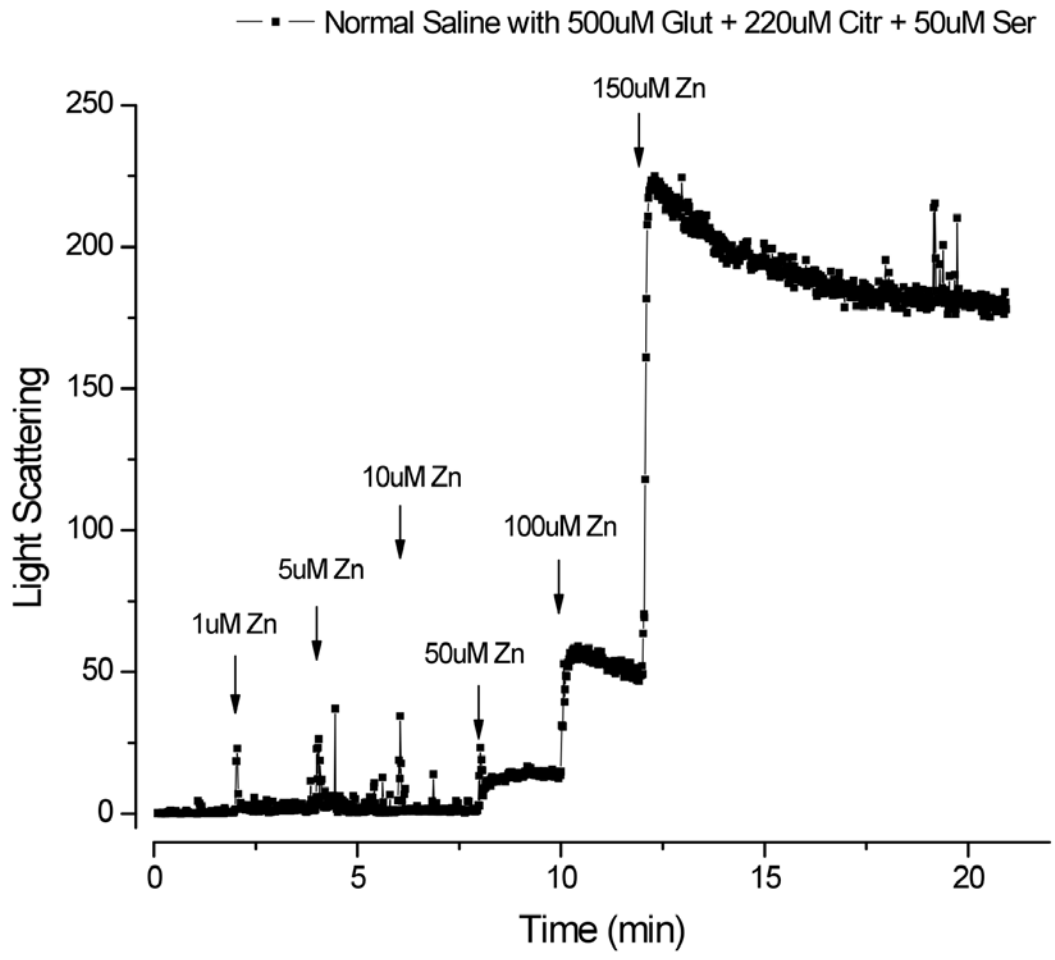

Figure 13. Combined effect of glutamine, serine and citrate on zinc solubility

---

Note: Light scattering experiment where increasing concentrations of zinc are added to normal saline containing 500 μM Glutamine, 220 μM Citrate and 50 μM Serine.

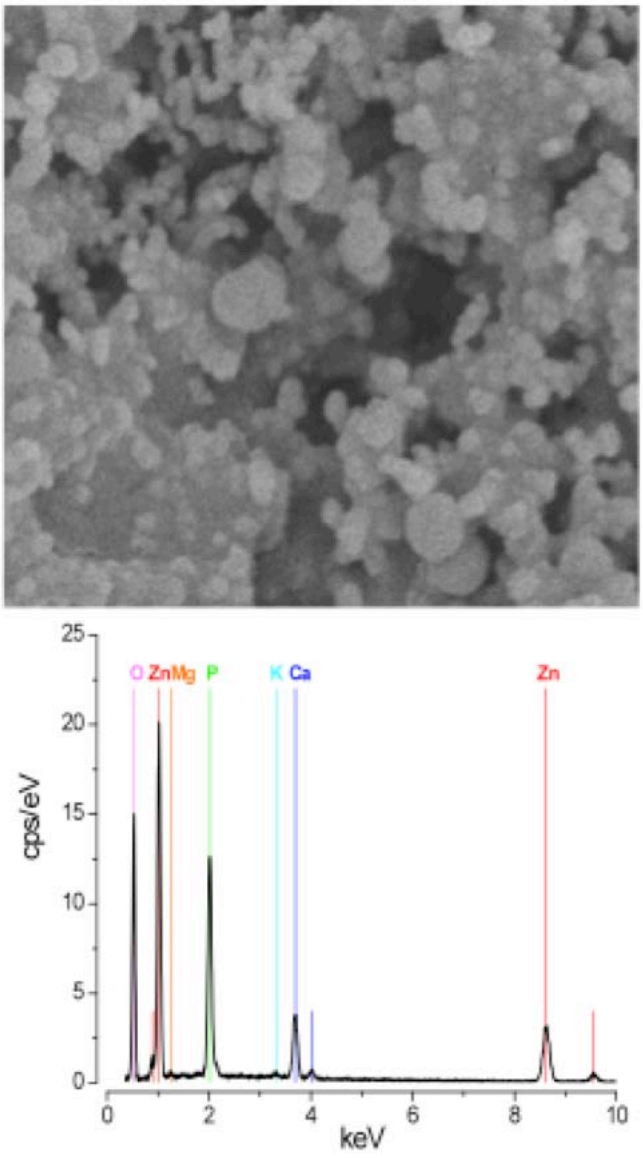

Figure 14. Zinc-phosphate precipitate characterization

Note: SEM image of the zinc precipitate formed and EDS analysis of the composition of the precipitate.

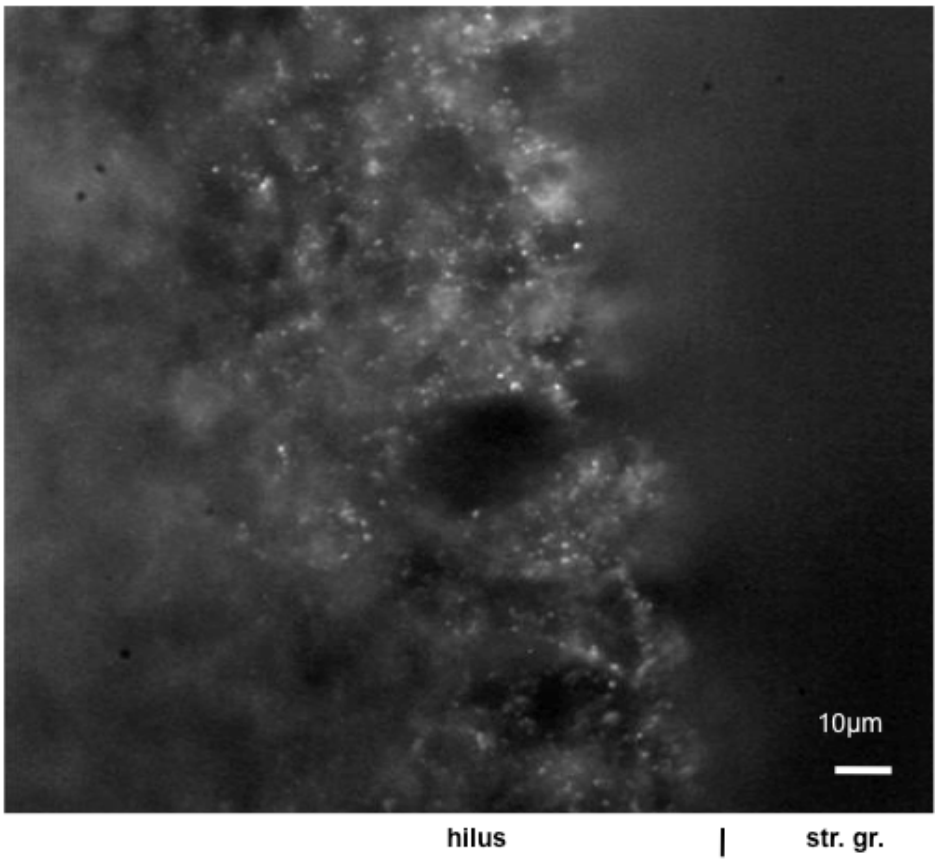

Figure 15. FZ-3-AM internalization into synaptic vesicles

Note: A fluorescent image of a hippocampal slice stained with FZ-3-AM. Hilus refers to the area that contains synaptic terminals whereas the stratum granulosum contains the cell bodies. The fluorescence is very punctuated which suggests that FZ-3-AM stains mainly the synaptic vesicles.

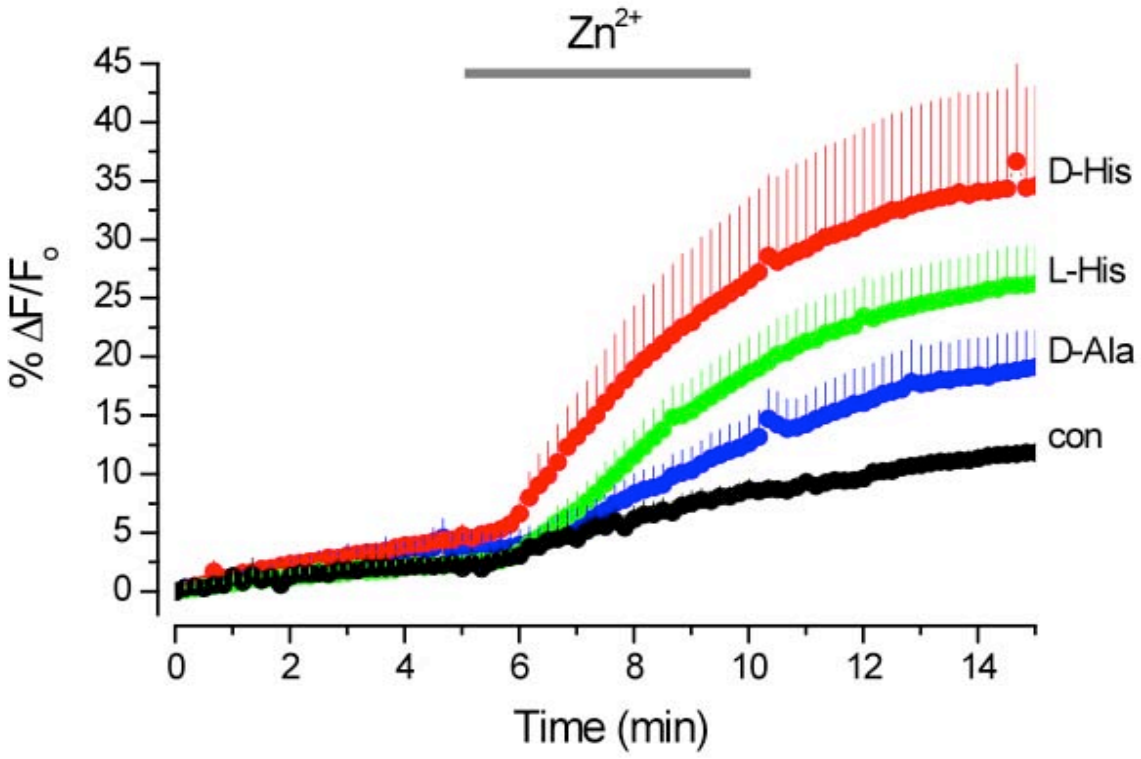

Figure 16. The influence of Pi and histidine on the influx of zinc into neocortical slices

---

Note: In all experiments the fluorescence was measured in slices loaded with FluoZin-3 AM in an area of interest roughly midway through the neocortex. (a) Influences of amino acids (200 μM) on zinc uptake in normal saline. The period of zinc (100 μM) and amino acid application is indicated by a horizontal bar. Control (con) no amino acid was added (n=4), D-Ala (n=4), L-His (n=41) and D-His (n=6).

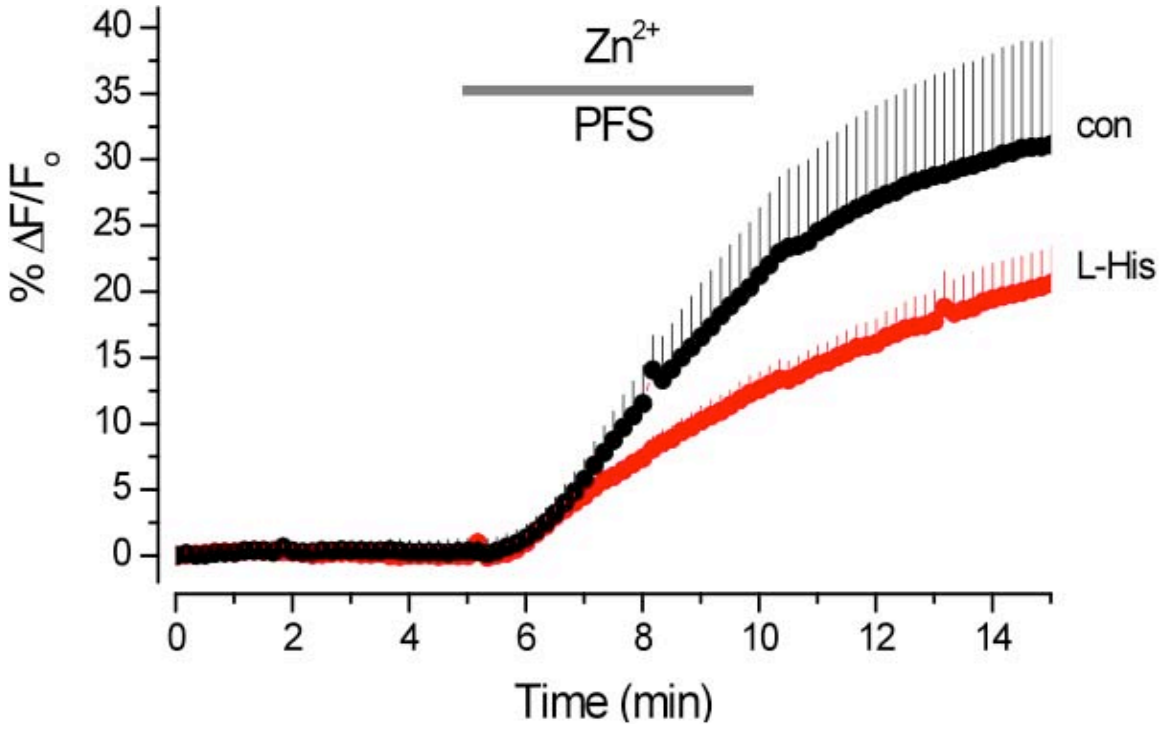

Figure 17. Zinc uptake in phosphate free saline

Note: The gray bar represents the application time for Zinc and Histidine. Control (con, n=5) and L-His (n=5).

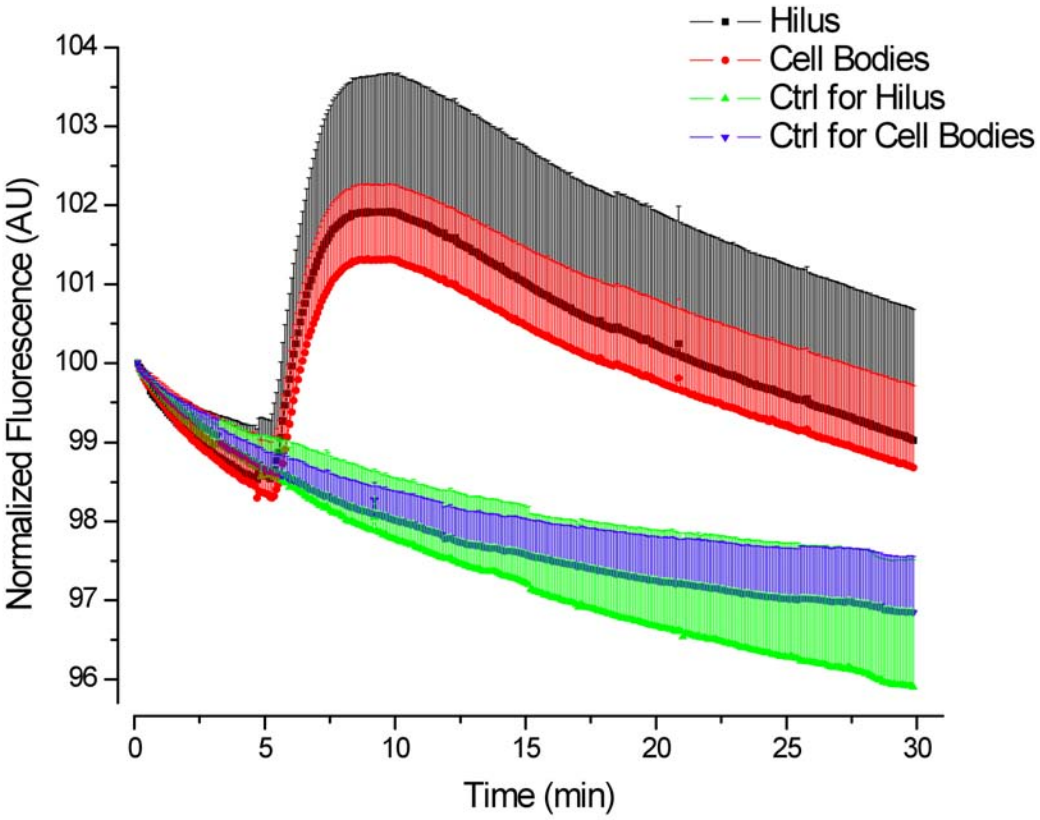

Figure 18. Fluorescent response of injected FZ-3-AM to Zinc/His application

---

Note: Slices were injected for at least 30 min and then Zn/His was applied for 5 min. The bar indicates the time and duration of Zn/His application. In all cases n=5 and error is given as SEM.

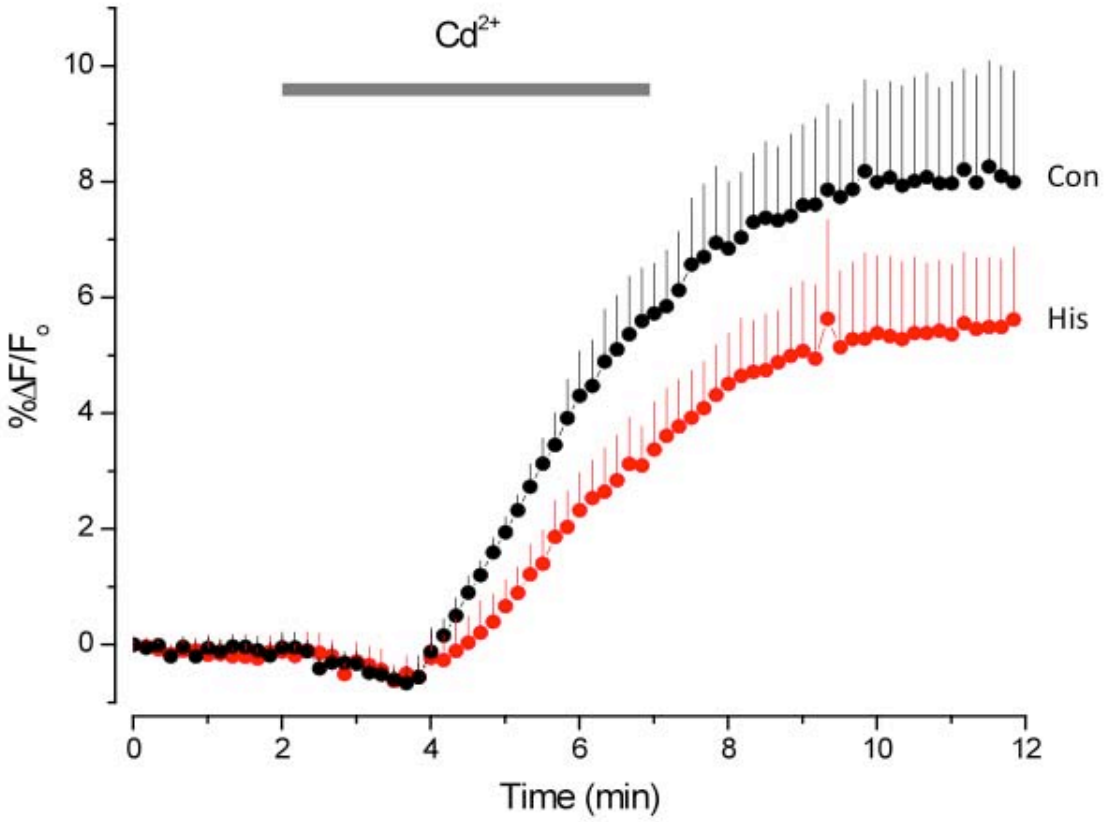

Figure 19. FZ-3-AM response to cadmium application

Note: The bar represents the time and duration of cadmium application. Con (n=5) – black curve, his (n=5) red curve. Error is given as SEM. There is no change in fluorescence during His application vs. control slices.

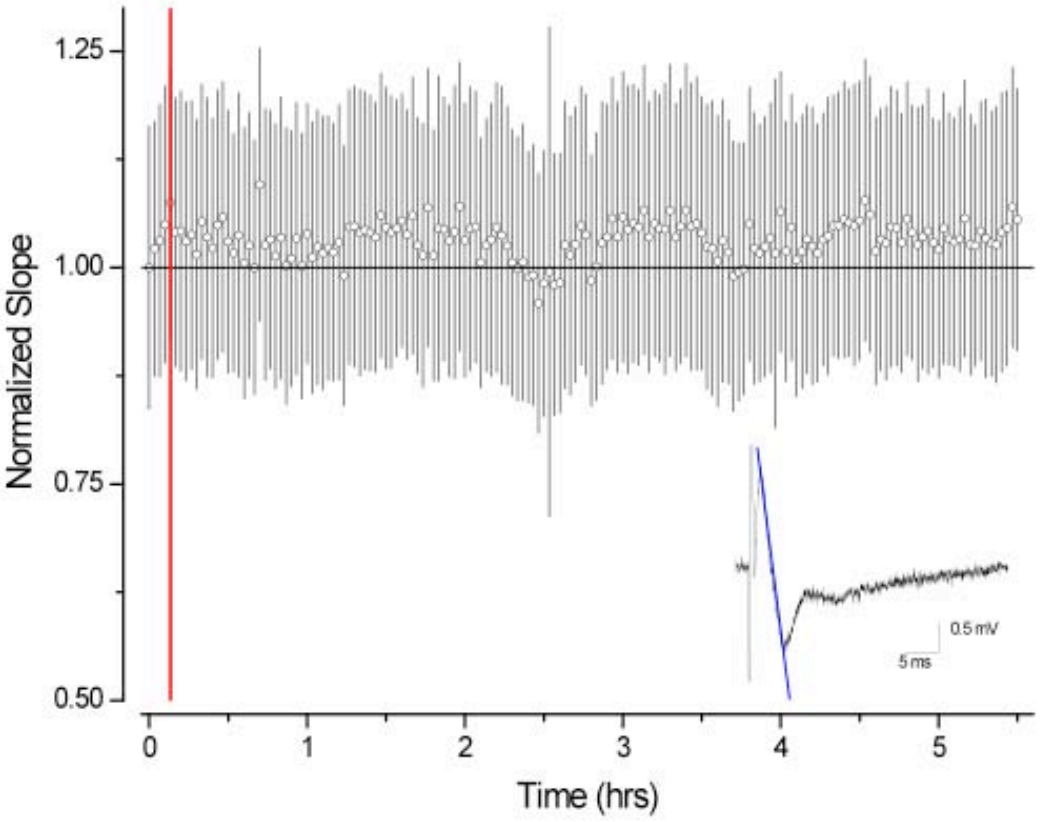

Figure 20. Effect of Pi removal from saline solution on synaptic activity

---

Note: The data represents the normalized slope of EPSP (excitatory post-synaptic potential) collected over 5.5 h of recording. The red line indicates the time of Pi removal from the saline solution. The inset is a representative of a typical field EPSP observed during electrical recording. The blue line represents the slope of fEPSP, which is measured and normalized. The scales of the inset are (horizontal) 5 ms and (vertical) 0.5 mV.

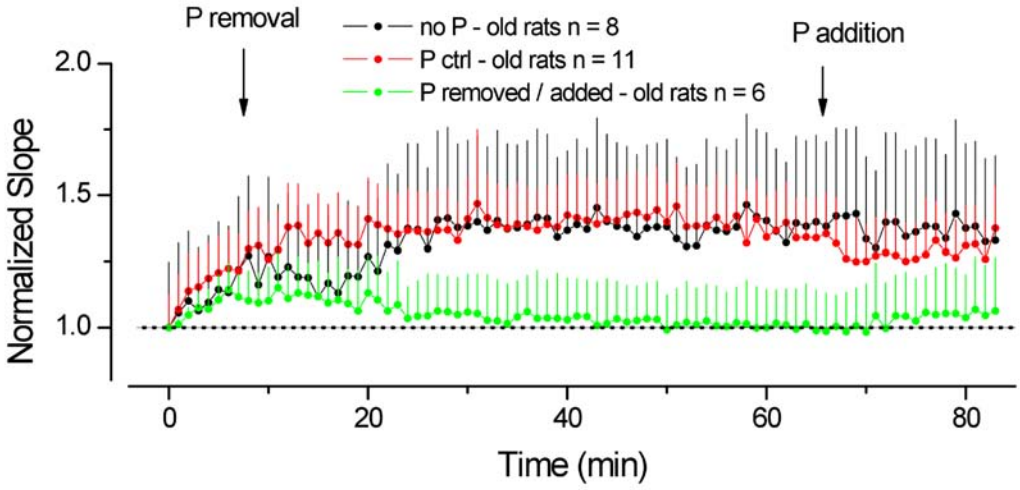

Figure 21. Effect of removal or re-introduction of Pi on synaptic activity of old rats

---

Note: The arrows indicate the time of the removal from and addition of Pi to normal saline. Data is given as normalized fEPSP slopes (see fig 20) and error is given as SEM.

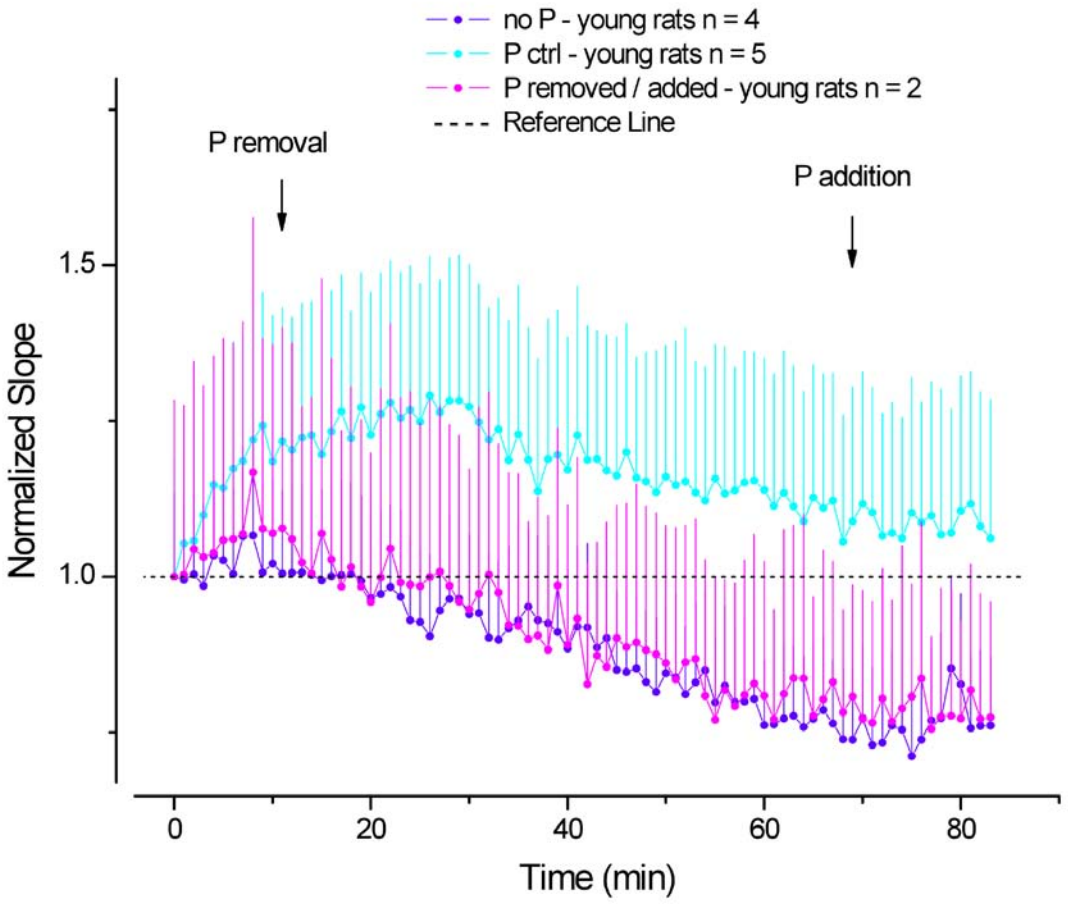

Figure 22. Effect of removal or re-introduction of Pi on synaptic activity of young rats

---

Note: The arrows indicate the time of the removal from and addition of Pi to normal saline. Data is given as normalized fEPSP slopes (see fig 20) and error is given as SEM.

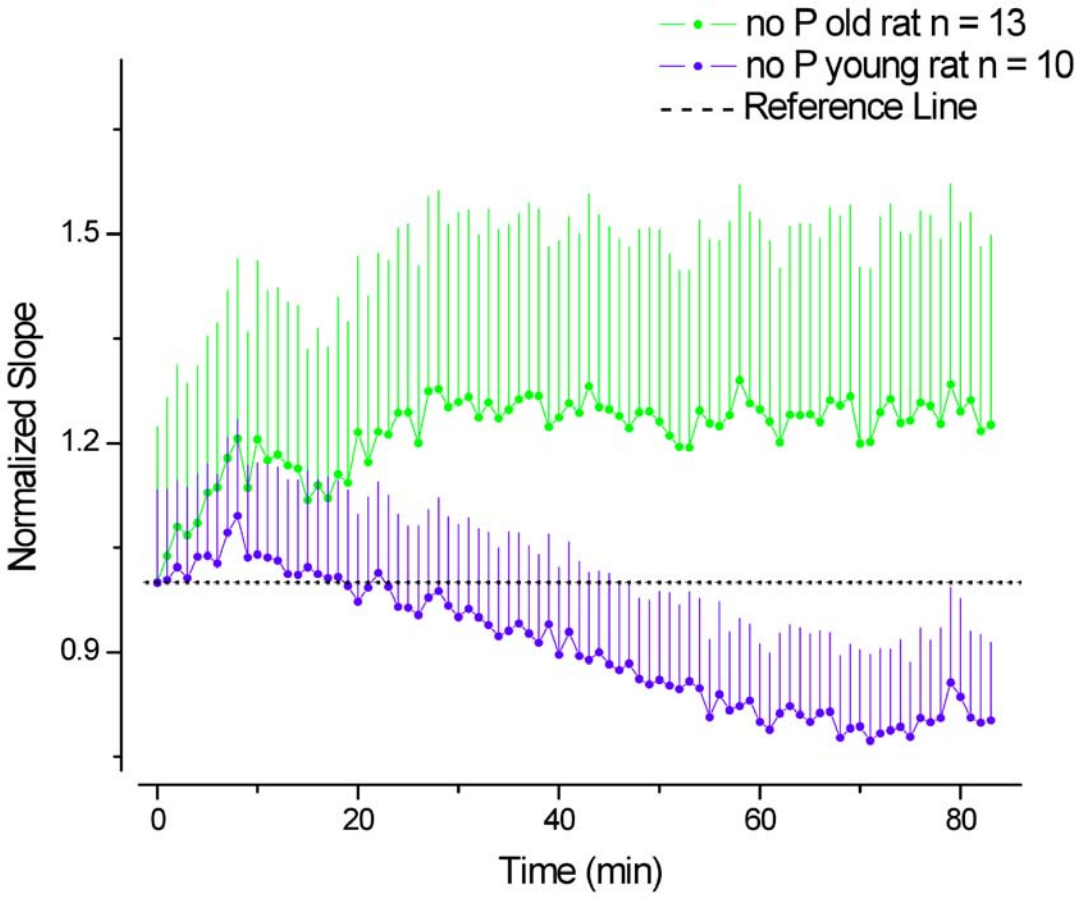

Figure 23. Effect of Pi removal on synaptic activity of young and old rats

---

Note: A comparison between the effect of Pi removal from normal saline solution upon fEPSP slopes in old and young animals. Error is given as SEM.

CHAPTER V.

ZINC HOMEOSTASIS

Introduction

A very important question to be considered is zinc homeostasis and buffering in brain cells. Even though it has been established that zinc plays an important role in many processes, zinc homeostasis and regulation both intracellularly and extracellularly still remains poorly understood. Findings such as zinc modulation of protein kinase C signaling pathways (Korichneva et al., 2002) and zinc inhibition of GABAergic neurotransmission (Hosie et al., 2003b) seem to indicate that the concentration of zinc, whether intracellular or extracellular could be important in cell signaling activity. Zinc in the extracellular space is estimated to be in the nM range (Takeda, 2000), while the total zinc concentration in the cytoplasm of a typical neuronal cell is estimated to be upward of 590μM (Tarohda et al., 2004), with most of the zinc sequestered by metal-binding proteins such as metallothionein, zinc-finger proteins and zinc-dependent enzymes (Burdette and Lippard, 2003; Maret, 2003; Palmiter, 1998). Estimated intracellular concentrations of free zinc varies widely from sub-nanomolar (0.4 nM) to sub-micromolar (0.18 μM) (Canzoniero and Sensi, 1997; Dittmer et al., 2009; Finney and O'Halloran, 2003; Thompson et al., 2002; Vinkenborg et al., 2009). The large variability in free zinc concentration values stem from the different methods used to estimate it. The low intracellular free zinc concentration points to the tight balance and control between zinc transport, efflux and influx and zinc exchange from transport proteins to newly synthesized metalloproteins or enzymes (Eide, 2006). It is well established that Ca^{2+} acts as a second messenger, therefore the cell tightly regulates the intracellular Ca^{2+} concentration, but allows transient changes to occur that are rapidly damped out. The large number of binding sites for Ca^{2+} cause transient Ca^{2+} currents both spatially and temporally (Pozzan et al., 1994). If a Ca^{2+} probe is utilized to assess Ca^{2+} buffering in the

cytoplasm, a transient increase in fluorescence is observed and the signal decays within seconds. Little is known however whether the cell responds the same way to zinc influxes, or whether other mechanisms of buffering are in place. In this work, we attempted to understand zinc buffering in hippocampal slices by using the fluorescent probe, FZ-3-AM.

Results

In our previous experiments, it was already found that zinc concentration is limited by the presence of phosphate in the extracellular medium, so zinc was co-applied with pyrithione (pyr) to FZ-3-AM loaded slices for 5 min and then normal saline wash was resumed (figure 24). FZ-3-AM is the non-fluorescent acetoxymethyl ester form of the dye FZ-3. FZ-3-AM passively diffuses into the cell and once in the cytoplasm, endogenous esterase enzymes cleave the ester groups and the dye is converted to the acid form FZ-3, which becomes trapped in the cell due to its negative charge. FZ-3 then binds zinc and becomes fluorescent. Intracellular concentration of FZ-3 can become 2-5 times the extracellular concentration (Krężel and Maret, 2006); due to the fact that FZ-3-AM is constantly being converted to FZ-3 and the shift in equilibrium is maintained. Pyrithione (pyr) is a compound that acts as an ionophore, forming a 2:1 complex with zinc and allowing it to cross both cell and synaptic vesicle membranes. If zinc is being buffered similarly to Ca^{2+}, then a transient increase in cell body (cytoplasm) fluorescence should be observed followed by a rapid decay in fluorescence signal. Synaptic vesicles, on the other hand, contain a high amount of chelatable zinc, so the fluorescence signal in vesicles should increase and stay up since this zinc is loosely buffered.

The fluorescent signal increases shortly after the application of zinc/pyr and remains elevated for minutes (figure 24). The signal behaves the same in both the hilus and the cell bodies. The inset shows a difference image between the image with the maximal fluorescence increase and the image just before zinc/pyr was applied.

Experiments performed with cortex slices yielded the same type of fluorescence increase, which lasted for up to 90 min with fluorescence falling only 2% from the value of the initial increase (data not shown). This is an interesting result since it indicates that zinc seems to be getting into both the cytoplasm and synaptic vesicles at the same time. It is not very clear from these results if zinc elevations are occurring in the cytoplasm itself or in cytoplasmic compartments. It is worthwhile noting that in cuvette experiments pyr addition to FZ-3 does not affect its fluorescence.

In all fluorescent dye experiments, it is very important to identify the location of the dye, since mistaking the location has significant implications for data interpretation. We attempted to differentiate whether FZ-3 accumulates in synaptic vesicles or in the cytoplasm. If CaEDTA (a membrane impermeable chelator) is first applied to unstimulated slices, fluorescence is not affected indicating that FZ-3-AM is internalized (see figure 26 – from min 5 to min 10). If 50 mM KCl is applied to loaded slices for 30 s and then normal saline wash is resumed, followed by the application of 1 mM CaEDTA (figure 25), the fluorescent signal decreases below control levels. This indicates that the dye moves into the vesicles and upon KCl stimulation it becomes available for CaEDTA chelation. It also suggests that part of the fluorescence observed is associated with vesicles. This conclusion is further reinforced by the punctate fluorescence seen in the image in figure 25, since the fluorescence would not have appeared as puncta if the dye was localized in the cytoplasm.

In the course of our experiments, we found that application of pyr by itself led to an increase in fluorescence (see black curve in figure 26). The signal increases the same way as if exogenous zinc was co-applied with pyr. This probably indicates that there must be some extracellular zinc, which is being transported inside. The source of this zinc is most likely what has been termed “zinc veneer” (Kay, 2003), which is zinc that is coordinated to molecules in the outer cell membrane and is present whether or not the cells are stimulated. To determine whether the zinc was coming from the solution, or

from the zinc veneer, we treated the slices with CaEDTA for 5 min (red curve – figure 26), and then slices were washed for another 5 min before pyr application. The application of CaEDTA prior to pyr addition greatly reduces the increase in signal that is observed upon pyr application, indicating that pyr is indeed stripping the zinc off the veneer and carrying it inside. It also excludes the possibility of pyr liberating zinc from intracellular sites, as CaEDTA application prior to pyr addition would have not lowered the fluorescence if the source of the fluorescence increase were zinc from intracellular stores. In addition, it eliminates the saline solution as the source of extracellular zinc as the slices are washed with saline after CaEDTA application and before pyr addition. Finally, pyr additions to FZ-3 in a cuvette do not increase the fluorescence, indicating that pyr itself is not contaminated with zinc.

To further explore the interaction between pyr and the zinc veneer, 20 μM pyr and 1 mM CaEDTA were co-applied for 5 min (black curve – figure 27). The fluorescence signal increases initially similar to the increase observed with pyr alone, however the signal then starts to decrease and eventually falls to initial value. This can be explained by the fact that CaEDTA is slow to strip zinc off from the veneer since it is saturated with Ca^{2+}, so pyr can transport some of the zinc from the veneer intracellularly. Once the zinc veneer is chelated, the signal starts to drop. The signal drops further due to the fact that pyr acts as an ionophore allowing zinc to cross the cell membrane and move extracellularly. CaEDTA chelation of zinc maintains a low extracellular zinc concentration. Zinc is therefore able to flow extracellularly down its concentration gradient. To determine if the sluggishness of CaEDTA binding zinc from the veneer is really why the signal goes up and then decreases, 200 μM EDPA was added simultaneously with pyr for 5 min. EDPA does not bind Ca^{2+} and Mg^{2+} as tightly as EDTA and thus binds zinc faster (Kay, 2003). The signal increase is largely abolished indicating that EDPA quickly chelates the zinc veneer preventing pyr from carrying much zinc in (red curve – figure 27). The signal also drops below control levels as a result of

zinc flowing down its concentration gradient since EDPA reduces the extracellular steady-state zinc concentration lower than that of CaEDTA. Both experiments are consistent with our interpretation that pyr is carrying the zinc from the veneer intracellularly and that it acts as a reversible ionophore.

To optimize the concentration of pyr, experiments were performed varying both zinc and pyr concentrations. Values for pyr experiments are around 20μM and since pyr forms a 2:1 complex with zinc, we used the same ratio for our initial optimization. 1, 3.3, 10, 33 and 100 μM zinc were applied together with twice the amount of pyr (figure 28b-f). It is interesting to note that in the experiments with 1, 3.3 and 10 μM zinc, the fluorescence increases only transiently. A likely explanation is that the excess pyr can shuttle zinc down its concentration gradient (similar to what was observed in figure 27). The biggest increase after zinc/pyr is washed off is the one observed with 33 μM zinc. An interesting phenomenon was observed when the zinc concentration reached 100 μM. The fluorescence signal decreased with zinc/pyr application instead of increasing as in all other cases. It could be that the concentration of pyr is so high that it allows more zinc to flow out than it is flowing in. The change in fluorescence was plotted as a function of zinc concentration in both the hilus and the cell body (figure 28a). The fluorescence change is pretty steady for the lower concentrations of zinc used and is the largest when zinc reaches 33 μM, but after that it sharply decreases. Fluorescence change is statistically the same in both the cell body and the hilus.

To see if an excess of either zinc or pyr would increase the zinc influx into the cell, 10 μM pyr was used with varying concentrations of zinc (1, 3, 10, 15 and 30 μM – figure 29) applied for 5 min. The fluorescence change was the largest at equimolar zinc and pyr (figure 29) and did not change much with subsequent zinc concentration increases. A typical response of fluorescence signal vs. time after 10 μM pyr and varying zinc concentrations were applied is given in the inset of figure 29. It was determined that an excess of zinc (meaning zinc concentrations that are larger than half the pyr

concentrations) is better than a 2:1 ratio, therefore we decided to use 10 and 15 μM zinc and pyr concentrations respectively.

We also co-applied zinc with another zinc ionophore Clioquinol, which allows zinc to move only into the cytoplasm. The fluorescence increase was the same as that observed with pyr (see figure 30), once again suggesting that the dye might be in cellular compartments rather than in the cytoplasm.

From the above data, it is difficult to distinguish whether zinc is getting into synaptic vesicles or cytoplasm, or both. There seems to be no difference in signal between the cell body and hilus or cytoplasm and synaptic vesicles respectively. To investigate in which compartments zinc influxes are being detected, we performed experiments with ZnT3 knock out (KO) mice and either zinc/his or zinc/pyr application. ZnT3 is a zinc transporter protein that is responsible for loading zinc into the synaptic vesicles (Cole et al., 1999; Palmiter et al., 1996; Wenzel et al., 1997b).

To confirm that synaptic zinc was eliminated in ZnT3 KO mice, hippocampal slices were stained with the membrane permeable probe ZnAF-2. There was no ZnAF-2 staining of the hilus and mossy fibers as seen in the wild type (WT) mice, indicating that KO slices do not contain synaptic zinc.

The average initial fluorescence value of the WT cell body layer is higher than that of KO mice (see table 1), indicating that some of the fluorescence that arises from the cell body layer is vesicular and not cytoplasmic. New synaptic vesicles are synthesized in the endoplasmic reticulum and are stocked with zinc through the action of ZnT3; therefore some of the fluorescence that is observed from the cell body area could arise from these newly synthesized vesicles.

Zinc and pyr were then co-applied to FZ-3-AM loaded slices of WT and KO mice for 5 min and then normal saline wash was resumed (see figure 31). The fluorescence response in the WT increases similarly to rat hippocampal slices, but at a slower rate. Fluorescence increase is larger in both the cell bodies (figure 31 – black filled squares)

and hilus (figure 31 – black open squares) of WT mice than in KO mice (figure 31 – red filled squares – hilus and red open squares – cell bodies). In KO mice however, there was no response to zinc application in either the cell bodies, or the hilus. This indicates that either little dye is localized in the cytoplasm, or that zinc is tightly buffered.

It could be argued that pyr can shuttle zinc out of the cell and may explain the lack of fluorescence increase. To determine whether this is the case, we co-applied zinc/his in WT and KO slices and found that slices responded the same as with zinc/pyr treatment (figure 32 – black filled squares – WT hilus and black open squares – WT cell bodies and figure 32 – red filled squares – KO hilus and red open squares – KO cell bodies). This lack of fluorescence increase in KO cell body layer during zinc/his application further supports the hypothesis that either little dye remains in the cytoplasm, or zinc is tightly buffered, since his can only facilitate zinc transport through the cell membrane and not directly into the cytoplasmic compartments.

To differentiate whether zinc is being strongly buffered as soon as it enters the cell, so that the zinc concentration does not increase much (even transiently) or whether the dye is localized in the cytoplasm at all, experiments were carried out with an oxidizing agent 2,2'-dithiodipyridyl (DTDP). DTDP is expected to oxidize any cytoplasmic proteins containing sulfhydryl groups (SH), such as metallothioneins (MTs) or glutathione (GSH) and zinc finger proteins. Oxidation of the SH group should liberate bound zinc and the fluorescence signal in the cytoplasm should undergo a sudden increase. DTDP was first added to pre-loaded FZ-3-AM slices. A large increase in fluorescence was observed in both the cell body and the hilus. Fluorescence intensity in either cell body or hilus did not decrease even after 1 h of recording (data not shown). This prolonged increase in cell body fluorescence is a result of zinc influx into cellular compartments instead of zinc influx into the cytoplasm itself. One of the reasons for the inability to observe zinc influx in the cytoplasm is the fact that the dye may be pumped

out of the cytoplasm (into cellular compartments or outside the cell). Addition of DTDP to slices while they are loading with FZ-3-AM would eliminate this possibility.

FZ-3-AM was added to unstained slices at 30s and allowed to stain for about 4 min. 1 mM DTDP was added at min 5 and zinc/pyr added at min 10 (figure 33). Fluorescence was monitored both in the hilus (filled squares – figure 33) and the cell body (open squares – figure 33) to see if the fluorescence response would be different. Fluorescence signal increased similarly to when external zinc and pyr were co-applied and there is no sharp increase in fluorescence that decays with time, as it would be expected if external zinc moves into the cytoplasm. The inset in figure 33 is a difference image between the image just before zinc/pyr was introduced and the image just before DTDP was introduced (difference between image at min 10 and at min 5).

The zinc influx from pyr application is induced through the plasma membrane and should lead to a larger increase in the cytoplasm of synaptic vesicles than that in the cytoplasm of the soma, because of the larger surface to volume ratio for a small compartment relative to a large compartment. However in the case of DTDP, because it is releasing zinc from bound sites within the cytoplasm, the increase should be larger in the cytoplasm of the soma than that of the synaptic boutons. This assumes that the concentration of zinc-binding proteins is the same in both. This phenomenon can be revealed if a ratio between the cell body fluorescence over the hilus is taken (see figure 34). If this were true, then the ratio of the cell body/hilus should increase over the DTDP application time. This ratio however is constant over the DTDP addition. A higher concentration of DTDP (5 mM) was also used to test if it would bring about a sharp increase in cell body fluorescence, however the results were the same as with the lower concentration of DTDP (data not shown). Figure 35 shows a sequence of difference images taken by subtracting the image before 1 mM DTDP application from the entire image sequence. It is easier to visualize small fluorescence changes over time if difference images are taken. Once again, fluorescence is largest in the hilus and not in the

cell body, with no sharp and sudden increases in signal as would be expected if there were transient zinc increases in the cytoplasm.

One of the reasons why transient increases in cytoplasmic zinc are not observed could be the fact that FZ-3 may be quenched or silenced by the interference of another metal ion. To exclude the possibility that FZ-3 fluorescence is being quenched by Fe^{2+} ions, an iron chelator 2-2'-dipyridyl was added to slices and fluorescence was observed (data not shown). If FZ-3 fluorescence were being quenched by iron, one would expect that the application of an iron chelator would bring about an increase in FZ-3 fluorescence. Fluorescence is not affected at all upon dipyridyl application, neither in the cell body, nor in the hilus. Fluorescence is also not affected when dipyridyl and zinc/pyr are co-applied.

Another explanation why we don't appear to observe zinc increases in the cytoplasm could be that zinc is very tightly buffered in the cytoplasm, so tightly in fact that any zinc that enters the cell is immediately bound by proteins or molecules. One possible candidate for this regulatory protein or molecule could be MT, however, MTs are typically saturated with metals and it would be difficult to buffer that much zinc so quickly. Another possibility could be glutathione (GSH), a tri-peptide molecule that plays an important role in redox buffering in cells. Fluorescence cuvette experiments were conducted to understand the buffering capacity of GSH for zinc. Different zinc concentrations (10 nM, 30 nM, 100 nM, 300 nM, 1 μM, 3 μM, 10 μM, 30 μM and 100 μM) were added to 1 μM FZ-3 in a cuvette and fluorescence was observed over time. These zinc titrations were also carried out in the absence, and in the presence of 1 mM, 3 mM and 10 mM GSH. Fluorescence intensity in the absence and in the presence of 1mM, 3 mM and 10 mM GSH vs. log of zinc concentration is plotted in figure 35. It was found that in the absence of GSH fluorescence increases were observed with even as low as 30 nM zinc addition and anything larger than 1 μM is likely to induce a large fluorescence increase (figure 36 – black curve). As expected, the buffering capacity for zinc increases

with increasing concentration of GSH. These results suggest that GSH may be closely involved in buffering zinc tightly in the cytoplasm although this would depend on the concentration of reduced GSH at any given time. The exact zinc buffering capacity of GSH is hard to determine since the concentration of GSH in the cytoplasm is not known with certainty. Literature values for GSH range from 1 mM to 10 mM (Smith et al., 1996), and one could see in the light of our experiment that this broad range in concentration can make a huge difference on our data interpretation.

Citrate is another possible endogenous chelator for zinc, so we repeated the same cuvette experiments with 300 μM and 500 μM citrate and the fluorescence intensity vs. log of zinc concentration was plotted in figure 37. It was found that citrate does not buffer zinc much, which is possible in view of the fact that citrate is a weaker chelator for zinc than GSH.

Discussion

Zinc is a very important transition metal that is required for the proper function of many enzymes and proteins. Little is known however, about how zinc is transported and buffered not only from the extracellular space, but also within the cytoplasm and into cellular compartments. Zinc transporters have been identified, but little is known about the mechanism of zinc cellular transport and trafficking. Once inside the cell, does zinc bind to MTs, or GSH and remain in the cytoplasm, or is it shuttled immediately into cellular compartments?

Our data from the KCl stimulation experiment and the average initial values of the WT and KO mice suggests that exogenous zinc moves into both synaptic vesicles and vesicular compartments. There is no clear indication of how zinc passes from the cytoplasm into these compartments, although zinc has to first pass through the cytoplasm to reach them. It is possible that zinc is immediately bound to metalloproteins such as metallothionein upon crossing the cell membrane. The increase in zinc-protein complex

could then serve as a cellular signal for zinc transporters to pump zinc into vesicles or cellular compartments. This buffering of zinc is different than Ca^{2+} regulation where an increase in free cytosolic Ca^{2+} concentration acts as a cellular signal. The tight buffering of zinc could explain the lack of transient fluorescence increases in the cytoplasm. Another possibility could be that the dye is pumped out lowering its intracellular concentration. This is unlikely however as the pumping of the dye outside the cell takes many minutes and our experiments with DTDP applied shortly after FZ-3-AM loading (4 min) should exclude this possibility. Another explanation could be that these transient changes in zinc are so small that our probe is not sensitive enough to detect them.

Other experiments could be conducted such as immunocytochemical ones, where an antibody against FZ is used to specifically determine where the dye locates once it enters the cytoplasm, or FLIM experiments as the fluorescence lifetime of the dye measured in the cytoplasm or in other cellular compartments would be different due to a pH difference. Another experiment could be the addition of cyanide to slices to be able to visualize the zinc release in the cytoplasm as the cell is dying.

Conclusion

These experiments were an attempt to shed some light on zinc buffering and trafficking into the cell. Exogenously applied zinc in the presence of a zinc ionophore, induces a large and persistent increase in fluorescence signal indicating that zinc is transported to vesicles or cellular compartments. No transient elevations in fluorescence were found, which indicate that zinc is very tightly buffered in the cytoplasm.

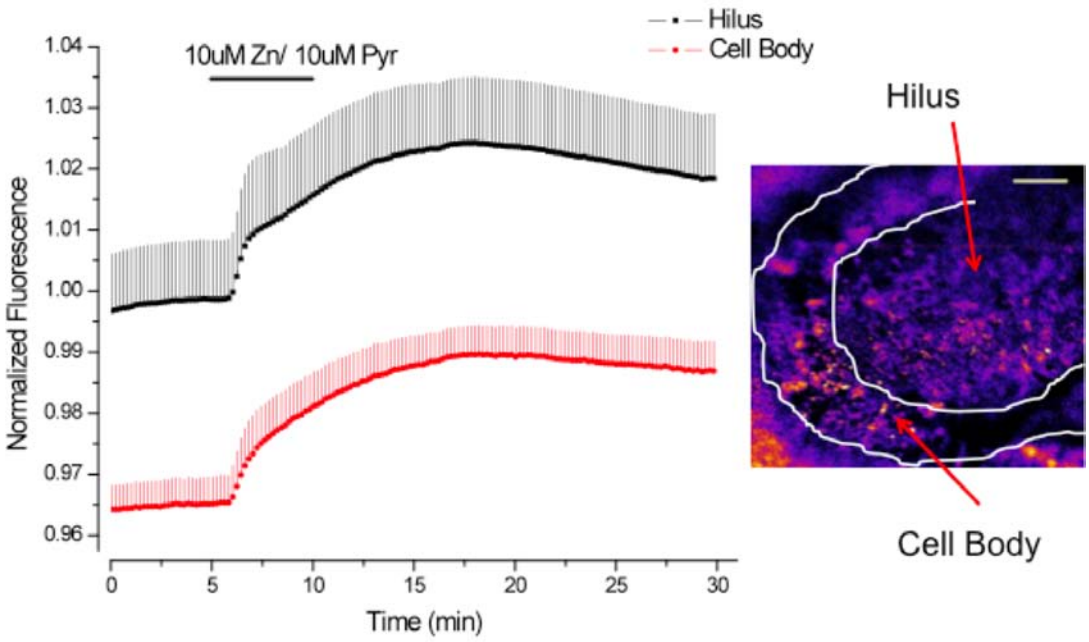

Figure 24. FZ-3-AM response of hippocampal slices to application of zinc/pyr

---

Note: Black curve represents the fluorescence in the hilus, whereas the red curve that in the cell body. The horizontal line represents the time and duration of zinc/pyr application followed by normal saline wash. Error given as SEM n=5. Inset is a difference image of a hippocampal slice treated with zinc/pyr. Image is the difference between the image with the maximal increase in fluorescence and the image just before the zinc/pyr was added. The arrows point to the hilus (synaptic terminal area) and the cell body layer. Scale bar is 50 μm.

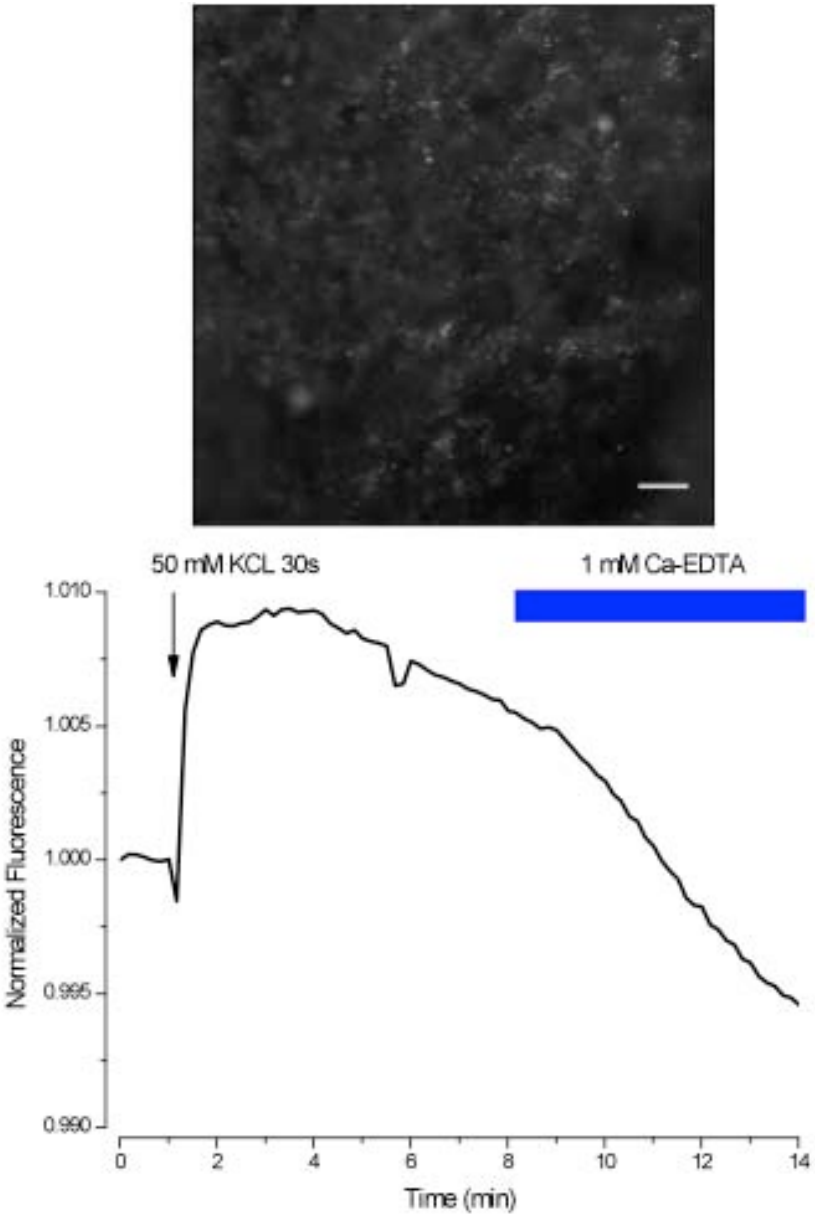

Figure 25. Fluorescence response of an FZ-3-AM slice after 50 mM KCl stimulation, wash and 1 mM CaEDTA addition

---

Note: Arrow indicates the time of KCl addition, which was applied for 30 s. The slice was then washed with saline till the application of CaEDTA. The blue bar indicates the time and duration of CaEDTA application. The raw image represents the punctuated fluorescence seen in FZ-3-AM loaded slices indicating that the dye is getting into synaptic vesicles. Scale bar is 20 μm.

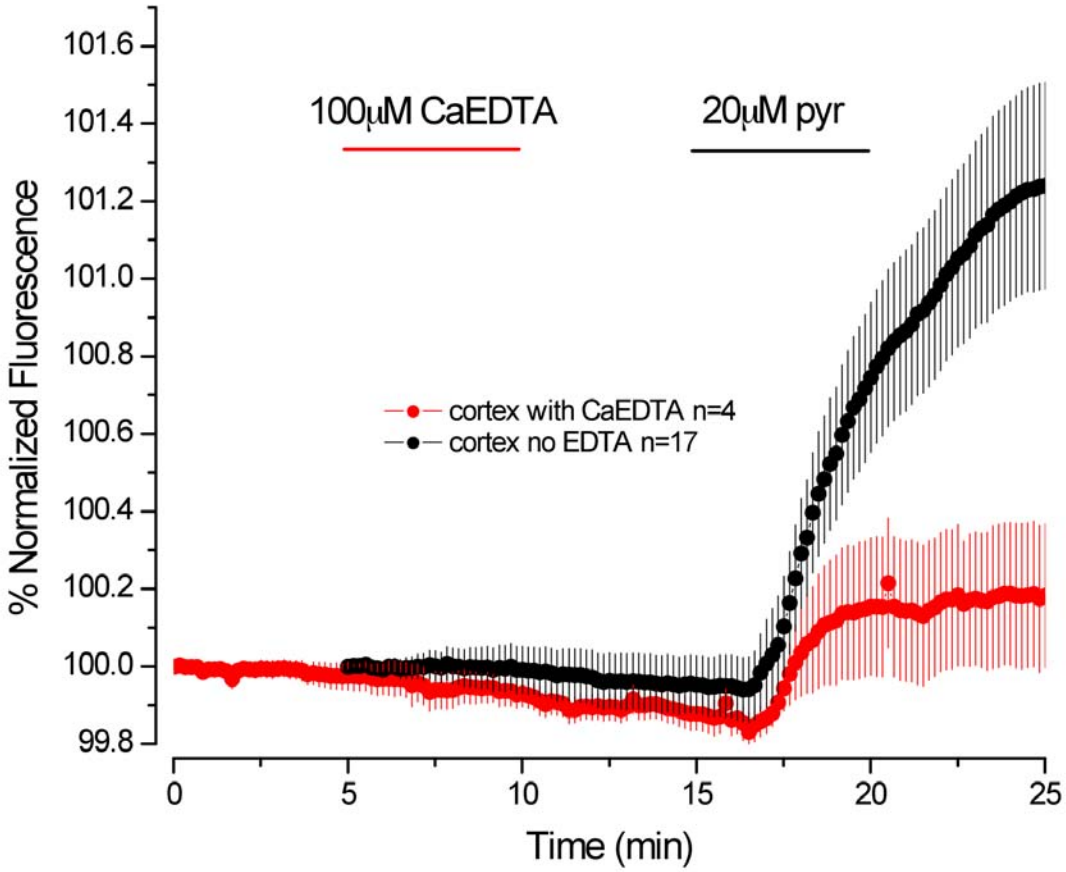

Figure 26. Fluorescence response of FZ-3-AM slices to pyr addition in the absence of CaEDTA or after CaEDTA treatment

---

Note: Black curve represents the fluorescence of slices after pyr application without prior CaEDTA treatment. The red curve represents the response to pyr application after slices were treated with 100 μM CaEDTA for 5 min and then washed with saline for 5 min. The horizontal lines indicate the time and duration of CaEDTA and pyr application. Error is given as SEM.

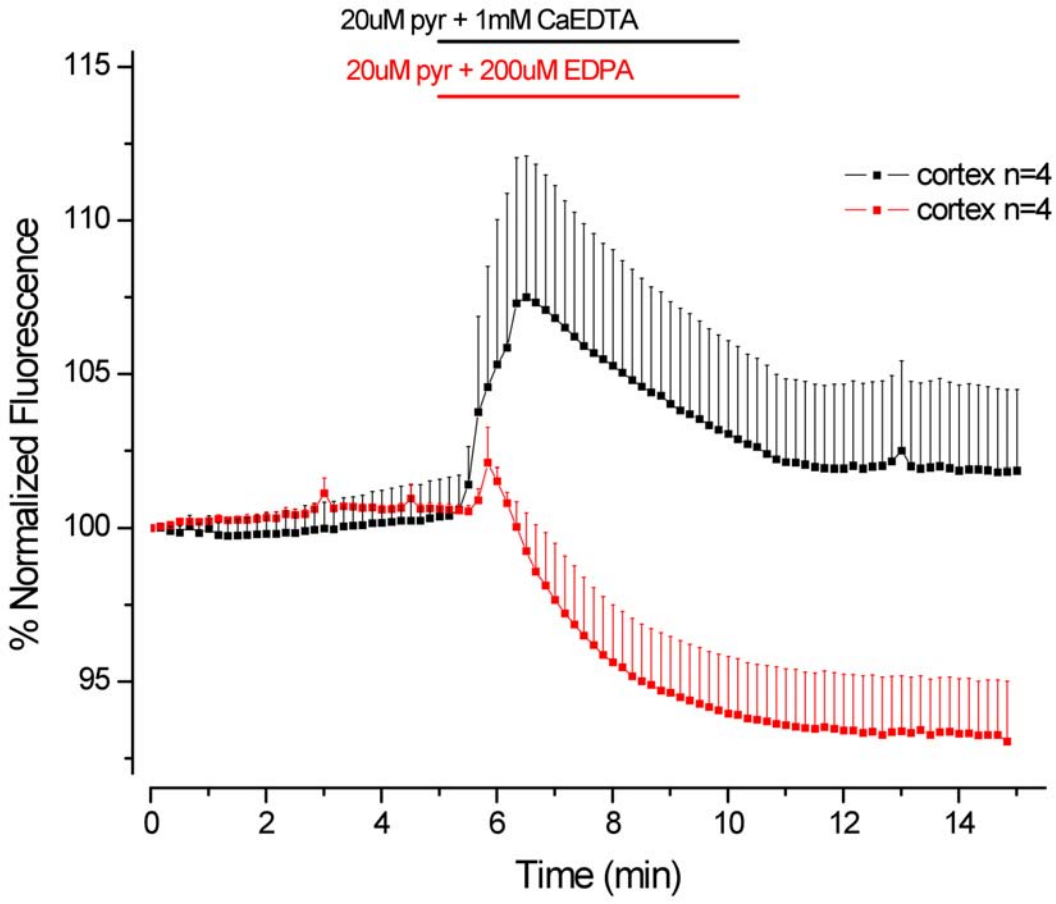

Figure 27. Fluorescence response of FZ-3-AM slices to simultaneous application of pyr with either CaEDTA or EDPA

Note: Black curve represents the fluorescence response to pyr and CaEDTA co-application and red curve represents the response to pyr and EDPA co-application. The horizontal lines indicate the time and duration of the application, which was followed by saline wash. Error is given as SEM.

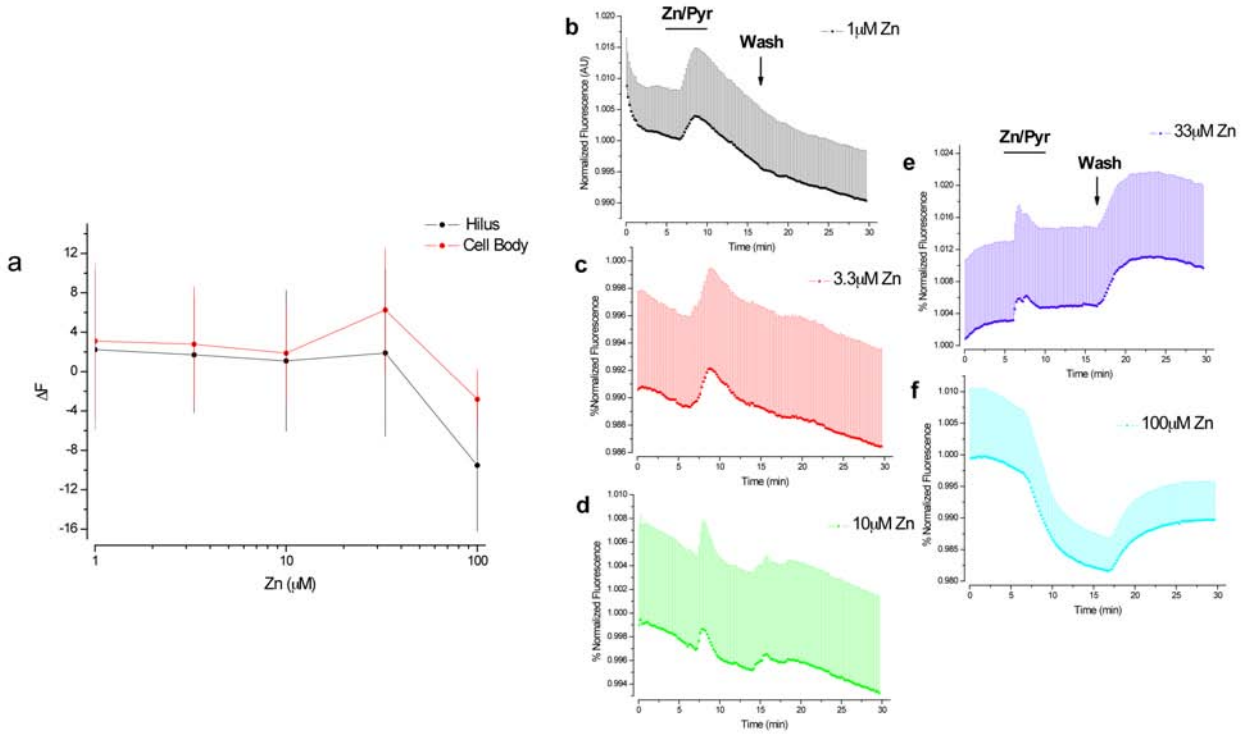

Figure 28. Fluorescence response to varying zinc and pyr concentrations in a 2:1 ratio

---

Note: Figure 28a represents the change in maximal fluorescence with zinc concentration for both hilus and cell body. Figures 28b-f represents fluorescence response of slices to varying zinc/pyr application (1, 3.3, 10, 30 and 100 μM zinc and 2, 6.6, 20, 60 and 200 μM pyr). Error is given as SEM n=5.

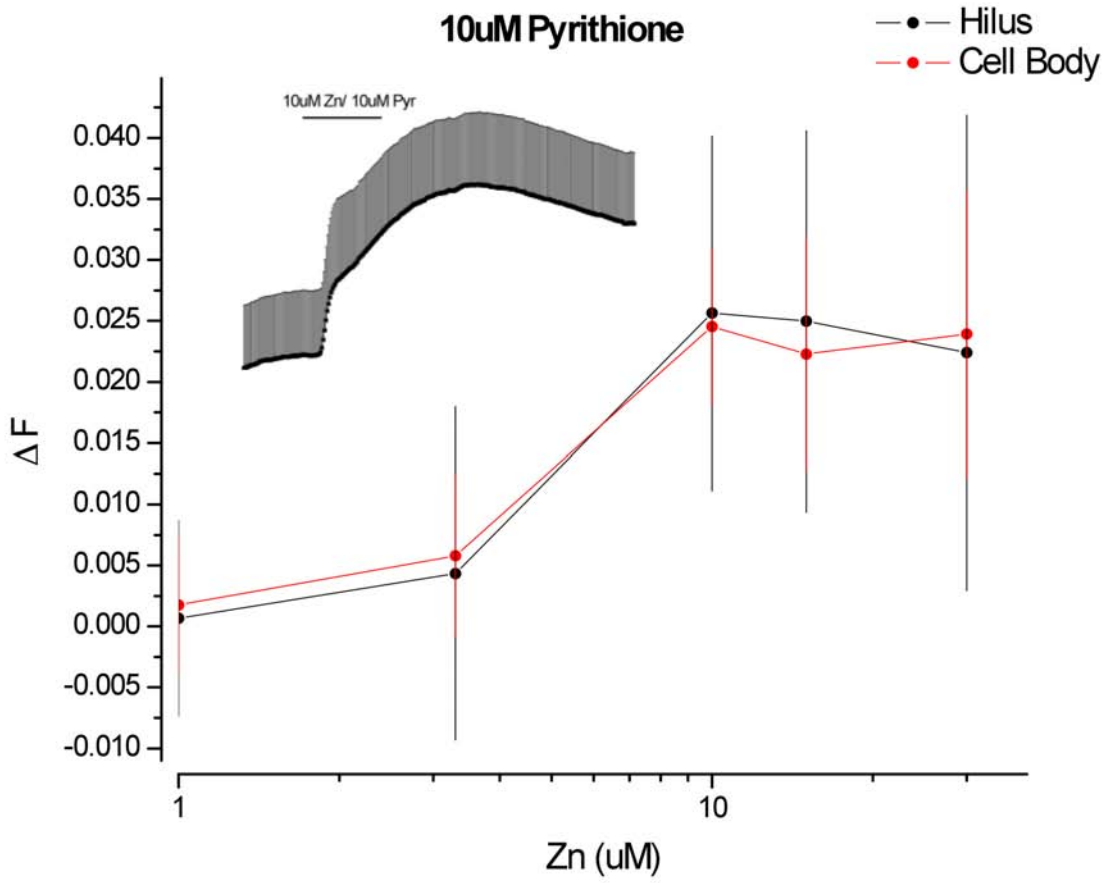

Figure 29. Change in fluorescence vs. zinc concentration at 10 μM pyr concentration

---

Note: Change in maximal fluorescence vs. zinc concentration for both hilus (black circles) and cell body (red circles) with 10 μM pyr application and varying zinc concentrations (1, 3, 10, 15 and 30 μM). The inset represents the typical fluorescence vs. time response observed with all the zinc concentrations in both hilus and cell body.

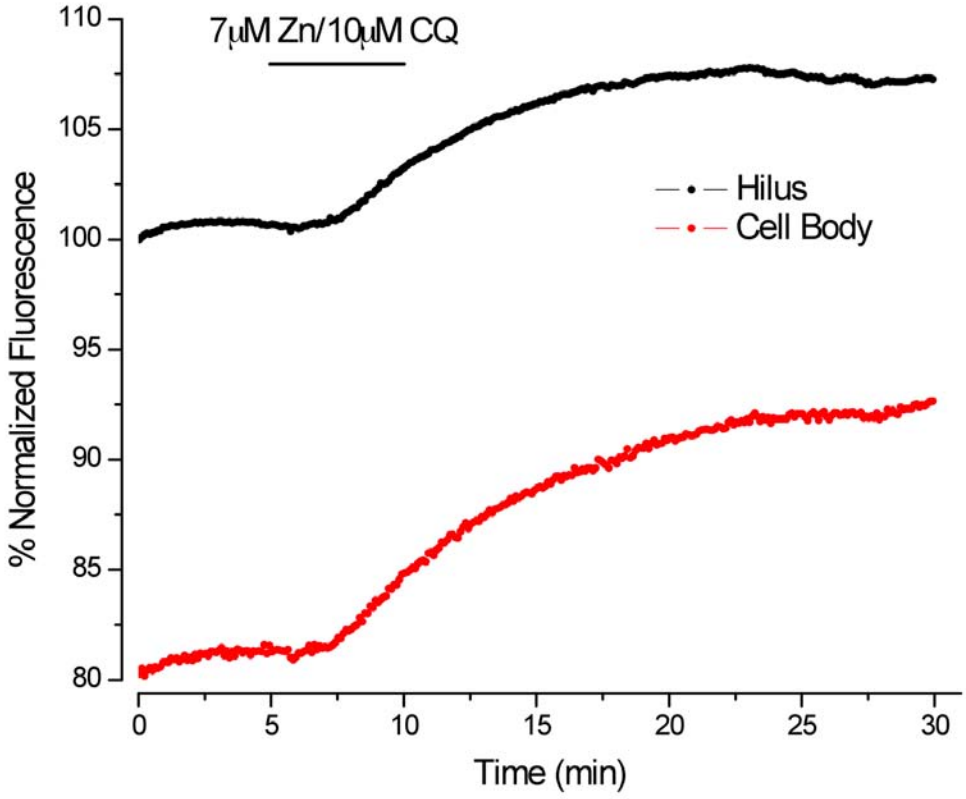

Figure 30. Fluorescence response of FZ-3-AM slices after zinc/CQ application

---

Note: 7 μM zinc and 10 μM CQ were co-applied to slices loaded with FZ-3-AM. Bar indicates the time and duration of zinc/CQ application.

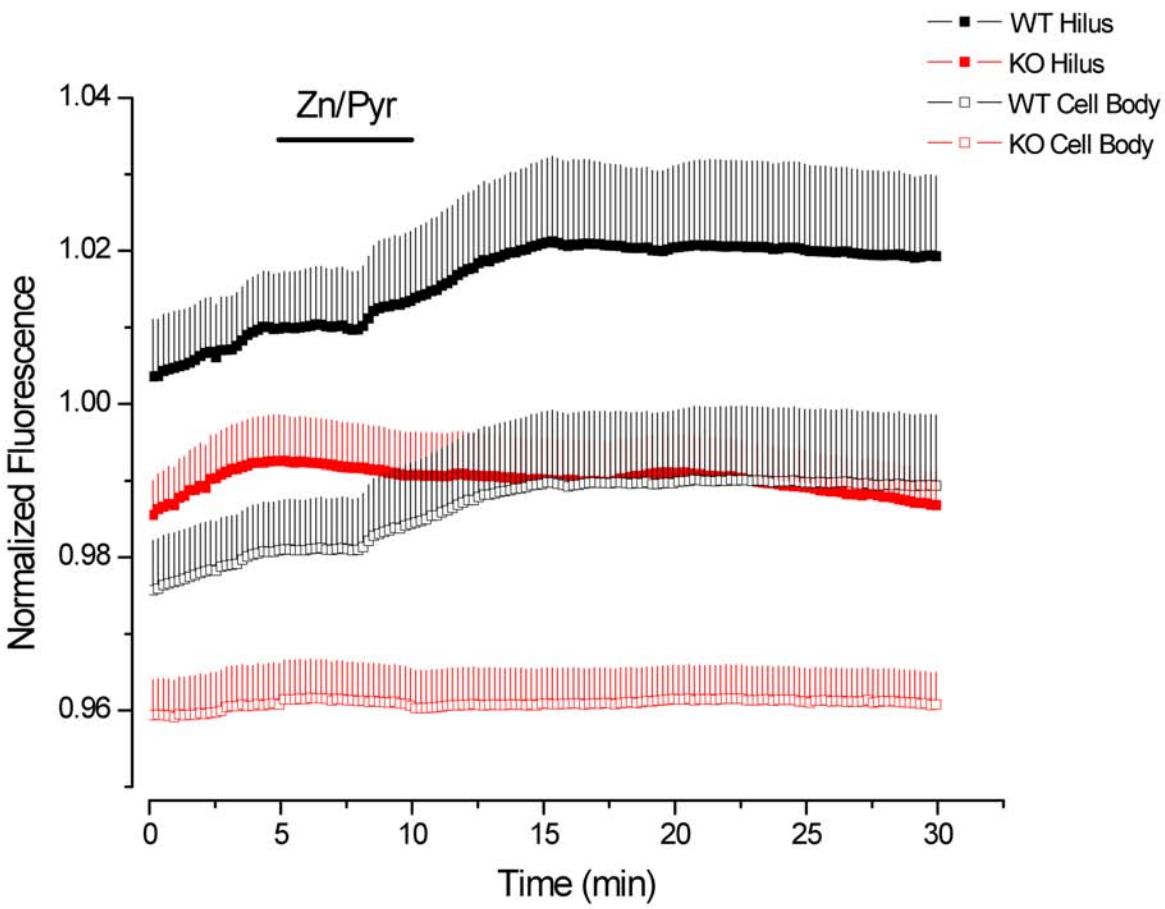

Figure 31. Fluorescence response of WT and KO mice to zinc/pyr application

---

Note: Black squares represent fluorescence in WT hilus (filled) and cell body (open). Red squares represent fluorescence in KO hilus (filled) and cell body (open). The bar represents the zinc/pyr application time, which was followed by saline wash. All data was normalized to the average of the first value of the WT hilus. Error is given as SEM n=5.

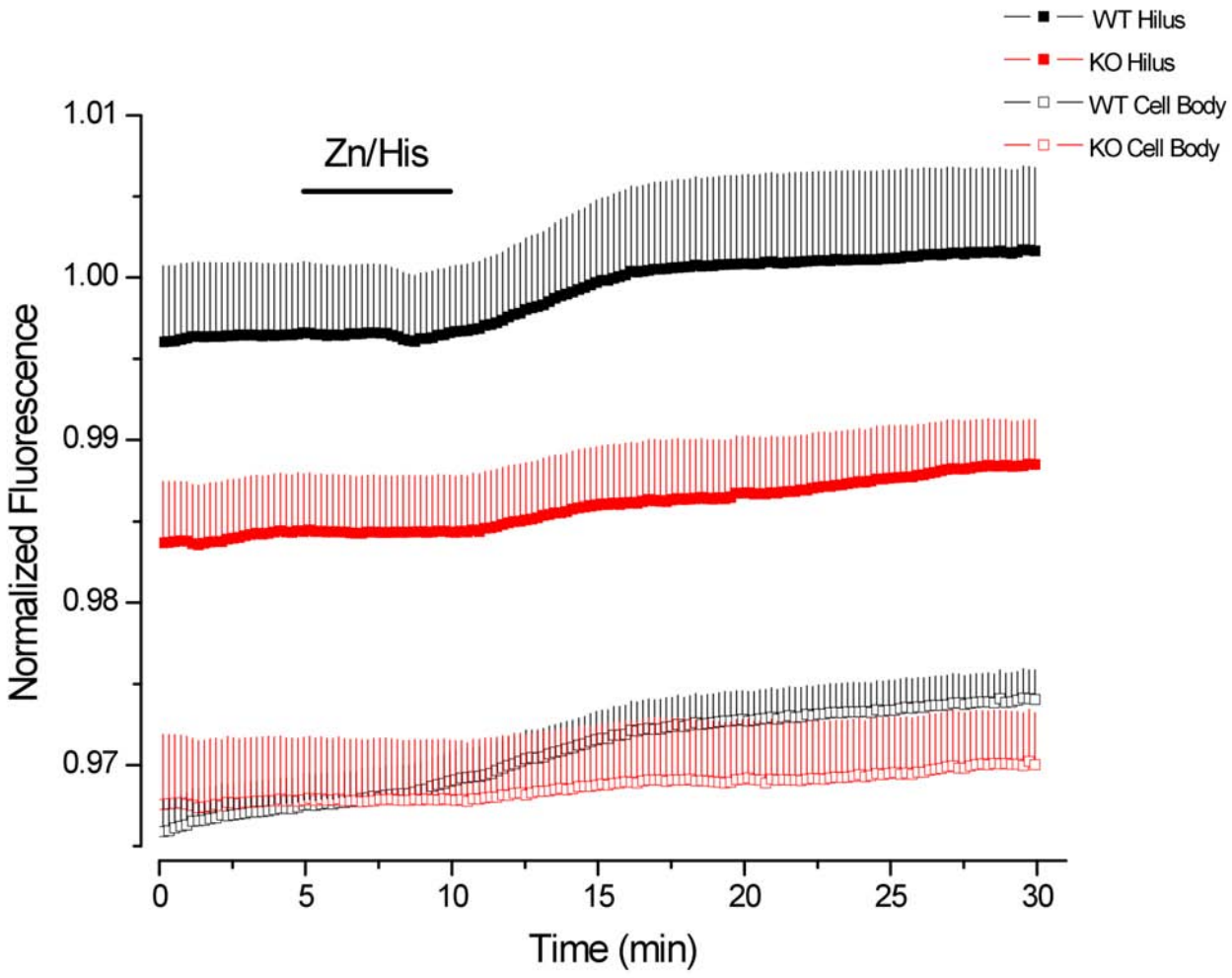

Figure 32. Fluorescence response of WT and KO mice to zinc/his application

---

Note: Black squares represent fluorescence in WT hilus (filled) and cell body (open). Red squares represent fluorescence in KO hilus (filled) and cell body (open). The bar represents the zinc/his application time, which was followed by saline wash. All data was normalized to the average of the first value of the WT hilus. Error is given as SEM n=5.

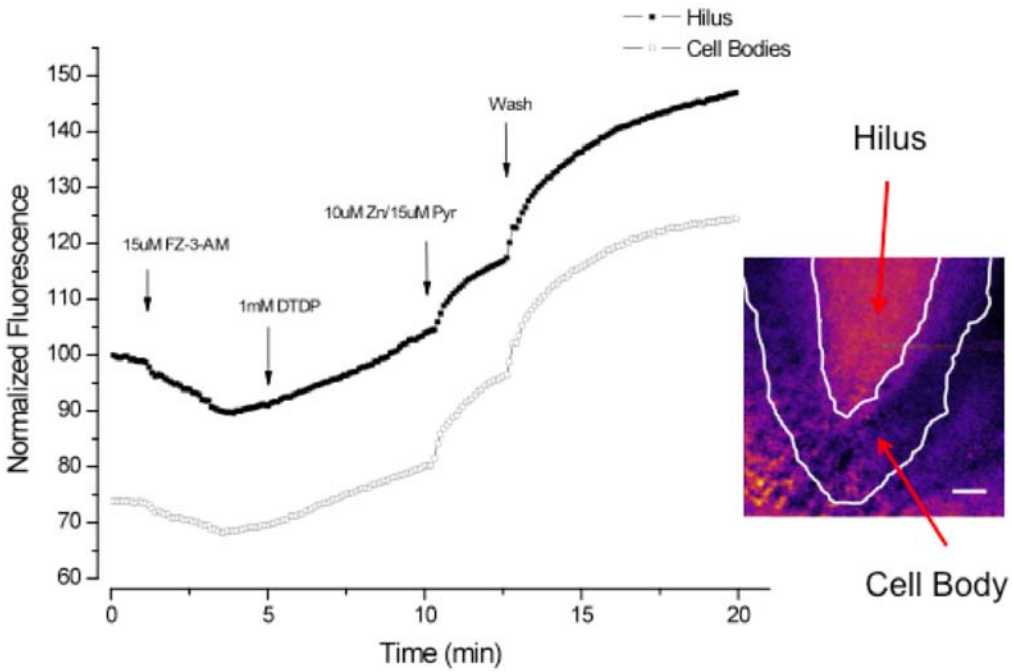

Figure 33. Fluorescence response of slices to the oxidizing agent dithiodipyridyl (DTDP)

Note: 15 μM FZ-3-AM was added to unstained slices at 30 s and allowed to diffuse into the slice. 1 mM DTDP was added at min 5 followed by zinc/pyr at min 10. Filled squares represent the hilus and open squares represent the cell bodies. The inset is a difference between the image at the end of DTDP addition with the image right before DTDP application. The scale bar is 50 μm.

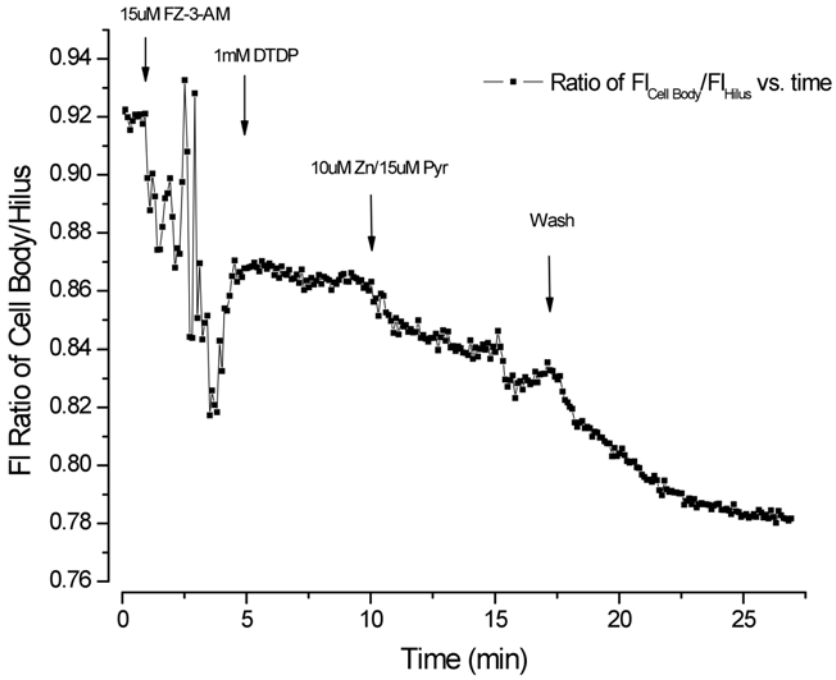

Figure 34. Fluorescence ratio between the cell body and hilus treated with DTDP

Note: Graph represents the ratio between the fluorescence of the cell body over the hilus from figure 33. If transient changes in cell body fluorescence after DTDP addition were to occur it would be easily revealed as a ratio between the cell body and hilus. The ratio is constant over the DTDP application.

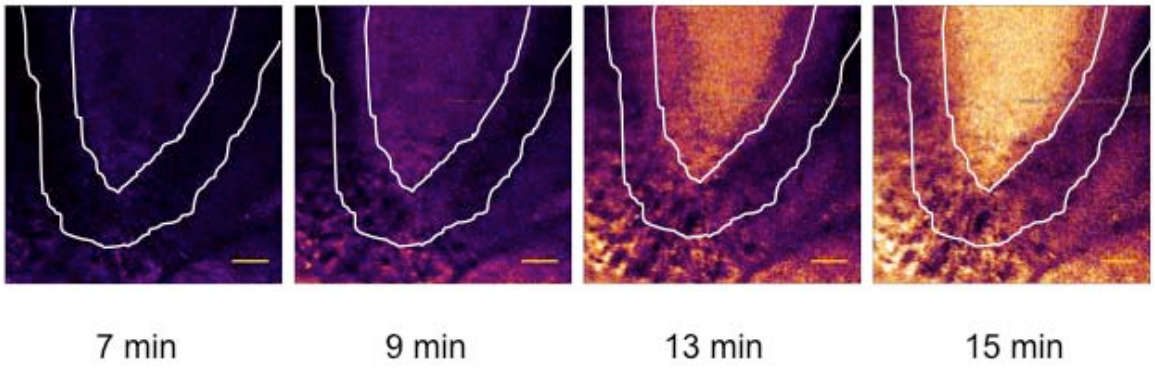

Figure 35. An image sequence of a slice during DTDP addition

Note: The sequence was obtained by subtracting the image right before DTDP was added from the rest of the images collected during DTDP application. No sharp elevations in the cell body layer are observed. Scale bar is 50 μm.

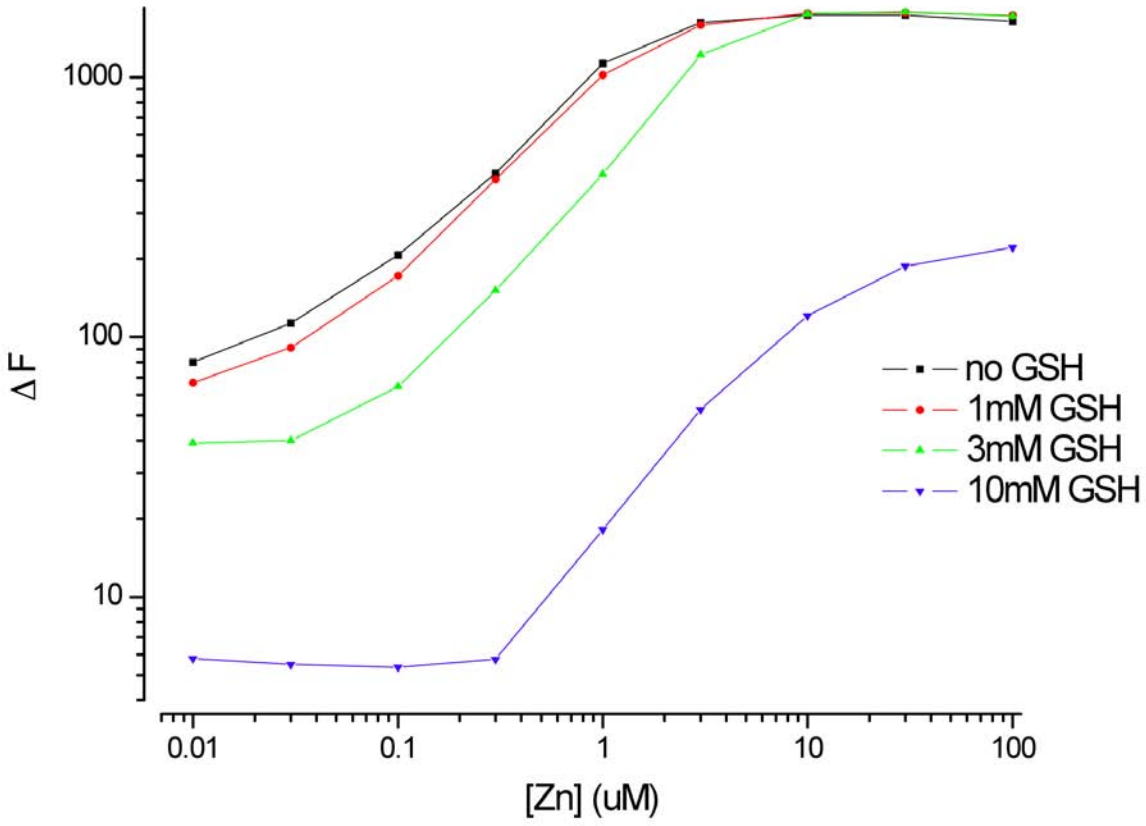

Figure 36. Change in FZ-3 fluorescence with increasing zinc concentration in the absence and presence of GSH

Note: Black line – no GSH, red line – 1 mM GSH, green line – 3 mM GSH and blue line – 10 mM GSH. 10 mM GSH has the largest zinc buffering capacity followed by 3 mM.

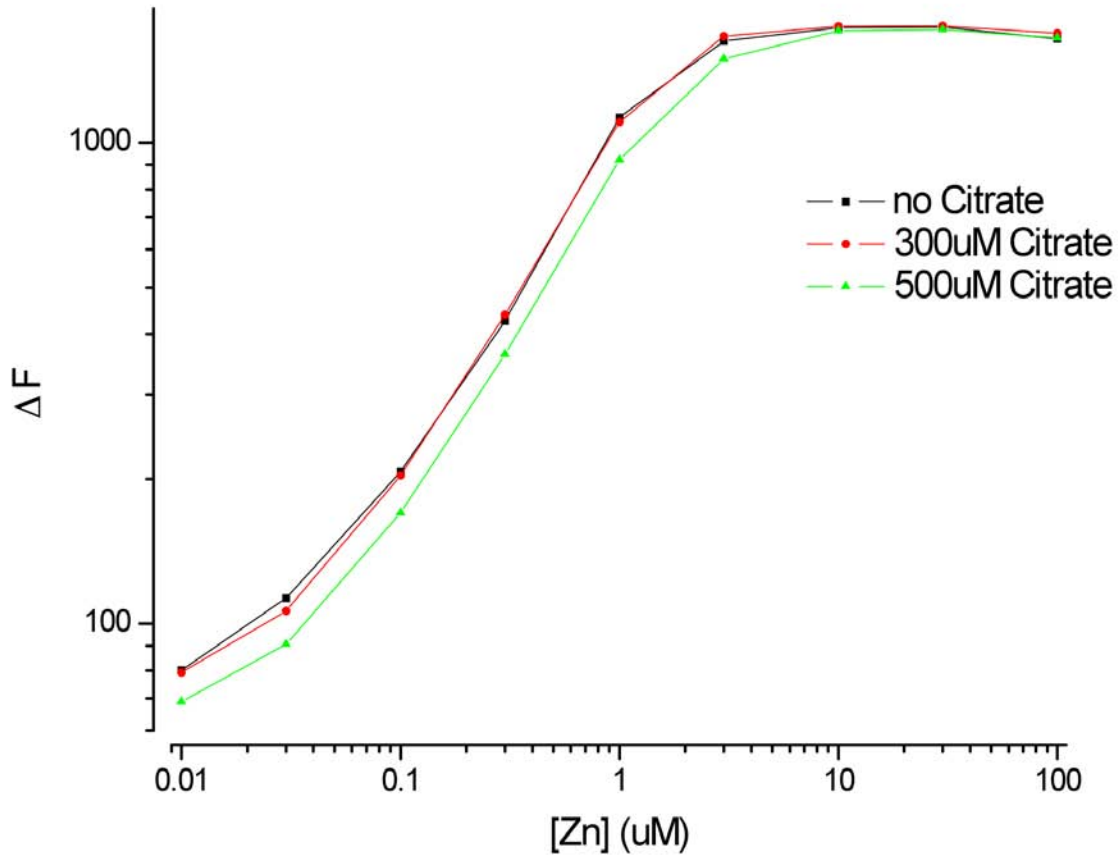

Figure 37. Change in fluorescence vs. zinc concentration in the absence and presence of Citrate

---

Note: Black line – no citrate, red line –300 μM citrate and green line – 500 μM citrate. Citrate (in neither concentration) seems to buffer zinc very well.

Table 1. A comparison of the average initial fluorescence values in the hilus and cell bodies of hippocampal slices of WT and KO mice

	WT (n=19)	**KO** (n=20)
	Average ± SEM	
Cell Body	562 ± 2	558 ± 2
Hilus	579 ± 3	568 ± 2

CHAPTER VI.
TESTING THE ZINC-RELEASE HYPOTHESIS WITH ZINC-SELECTIVE FLUORESCENT PROBES

Introduction

As mentioned in chapter 2, chelatable zinc is found at high concentrations in about 50% of glutamatergic pathways in the mammalian forebrain (Frederickson, 1989; Frederickson et al., 1990; Frederickson and Moncrieff, 1994; Kay, 2006; Kay et al., 2006; Kay and Toth, 2006, 2008). Other neurotransmitters that are co-packaged with zinc exist and include glycine and γ-aminobutyric acid or GABA (Frederickson et al., 2005). Zinc containing glycinergic vesicles are mostly localized in the nervous system (spinal cord), while GABA/zinc neurons are found both in the spinal cord and the cerebellum (Birinyi et al., 2001; Danscher and Stoltenberg, 2005; Wang et al., 2002; Wang et al., 2001). Since zinc is mostly co-packaged with glutamate in synaptic vesicles, it has been postulated that zinc may be involved in glutamatergic neurotransmission, packaging and even act as a neuromodulator, regulating the post-synaptic response of glutamate (Frederickson et al., 1990). To act as a modulator, zinc has to be released in the synaptic cleft along with glutamate and bind to receptors in the post-synaptic cell, or diffuse through ion channels. This is known as the zinc release hypothesis. While it has been shown that zinc modulates post-synaptic receptors and voltage- and ligand-gated ion channels (Harrison and Gibbons, 1994; Smart et al., 1994) if applied exogenously, reports about the release of zinc from synaptic vesicles are inconclusive. The first reports of zinc release were published back to back in 1984 (Assaf and Chung, 1984; Howell et al., 1984) and apparently confirmed in other studies (Budde et al., 1997; Charton et al., 1985; Li et al., 2001a; Li et al., 2001b).

Most of the work on synaptic zinc has focused on the theory that zinc is completely released in the synaptic cleft during stimulation. This is known as the phasic

mode of release where zinc, once released is free to diffuse in the synaptic cleft and modulate pre- and/or post-synaptic receptors or ion channels (Kay and Toth, 2008). Concentrations of released zinc in the synaptic cleft are expected to be transient and would depend on how quickly zinc is cleared off the synaptic cleft. Another alternative to the phasic release mode that has been proposed is the tonic mode during which, a very small fraction of the total synaptic zinc is actually released in the extracellular medium (Kay and Toth, 2008). Under these conditions, zinc is not free to move out into the extracellular space, but is probably coordinated to certain molecules or proteins in the synaptic vesicle and remains so after vesicle fusion as well. Zinc would then be externalized and become part of what has been termed "the zinc veneer" (Kay, 2003). A molecule in the synaptic cleft may bind to zinc and form a ternary complex, become internalized and thus act as a possible retrograde messenger for the pre-synaptic cell (Kay, 2006; Kay et al., 2006; Kay and Toth, 2006, 2008). Previous work in our lab with zinc-selective fluorescent probes, has suggested that zinc might perhaps not be released into the extracellular medium. The purpose of this work was to use the zinc-selective dye ZnAF-2, to determine whether zinc is released during synaptic stimulation.

Results

In light of the two zinc release models and based on the results of our experiments we hypothesize that zinc is not being freely released in the extracellular space during the course of synaptic transmission, instead zinc is externalized while still coordinated as a ternary complex with a molecule not yet identified in the vesicular membrane. We also hypothesize that during synaptic transmission the vesicular zinc transporter ZnT3, gets activated and begins stocking synaptic vesicles with zinc. We observed that during synaptic stimulation, the fluorescence signal of the membrane permeable dye ZnAF-2 increased sharply and then remained elevated for minutes after the stimulus is removed, failing to drop below control levels even after 28 min of continuous washing with normal

saline (figure 38a – black curve). These observations do not support the classic zinc release hypothesis, which suggests that zinc is fully released (phasic release) into the extracellular medium, instead they suggest that zinc is externalized when synaptic vesicles fuse, but remains bound to a membrane protein in the form of a ternary complex. If these observations, upon further examination indicate that zinc indeed is just externalized and not fully released, then the role of zinc during synaptic transmission needs to be revisited as well. Therefore, the goal of the experiments presented in this work was two-fold; first, to understand why fluorescence increased upon stimulation and second why fluorescence intensity does not fall below control levels. To study zinc release during stimulation, we utilized zinc-selective fluorescent probes, which become fluorescent only upon zinc binding. Assuming that the zinc release hypothesis is true, two different fluorescent signals can be obtained using zinc-selective fluorescent probes depending on the location of the probe (see figure 39c – adapted from (Kay, 2006)). When using a membrane permeable dye the fluorescence signal should start out high as the dye is already bound to the chelatable zinc within the synaptic vesicles. After vesicles fuse to the cell membrane, if zinc is being fully released together with the dye, the signal should drop quickly below control levels, since the slice is being continually washed with saline solution and the probe-dye complex diffuses away. A membrane impermeable dye can enter neither the cell, nor the synaptic vesicles being localized extracellularly. If extracellular zinc levels are low, the dye should be in the zinc-free form and its fluorescence should start out low. During stimulation however, zinc becomes available for probe binding due to vesicle fusion to the cell membrane and as a consequence the signal should increase quickly and then drop to initial values as the probe-zinc complex diffuses away.

We used 50 mM KCl for 30 s (figure 38a – black curve) to stimulate slices of rat hippocampus that were loaded with 10 μM ZnAF-2 (for procedure refer to chapter 3). The saline flow was stopped for the addition of KCl while the solution was stirred and

oxygenated by a stream of oxygen. The saline flow was then resumed and slices were washed continuously for the remainder of the experiment. The fluorescent signal did not however, behave as expected. ZnAF-2 is a membrane permeable dye (Kay and Toth, 2006), thus under the zinc release hypothesis its fluorescence should show a monotonic decrease. This is not what was observed however, as ZnAF-2 fluorescence increased upon stimulation and never fell below control levels (figure 38a – red curve). This behavior is not consistent with the phasic release of zinc from synaptic vesicles predicted by the zinc release hypothesis for two reasons; one, fluorescence should not initially increase upon KCl stimulation and two, fluorescence should drop below control levels due to diffusion of the zinc-probe complex. We obtained similar results with other membrane permeable dyes such as ZP1 (figure 44a – red curve) and Zinquin.

One could argue that 50 mM KCl causes a large stimulation and is also unnatural compared to physiological stimulation so the increase in fluorescence might not be observed during the normal course of stimulation. To see if this was indeed the case, stimulation experiments were conducted by using electrical stimulation (500 pulses at 100 Hz) instead and we observed the same increase in fluorescence (figure 40c). This increase is smaller, which is consistent with the fact that the slice is only stimulated locally vs. whole slice stimulation with KCl. Fluorescence levels still remain elevated, even with continuous washing similar to that observed with KCl stimulated slices. The same phenomenon is also observed with 500 mM Sucrose stimulation (see figure 40d), which is a widely used technique for eliciting synaptic release.

Since 50 mM KCl might be considered a little too high of a concentration for slice stimulation and might damage the slices, we also decided to use a smaller amount of KCl (15 mM) for slice stimulation. The response is the same as with higher K^+ stimulation although the amplitude of the fluorescence increase is smaller (6.35) than that of 50 mM KCl (10.65). Fluorescence levels however, do not drop below control. We also tried to perfuse slices with elevated KCl instead of stopping the flow. The problem with this

approach was that perfusing required higher amounts of KCl (100 mM KCl for 45 s) to achieve stimulation due to the dilution of KCl as it moves through the chamber.

To ascertain if 50 mM KCl was damaging the slices multiple stimulations on the same slice were performed and the time between stimulations was varied (figure 41). Re-stimulation of the slice as low as 15 min after first stimulation (black curve – figure 41) elicited the persistent fluorescence response, albeit smaller, than what was previously observed, indicating that the slice is not irreparably damaged, even though it needs some time to recover.

This persistent ZnAF-2 fluorescence increase is very puzzling in light of the location of the probe, so we set out to understand the phenomenon behind it. Our working hypothesis was that zinc in synaptic vesicles is not entirely free, but it exists in a coordinated form together with a membrane protein or another molecule and little if any is released during stimulation. This zinc is however externalized during stimulation and can still interact with molecules in the extracellular space (including chelators). If zinc is indeed released in the course of stimulation, then applying an extracellular chelator should strip the zinc off and cause the dye fluorescence to drop. To test this hypothesis we used the extracellular chelator, EDPA. EDPA has a lower affinity for zinc as compared to EDTA, but it also binds calcium and magnesium less tightly than EDTA therefore it binds zinc faster. 1 mM EDPA was first applied to unstimulated slices loaded with ZnAF-2 (red curve in figure 42a and 42b). There seems to be a little delay in the EDPA response, but fluorescence levels fall below control levels to about 55% of initial fluorescence. This is in agreement with previous findings (Kay, 2003) that there seems to be a layer of chelatable extracellular zinc, previously christened “the zinc veneer”. EDPA is able to strip off the zinc veneer and fluorescence levels drop below those of control.

To see if the zinc veneer is being increased during stimulation by an increase in externalized zinc, we varied the timing of EDPA application with respect to KCl stimulation. If the zinc veneer does increase after KCl stimulation due to more zinc

becoming externalized, then adding EDPA after slices have been stimulated should lower the fluorescence more than just EDPA alone. KCl (50 mM) was applied for 30 s and then the slice was washed with normal saline for 3 min and 30 s. EDPA was then applied to the extracellular medium for the remainder of the experiment. If the veneer is somehow increased during stimulation, then the application of EDPA after stimulation should in fact strip off more zinc and the level of fluorescence should drop below that of EDPA application alone. This is not the case, however as the levels of fluorescence in both cases are the same (figure 42a – black and red curves). There can be several explanations for this; one being that the level of externalized zinc compared to the total fluorescence is so small that we are not able to distinguish it from biological noise level. Another explanation could be that EDPA is only able to strip the zinc veneer and not the zinc that is externalized during synaptic stimulation. However, this could not be the case since during simultaneous application of KCl and EDPA the large fluorescence peak is eliminated, suggesting that the externalized zinc from the vesicles is being stripped from the dye (since EDPA does not interact with the dye itself). Another possibility is that the ZnT3 transporter is somehow activated and is stocking the vesicles with zinc as fast as zinc is being chelated, keeping the zinc level at steady state (EDPA chelates the same amount of zinc whether the slices are stimulated or not). An interesting implication of this conclusion is that ZnAF-2 dye has to be recycled from the cytoplasm to these vesicles as well, so that the final fluorescence remains steady.

If KCl and EDPA are applied together then EDPA should be able to strip off the externalized zinc more easily. The concurrent application of EDPA and KCl all but got rid of the high fluorescence increase observed after KCl stimulation (red curve – figure 42b). As KCl stimulation occurs, fluorescence starts to increase and as soon as the vesicles start to fuse to the membrane, EDPA strips the zinc right off the dye, preventing the increase in fluorescence that is typically observed (see inset in figure 42b). Final fluorescence levels however, do not fall below those of EDPA alone. The fluorescence

seems to decay faster than EDPA alone suggesting that KCl stimulation somehow facilitates the stripping of zinc by EDPA.

This phenomenon differs somewhat in younger animals (14-18 days old) (figure 38b). While the increase in fluorescence due to KCl stimulation is similar (black curve – figure 37b) to older animals (21-35 days old), the response to EDPA application is slightly different. When 1 mM EDPA is applied after KCl stimulation and wash (red curve – figure 38b), fluorescence does not fall below control levels (blue curve – figure 38b). This suggests that the zinc veneer is not as large in younger animals compared to older ones. Application of EDPA before stimulation occurs seems to limit the increase in initial fluorescence, but once again does not bring fluorescence below control levels.

What happens to the fluorescence after multiple KCl stimulations of the same slice? To determine if the synaptic zinc is exhausted from multiple stimulations, we first stimulated slices 10 times with 50 mM KCl for 30 s each time and 5 min wash in between. The KCl solution also contained 1 mM of EDPA. Slices were held in a holding chamber fitted with netting on the bottom and submerged in 10 mL solution continually bubbled with O_2. We performed two different controls; one where we stimulated the slices with KCl 10 times, but without EDPA in solution and second a normal saline solution without KCl and without EDPA. The control slices were submitted to the same procedure in normal saline solution at the same time as the KCl/EDPA stimulated slices were being moved from the KCl/EDPA chamber to the wash chamber and vice versa. After the multiple stimulations, the slices were stained with ZnAF-2 for 30 min and stimulated once more with KCl for 30 s and an image sequence was collected. The average initial fluorescence value for the slices that were stimulated multiple times in the presence of EDPA was lower than that of control slices (either stimulated with no EDPA, or not stimulated at all – see table 2). This strongly indicates that zinc is not released in the extracellular medium, since the fluorescence value for slices that were stimulated in the absence of EDPA is not statistically different than the value for the unstimulated

slices. The fluorescence value for slices that were stimulated in the presence of EDPA is statistically different than the value for unstimulated slices, suggesting that EDPA is stripping the externalized zinc as the vesicles are fusing to the membrane.

We observed another interesting phenomenon after the multiple stimulations. Slices that had been subjected to multiple KCl stimulations in the presence of EDPA and then stained and re-stimulated, exhibited an increase in fluorescence that was almost 3 times (red filled squares – figure 43) the normal increase in fluorescence that we had previously observed (black open squares – figure 43). There was no difference in the fluorescence increase that was observed from slices that were stimulated multiple times in the absence of EDPA and the normal stimulation that had been previously observed (black open squares and blue filled squares – figure 43).

To differentiate whether this priming of vesicles is due to the chelation of the zinc from the veneer or the externalization, the following experiment was performed. Slices were placed in solution that contained 1 mM EDTA and no KCl for 30 s and then washed for 5 min in saline solution that also contained the same amount of EDTA. The slices were then stained with ZnAF-2 followed by KCl application. The fluorescence increase after KCl stimulation was only slightly lower than after 10 stimulations in EDPA (red open squares and red filled squares – figure 43). This suggests that removing the zinc veneer somehow causes a priming of slices for a large synaptic vesicle release. The difference between the increase observed with EDTA vs. EDPA could arise from the fact that since EDPA was co-applied with KCl is able to remove both the zinc veneer and the externalized zinc, suggesting that the removal of both the veneer and the externalized zinc is important in priming vesicles for release. The fact that removing only the zinc veneer gives rise to almost the same large fluorescence as removing both the veneer and externalized zinc could speak to the importance of the veneer in priming for vesicle release. The fluorescence observed could also be proportional to the amount of zinc that corresponds to the veneer vs. the externalized zinc (the fraction of externalized zinc is

much smaller than the zinc veneer so the fluorescence increase due to stripping of the externalized zinc is smaller than that observed from stripping the zinc veneer). The next step was to determine the minimum CaEDTA application time needed to induce this large increase in fluorescence. Slices were perfused with saline solution containing 1 mM EDTA for 15, 30 and 45 min, washed for two min and then stimulated with KCl. The large increase in fluorescence was observed with as low as 15 min of EDTA application time (black curve – figure 44) with the highest increase occurring at 30 min of application time (red curve vs. black and green curves– figure 44).

The pH within synaptic vesicles is around 5.5 and is rapidly alkalinized to pH 7.4, upon fusion with the plasma membrane. Fluorescence of the zinc – ZnAF-2 complex increases by a factor of ~7 when it is subjected to a similar change in pH (Hirano et al., 2000) and could account for the large increase in fluorescence that is observed upon KCl stimulation. To determine how much of the fluorescence increase observed after KCl stimulation is due to the large change in pH that vesicles undergo, NH_4Cl was used to alter vesicular pH before KCl addition. If the fluorescence change observed upon stimulation is due solely to the change in vesicular pH, then perfusing the slices with NH_4Cl should increase the fluorescence until the pH levels reach about 7.4 (zinc-ZnAF-2 fluorescence is almost constant at pH>7) and any additional fluorescence increase after KCl addition should be eliminated.

ZnAF-2 loaded slices were perfused with saline that contained 50 mM NH_4Cl for the duration of the experiment. After slices were pre-treated for 4 min with NH_4Cl, 50mM KCl was applied for 30 s and then saline wash (containing NH_4Cl) was resumed. The fluorescence increased upon NH_4Cl perfusion, however when KCl is applied there is another increase (red curve – figure 45a), indicating that the large fluorescence increase that is observed when the slice is stimulated is not completely due to the change in pH. An alternate explanation however could be that 4 min of NH_4Cl application prior to KCl stimulation is not enough time to fully change the vesicular pH from 5.5 to 7.4.

To see if a longer application time with NH_4Cl would completely get rid of the fluorescence increase after KCl application to NH_4Cl treated slices, we applied 50 mM NH_4Cl for 30 min and then applied KCl for 30 s (black curve – figure 45b). The treatment of slices with NH_4Cl for 30 min leads to a reduction of fluorescence observed after KCl stimulation, however fluorescence remains consistently higher than in control slices. This result indicates that NH_4Cl application may be partly responsible for the initial increase in fluorescence observed after stimulation, however is not responsible for the continued elevation of fluorescence since ZnAF-2 fluorescence is almost constant above pH 7.5. This NH_4Cl application time however, might be a little too long and inhibit slice stimulation altogether (as simultaneous electrical recordings show the disappearance of fEPSPs).

To determine if the peak of the fluorescence increase after KCl stimulation is only due to the vesicular pH change, we performed the same stimulation experiments with a different fluorescent dye, ZP1. If the persistent ZnAF-2 fluorescence increase observed during stimulation is due to an increase in ZnAF-2 quantum yield due to the alkalinization of vesicular pH, then using ZP1 in these experiments should abolish the increase in fluorescence upon stimulation since ZP1 fluorescence does not change much (even decrease a little) with increasing pH (Burdette et al., 2001).

ZP1 slices respond in a similar manner to KCl stimulation as ZnAF-2 loaded ones (compare red curve – figure 46a and black curve – figure 38a). Fluorescence increases upon KCl stimulation and remains elevated for minutes after the stimulus is removed. This result indicates that pH is not the only factor that influences the increase in fluorescence due to stimulation; since if that were the case, fluorescence of ZP1 loaded slices should decrease with increasing pH.

ZP1 slices were also submitted to 50 mM NH_4Cl treatment and then stimulated with KCl. After slices were pre-treated for 4 min with NH_4Cl, 50 mM KCl was applied for 30 s and then NH_4Cl wash was resumed for the duration of the experiment.

Fluorescence increased upon NH_4Cl perfusion, however when KCl was applied another increase was observed (black curve – figure 46a) similar to that in ZnAF-2 slices.

ZP1 fluorescence is constant between pH 5.5 and 6.5 (Burdette et al., 2001), therefore to exclude the possibility that 4 min of NH_4Cl treatment before KCl stimulation is not enough to completely change the vesicular pH to about 7.4, we treated ZP1 slices with NH_4Cl for 10 min and then stimulated them with KCl (NH_4Cl treatment was resumed after 30 s of KCl application). The peak fluorescence is greatly reduced as compared to KCl only, but fluorescence does not decrease, as it would be expected from pH effects on ZP1 fluorescence (black and red curves in figure 46b). This indicates once again that only part of the large increase in fluorescence observed with KCl stimulation of slices is due to pH changes. In the case of ZP1, increasing pH should not only eliminate the increase in fluorescence after stimulation, but it should cause a slight decrease, which is not observed.

Interestingly, fluorescence of ZP1 loaded slices starts to increase above control levels soon after NH_4Cl treatment and well before KCl application (black curve – figure 46b). This continued increase in fluorescence cannot be explained by increasing pH, since ZP1 fluorescence does not increase with increasing pH, instead it remains constant and decreases sharply with pH>8. So how can ZP1 fluorescence increase with increasing pH? We hypothesize that the change in vesicular pH, results in an increase in vesicular zinc concentration through the activation of the ZnT3 transporter. ZnT3 may become activated when the pH gradient is lost and begin pumping more zinc into the vesicles, leading to an increase in fluorescence. To make certain that ZP1 fluorescence does not change much between pH 5.5 and 7.4, a scan of zinc-ZP1 fluorescence in a spectrofluorimeter at both pH values was performed. The ratio between the total fluorescence intensity at pH 7.4 vs. pH 5.5 was 0.77, confirming previous data that increasing pH causes a decrease in ZP1 fluorescence intensity (Burdette et al., 2001).

A change in pH through direct action on the quantum yield of the dye can only account for a part of the persistent increase in ZnAF-2 fluorescence, since this increase also occurs with ZP1. The pH dependence of the dye might explain the large fluorescence increase observed after KCl application, but it cannot explain why the fluorescence levels do not decrease below control levels (compare 30 min NH_4Cl application – black curve and ZnAF-2 control – red curve in figure 45b). If fluorescence does not decrease below control levels, then zinc is probably not released in the extracellular space during stimulation.

How does vesicular zinc itself respond to pH change? We mentioned earlier that one of the reasons that the fluorescence levels with EDPA alone and fluorescence levels with KCl/EDPA together are not different, might be the fact that ZnT3 pump is activated and recycles zinc into the vesicles as fast as it is being removed. Most pumps work by using a pH gradient and given the results obtained with NH_4Cl treatment of ZP1- and ZnAF-2-loaded slices, we wanted to know if ZnT3 activity is affected by alkalinization of the intravesicular pH. Unstained slices were treated with 50 mM NH_4Cl for 15min and then stained for 30 min in ZnAF-2 saline solution that contained 50 mM NH_4Cl to maintain a high pH during staining. The fluorescence was then recorded and compared to control slices, which were held in normal saline solution for 15 min then stained with ZnAF-2 in normal saline for 30 min (table 3). If the ZnT3 pump is rendered inactive by an increase in pH, or if the zinc gradient inside the vesicle would be lost due to the pH increase, then the average level of initial fluorescence values for the NH_4Cl treated slices should be lower than that of control. If however, ZnT3 is activated by an increase in pH, then the opposite should be true. This is not the case, however since the two average initial values are statistically the same. This suggests that ZnT3 may not use a pH gradient to pump zinc into the vesicle, or that pH 5.5 is not necessary to retain vesicular zinc. Also, ZnT3 might require both an increase in pH and loss of vesicular zinc to

become activated therefore, if the increase in pH does not compromise the concentration of zinc inside the vesicle, then ZnT3 may not be activated.

To distinguish between what fractions of zinc gave rise to the fluorescence observed we also used membrane permeable chelators. These chelators are able to cross both the cell membrane and the synaptic membrane, and therefore are able to chelate zinc from the veneer and the synaptic vesicles. Different chelators can also strip off different amounts of zinc from the ternary complex it forms with the synaptic membrane protein, so two membrane permeable chelators, TPEN and DEDTC were used to study the fluorescence of ZnAF-2 loaded slices. TPEN is larger then DEDTC so it diffuses slower into the cell, however it has a much higher affinity for zinc so it binds it very tightly compared to DEDTC.

If TPEN is applied to unstimulated slices, fluorescence drops below control levels (compare blue curve – figure 47a to red curve – figure 38a) to about 30% of initial fluorescence value, validating the fact that TPEN is indeed diffusing into the cell and chelating zinc from the synaptic vesicles. To see if TPEN would be able to strip more zinc if the pH was increased, slices were pre-treated with NH_4Cl and then TPEN was added (green curve – figure 47a, NH_4Cl along with TPEN were applied for the duration of the experiment). There is a small fluorescence increase due to the pH change and then fluorescence drops quickly when TPEN is applied. However, the end fluorescence value is not any different than TPEN alone, suggesting that TPEN is not able to strip any more zinc off than at physiological pH. If the slice is stimulated with KCl first and the fluorescence allowed to peak, then TPEN is added (about 1min from addition of KCl) the end fluorescence value is different than the end value for TPEN alone (red curve – figure 47a), which indicates that during stimulation TPEN might be able to extract more zinc than in the non-stimulated state. TPEN may be able to penetrate the vesicles better if they are fusing to the membrane than in the non-stimulated state. Another possibility for the difference in fluorescence could be that TPEN alone was not allowed enough time to strip

all the possible zinc. There is also a possibility that KCl application may lower the autofluorescence of the slices. DEDTC confirmed the results obtained with TPEN. If DEDTC is added to unstimulated slices (blue curve – figure 47b), fluorescence drops to about 55% of the initial value. The drop is faster, because DEDTC is smaller and diffuses in quickly, but the end fluorescence value is higher than with TPEN since it does not bind zinc as strongly. The change in pH does not seem to affect how much zinc DEDTC can appropriate (similar to TPEN) since in slices that were pre-treated with NH_4Cl prior to DEDTC application, the end fluorescence value was the same (green curve – figure 47b) as that of DEDTC alone. NH_4Cl application might affect the rate of chelation however, so that in NH_4Cl treated slices, zinc might become more accessible and be chelated more rapidly than in non-treated slices. When slices were stimulated with KCl, allowed to reach peak fluorescence (1 min) and then DEDTC was added, fluorescence dropped quickly to the same level as DEDTC alone (red curve – figure 47b). The reason that the two are not different could lie in the fact that DEDTC has a lower affinity for zinc than TPEN and even though it can penetrate better and get to the vesicles be they in the stimulated or non-stimulated state, it does not strip as much zinc off. The fluorescence drop after DEDTC is applied to stimulated slices is very quick (about 5 min) as compared to TPEN (about 20 min) even though it is not as pronounced (to about 55% of initial fluorescence vs. 30% in TPEN).

The use of membrane permeable and impermeable chelators allows for the differentiation of various pools of zinc. As it was determined earlier, if EDPA is applied to unstimulated slices loaded with ZnAF-2, fluorescence intensity decreases below control levels indicating that there is a pool of zinc associated with the extracellular membrane and is termed the zinc veneer. The zinc veneer exists with or without slice stimulation. Similarly, if TPEN or DEDTC are applied to unstimulated slices loaded with ZnAF-2, fluorescence decreases more than when EDPA is applied, suggesting that the membrane permeable chelators are able to strip not only the zinc veneer, but another zinc

pool as well; the vesicular zinc. The remaining pool of zinc is termed externalized zinc and is a subset of the vesicular zinc. Since only a fraction of the synaptic vesicles fuse with the cell membrane during stimulation at any given time, not all vesicular zinc becomes externalized. To understand what pool of zinc the fluorescence comes from, we can compare the KCl stimulated slices with the EDPA chelated pool and the TPEN chelated pool (figure 48). If we assume that all the increase in fluorescence after KCl addition is due to the pH dependence of ZnAF-2 and divide that increase by 7 (the ZnAF-2 fluorescence increase due to pH is about 7 fold), that is the fraction of the synaptic zinc that is externalized (black curve – figure 48). Taking the difference between the final value of fluorescence with TPEN alone (orange curve – figure 48) and subtract it from the final value of control (gray curve – figure 48) would give the fluorescence that arises from all chelatable forms of zinc (assuming that TPEN chelates all three forms of chelatable zinc, which is a reasonable assumption, since TPEN is a membrane permeable chelator with a strong affinity for zinc). The difference between the final fluorescence value of EDPA alone and that of control corresponds to the fraction of chelatable zinc that is part of the veneer (green curve – figure 48). A different breakdown of the percentage of the different zinc pools is given in figure 49. Notice how the percentage of externalized zinc (in red) is so small as to be within measurement error. Synaptic zinc and veneer zinc are about the same percentage. EDPA and EDPA/KCl strip about the same amount of zinc, while TPEN/KCl strips off more zinc than TPEN alone, indicating that either there is some amount of zinc that is unable to be stripped with TPEN, or that the experiment was not long enough to allow for TPEN to strip off all the chelatable zinc (orange curve in figure 48 does not seem to fully reach steady state).

Another interesting question is the localization of ZnAF-2 with respect to intracellular compartments. We utilized histidine (his) and pyrithione (pyr) to visualize where ZnAF-2 is located (mainly in the cytoplasm or in the synaptic vesicles). His is a membrane impermeable zinc chelator, which forms both mono- and bis – zinc complexes

and facilitates its solubility in the extracellular medium (Rumschik et al., 2009), but it does not act as a zinc transporter. As a result, if zinc and His are co-applied extracellularly, zinc should be able to enter the cell, but not the synaptic vesicles. If ZnAF-2 is located mostly in the cytoplasm, when zinc and his are applied, there should be a surge in fluorescence as extracellular zinc makes its way into the cell. We applied zinc/his (100:200 μM – for ratio optimization see chapter 4) to slices loaded with ZnAF-2 and observed a slight increase in fluorescence (see figure 50) as compared to other dyes such as FZ-3-AM. This could be because ZnAF-2 is preferentially localized in the synaptic vesicles where the chelatable zinc is located, rather than in cytoplasm. There was no difference in the fluorescence increase from the cell body (figure 50 – open squares) from the increase in synaptic vesicles (figure 50 – closed squares). This indicates that either ZnAF-2 is not localized in the cytoplasm, but preferentially moves into the synaptic vesicles, or that zinc is very tightly buffered once it enters the cytoplasm (refer to chapter 5).

Pyrithione (pyr) on the other hand, is a zinc ionophore and allows zinc to cross both the cellular membrane and the synaptic membrane (it does this by forming a 2:1 complex with zinc and shuttling it across membranes, see figure 51). When pyr/zinc (15:10 μM – for ratio optimization see chapter 5) is co-applied, a large increase in fluorescence should be observed as seen with FZ-3-AM (see figure 24 in chapter 5). However, a decrease in fluorescence was observed after zinc/pyr application in both the cytoplasm and the synaptic vesicles. This phenomenon needed further probing, so we set out to understand what was causing the decrease in ZnAF-2 fluorescence. We performed fluorimeter experiments with 500 nM ZnAF-2. ZnAF-2 fluorescence increases upon zinc (10 μM) binding, but decreases to about 1/3 of the fluorescence after 15 μM pyr is added to the buffered solution. Subsequent additions of zinc (up to 40 μM total concentration) do not seem to restore the fluorescence value, indicating that pyr quenches ZnAF-2

fluorescence. We also studied the quenching of ZnAF-2 with varying pyr concentrations and found that quenching occurs in pyr concentrations as low as 0.33 μM (see figure 52).

We then tried to find another compound that would act as a zinc ionophore, but would not quench ZnAF-2 fluorescence. Clioquinol (CQ) is another ionophore and a substance that has been used for Alzheimer's disease with some success. We started out by treating the slices with 10 μM CQ and 7 μM zinc (blue line – figure 53) and then stimulate with KCl. No increase in fluorescence is observed prior to KCl stimulation, which can be explained by the fact that zinc is tightly buffered once it enters the cell. This explanation does not exclude the fact that ZnAF-2 could be located only in the synaptic vesicles, since if ZnAF-2 were in the cytoplasm it could see influxes of zinc however transient. Interestingly, application of 10 μM CQ and 7 μM Zn to FZ-3-AM loaded slices induces an increase in fluorescence, unlike ZnAF-2. This could indicate once again that ZnAF-2 may indeed preferentially move into synaptic vesicles where the concentration of chelatable zinc is large. Fluorescence does not decrease either, indicating that CQ does not quench ZnAF-2 fluorescence. In the course of the CQ study a very interesting phenomenon was observed. If trace amounts of CQ are present, the response to KCl stimulation is 4 times larger (red curve – figure 53) than in our previous stimulations (black curve – figure 53). CQ is very hydrophobic and it sticks to the walls of the tubing used to perfuse normal saline solution containing CQ. In fact, the only way to get rid of CQ was to replace the tubing. Due to the fact that the unusual increase in fluorescence after KCl stimulation was observed after trying to flush CQ from the tubing by continuous washing, it was difficult to determine what concentration of CQ was causing the large increase in fluorescence, therefore it was termed "trace amounts". To determine how low of a concentration of CQ could bring about the large fluorescence increase slices were treated with 10 μM CQ (green curve – figure 53) for 5 min and then stimulated. The increase in fluorescence upon KCl stimulation is similar to the one observed with trace amounts, although it is not as large, implying that CQ levels need to be lower to reach as

large of a fluorescence increase upon KCl stimulation. CQ does not seem to affect the fluorescence after KCl stimulation even with a concentration as low as 1 μM (magenta curve – figure 53). We are not sure how CQ affects the slice stimulation, but one possible way could be that it somehow primes the slice for a massive synaptic vesicle fusion. CQ does not seem to have an effect on ZnAF-2 fluorescence itself, since its application before KCl addition does not affect the fluorescence at all (blue curve – figure 53).

Discussion

Our experiments provide evidence against the notion that zinc is freely released during the course of synaptic stimulation. The fact that the fluorescence signal sharply increases and does not diminish with time after continuous washing of the slices indicates that zinc is not being freely released. Our data provides evidence to support what we have previously hypothesized, that zinc is being externalized (Kay, 2006) during synaptic transmission instead of being released in the extracellular medium. Some reports of zinc release have also found similar increases in fluorescence after stimulation that have lasted for several minutes after stimulation was induced, however the source of the fluorescence increase was not addressed (Qian and Noebels, 2005; Ueno et al., 2002; Varea et al., 2001). It could be argued that the increase in fluorescence is due to the change in pH the fluorescent dye undergoes when the vesicles fuse to the membrane (Sankaranarayanan et al., 2000). ZnAF-2 fluorescence increases 7-fold when the pH is changed from 5.5 to 7.4 (Hirano et al., 2000), giving rise to the sharp increase observed under KCl stimulation. Our results obtained with NH_4Cl treatment of the slices, where fluorescence increased due to the pH change, but was smaller than the increase observed with KCl stimulation, support the conclusion that the total fluorescence increase observed with stimulation is not all due to the pH change. It could be that treatment of slices with NH_4Cl may not induce a complete change in pH (up to 7.4), however slices were treated with 50 mM NH_4Cl, which should be a large enough concentration to induce such a change and

NH_4Cl is also a small molecule and it diffuses very quickly, penetrating even into the depth of the slice. One other possibility could be that the cells are somehow pumping NH_4Cl out as it diffuses in, which can be the reason why the pH may not get to 7.4, however the concentration of NH_4Cl is large enough to change the vesicular pH very quickly and keep it so, since it is applied for the length of the experiment. These vesicles are very small (50 nm diameter) so they do not require large changes in H^+ concentration to achieve large pH changes. It could also be that as the pH is changing in the vesicle, the pH pumps get activated and begin to counteract the action of NH_4Cl, by lowering the pH. Since synaptic vesicle size is below the resolution of optical microscopes it would be impossible to determine if the pH of vesicles responds homogenously to NH_4Cl and that all vesicles achieve a pH of 7.4. We shied away from the idea of using pH sensitive dyes, since in tissue studies there would be a distribution of pH values and it would be very hard to distinguish whether the pH is indeed changing in the synaptic vesicle area only. The data obtained with ZP1 loaded slices, whose fluorescence decreases with increasing pH (Burdette et al., 2001), seem to refute the idea that all fluorescence increase is due to pH change, since the same phenomenon of fluorescence increase observed with ZnAF-2 is observed with ZP1.

The pH-dependent increase in fluorescence however only accounts for a fraction of the increase in signal after stimulation, but it does not explain why the signal does not fall below control levels. If the zinc-dye complex is freely diffusing in solution, the signal should fall quickly due to washing, but this is not observed. However, it could be possible that the dye immobilizes zinc somewhat by forming a stable ternary complex with zinc and some other membrane bound molecule and keeps the zinc from diffusing into the synaptic cleft.

The average initial fluorescence value for multiple KCl stimulated slices in the presence of EDPA was lower than the one for control (no stimulation at all, or stimulated in the absence of EDPA). The more telling result is the fact that the initial fluorescence

value for slices that were stimulated multiple times with KCl in the absence of EDPA was statistically the same as the value for the non-stimulated slices. This indicates that either zinc is not being released, or that zinc is recycled back into the slice. A different explanation for this could be that the slices are appropriating zinc from the saline holding solution, even though we take careful precautions to keep the concentration of zinc in solutions at a minimum (20 nM).

EDPA applied simultaneously with KCl does not seem to strip off any more zinc than EDPA applied to unstimulated slices, however the multiple stimulation experiments provide evidence that zinc is only externalized and becomes available for EDPA chelation. The difference between zinc stripped off by EDPA alone, or by co-application of EDPA and KCl could be small enough to fall within experimental error (we are able to see the difference only with multiple stimulations of the same slice). In our breakdown of the fluorescence signal, externalized zinc only accounts for about 3.4% of the total fluorescence observed, whereas zinc veneer and synaptic zinc give rise to over 95% of the fluorescence observed. The fluorescence that comes from externalized zinc is within experimental error and we are not able to see the difference between how much zinc can be stripped from EDPA and EDPA/KCl application.

The phenomenon of the unusual fluorescence increase observed during multiple stimulations (figure 43) deserves some attention as well, even though we have not performed follow-up experiments. The result that stripping the veneer is enough to cause the large fluorescence increase indicates that loss of the veneer is somehow affecting vesicle release. More experiments are needed in order to determine the relationship between the veneer and the efficacy of synaptic transmission.

Conclusion

In conclusion, we have presented evidence that refutes the traditional zinc release hypothesis, which claims that zinc is being freely released during synaptic transmission.

Our data indicates that zinc is being externalized instead, as a ternary complex with a yet-to-be-identified synaptic membrane molecule or protein. Our data throws doubt on the hypothesis that ZnT3 uses a pH gradient to drive zinc uptake into the vesicles. The stripping of zinc from the veneer via extracellular chelation leads to a large increase in the stimulus-induced increase in fluorescence, suggesting that the role of the veneer may be important in normal cell physiology.

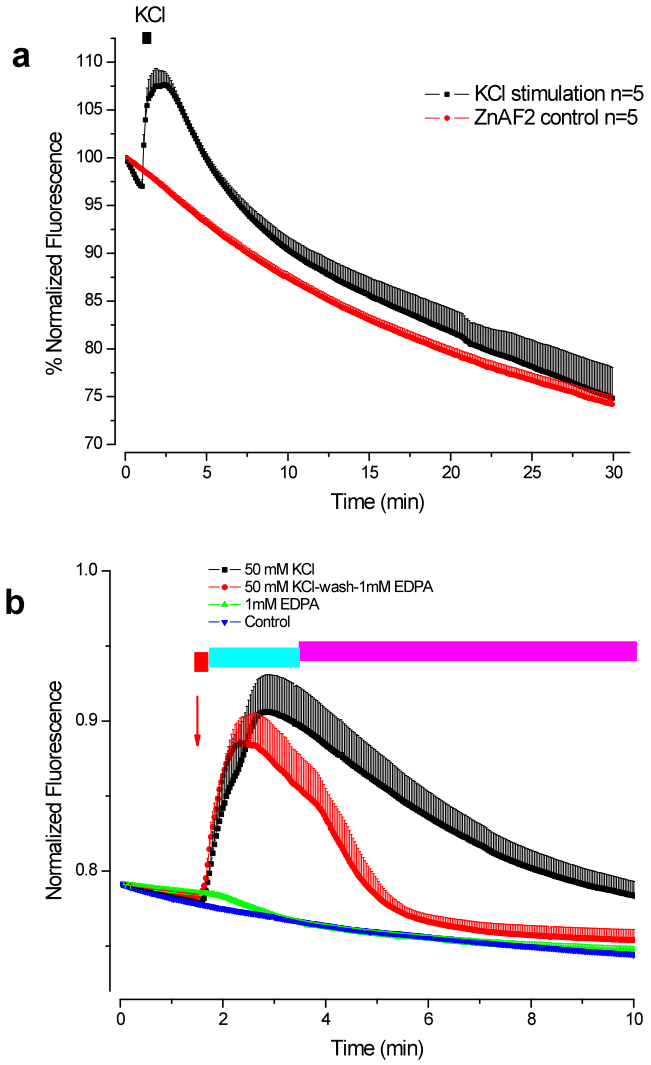

Figure 38. KCl stimulation and EDPA chelation of Zinc in older and younger animals

---

Note: Graph a – black curve represents fluorescence response to 50 mM KCl. Arrow indicates the addition of KCl, which lasted for 30 s. Red curve – control. Graph b – black curve – fluorescence response to KCl stimulation in young animals, arrow denotes the time of application and the red bar denotes the duration of KCl stimulation (15 s). Red curve – fluorescence response to KCl stimulation followed by 2 min washing and then 1 mM EDPA application; the aqua bar represents the duration of normal saline wash, whereas the magenta bar the duration of EDPA application. The green curve represents the fluorescence response of unstimulated slices to EDPA addition and the blue curve is the control curve.

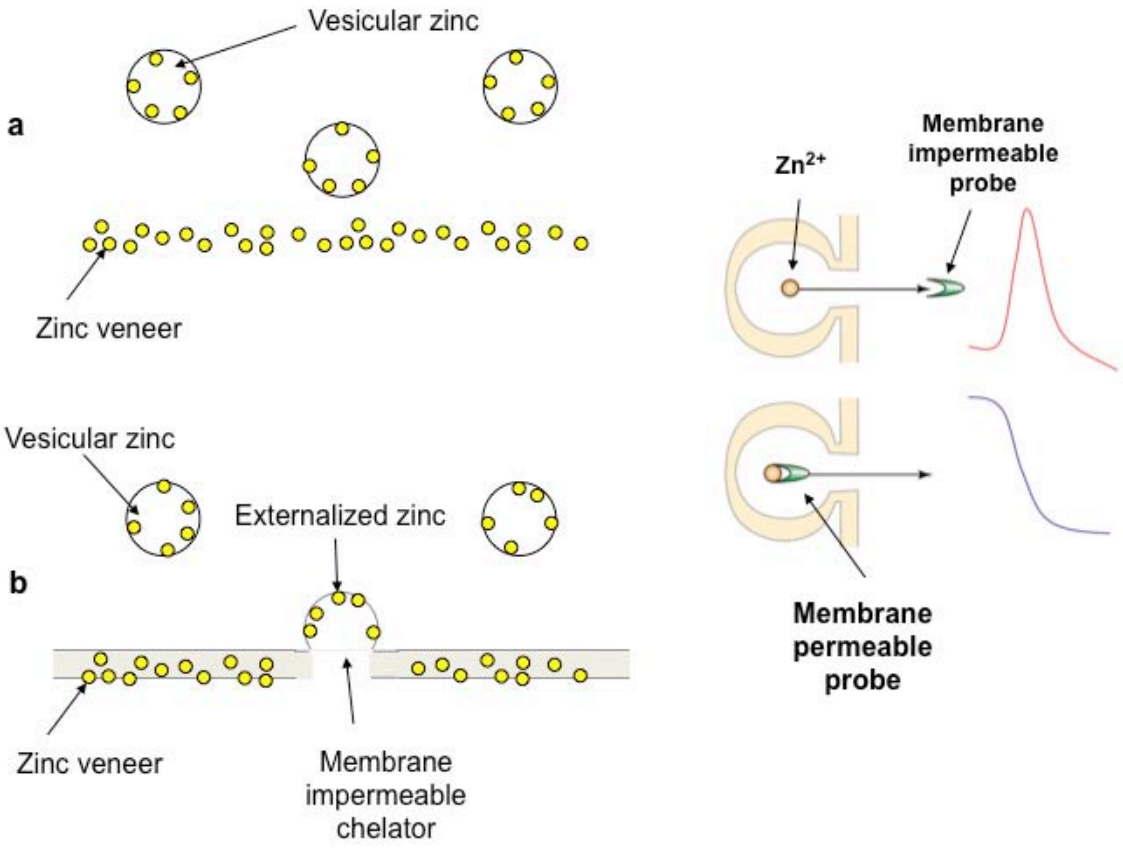

Figure 39. Importance of location and membrane permeability of the probe and chelator

Note: Panel a – synaptic and veneer zinc in unstimulated slices. Large circles represent synaptic vesicles whereas small ones represent chelatable zinc within the vesicles. Panel b – during stimulation the vesicles fuse to the membrane exposing zinc to the extracellular space where it can be stripped off from an extracellular chelator. Panel c – general schematic of the fluorescence signal that is expected if the fluorescent probe is membrane permeable and membrane impermeable. These scenarios are true if the zinc is being fully released (Kay, 2006).

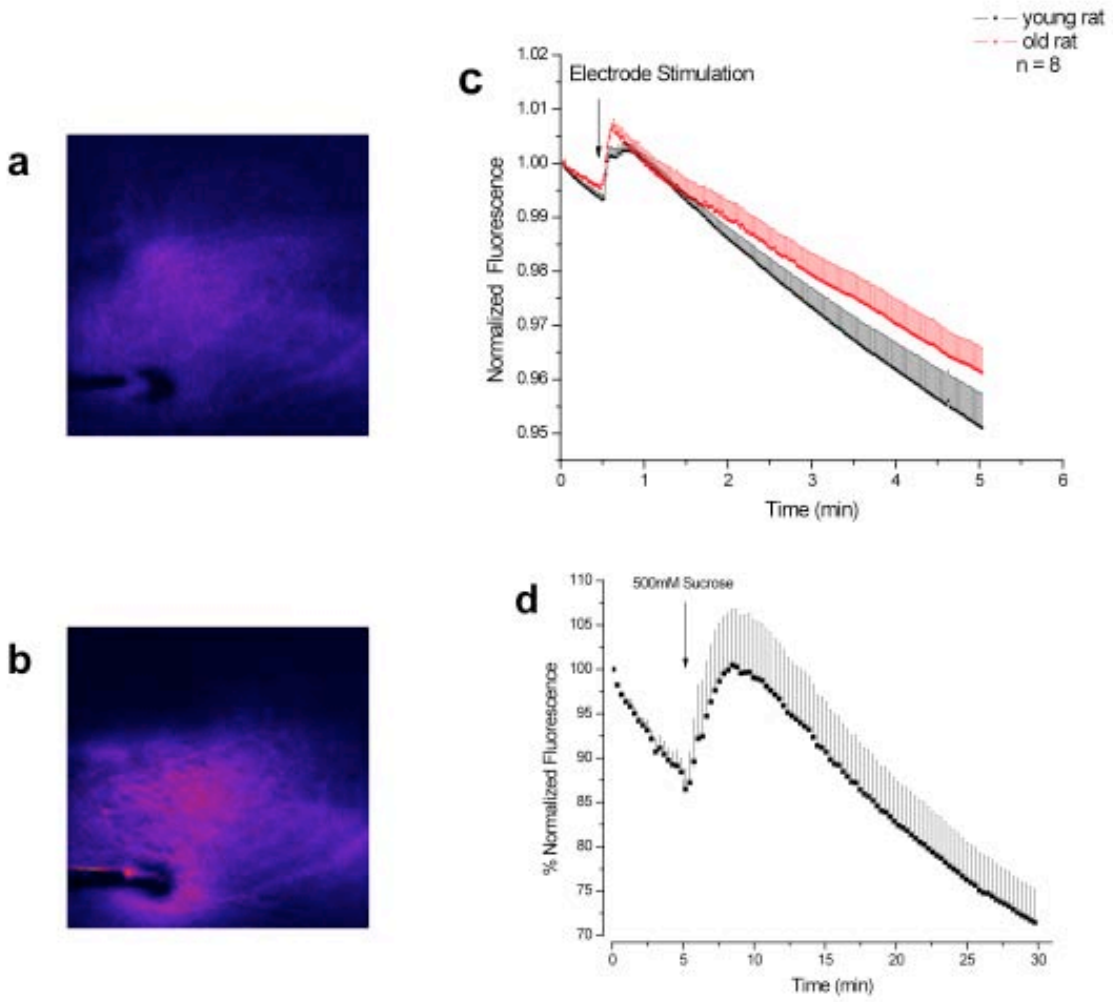

Figure 40. Fluorescence response to different types of stimuli

---

Note: Images of a slice that is being electrically stimulated (500 pulses, 100 Hz), when stimulation starts (image a) and at the peak of fluorescence increase (image b). Graph c represents fluorescence response of electrically stimulated slices in young (black curve) and old (red curve). The arrow indicates the start of the electrical stimulus. Graph d represents the fluorescence response of slices stimulated with 500 mM sucrose for 30 s. Arrow indicates the time of sucrose application.

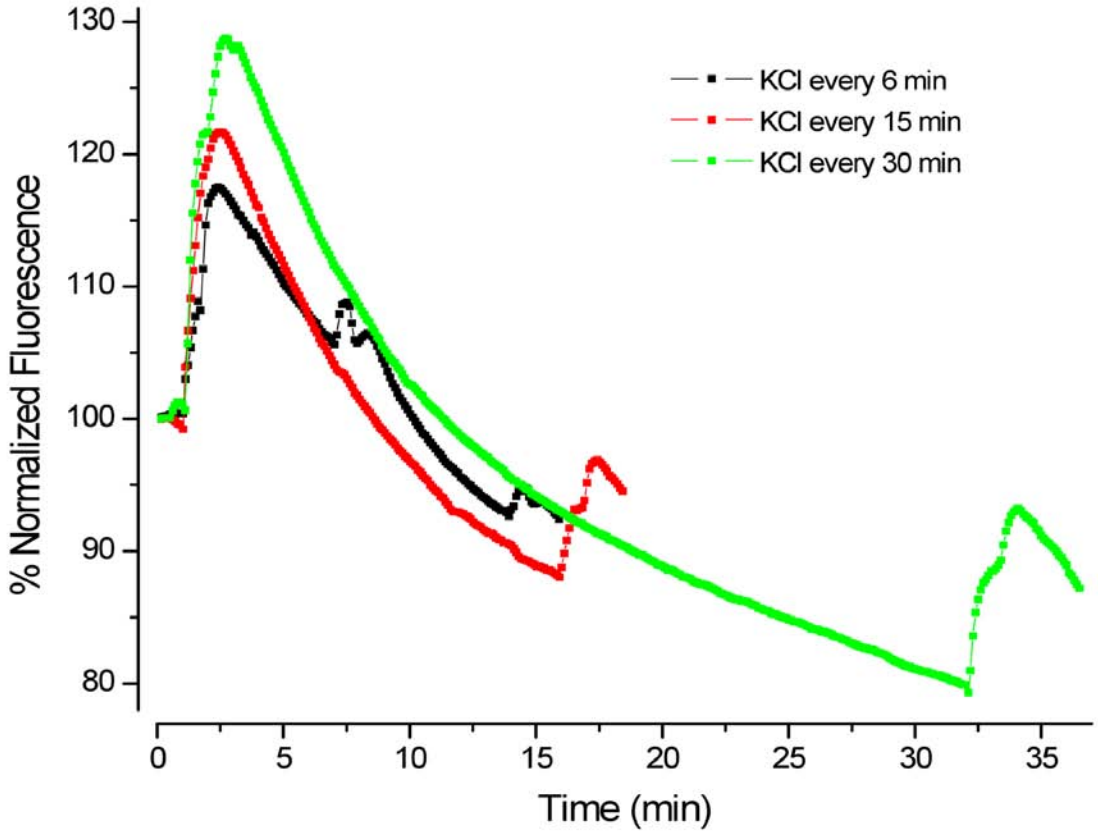

Figure 41. Multiple KCl stimulations of the same slice

Note: The timing of 50 mM KCl application was varied every 6 (black curve), 15 (red curve) and 30 min (green curve).

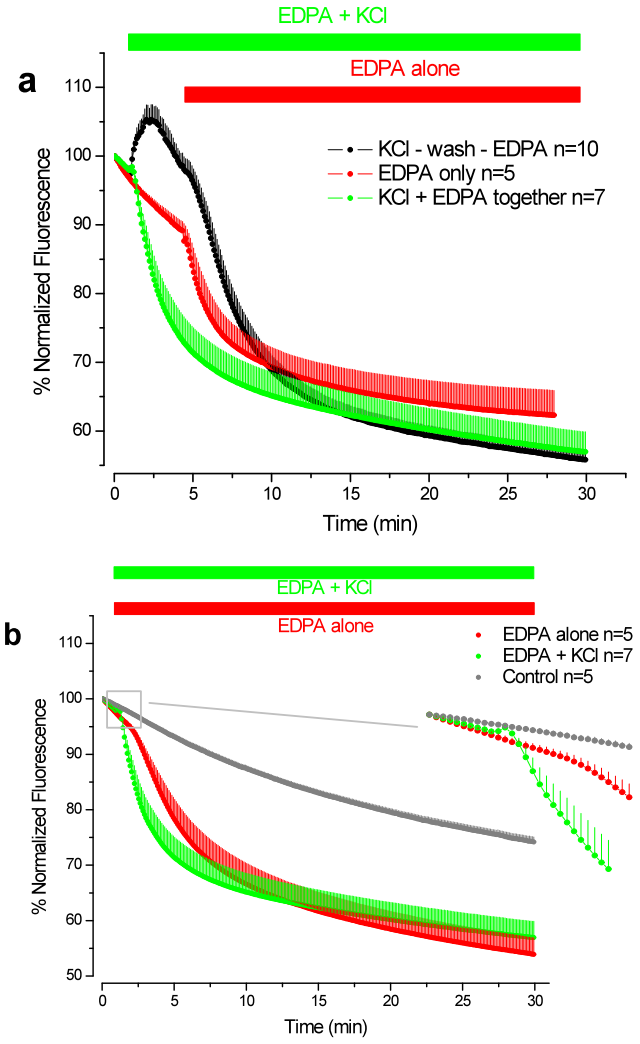

Figure 42. EDPA chelation in ZnAF-2 loaded slices

Note: Graph a – black curve represents the addition of 1 mM EDPA after 50 mM KCl addition followed by saline wash. Red curve – EDPA addition to unstimulated slices. Green curve – simultaneous addition of EDPA and KCl. Lines indicate the time of application, KCl 30 s, EDPA for the remainder of the experiment. Graph b, green curve – EDPA addition to unstimulated slices. Red curve – simultaneous EDPA and KCl addition. Gray curve – control slices. Inset shows a blow-up of the graph around the application of EDPA and EDPA/KCl.

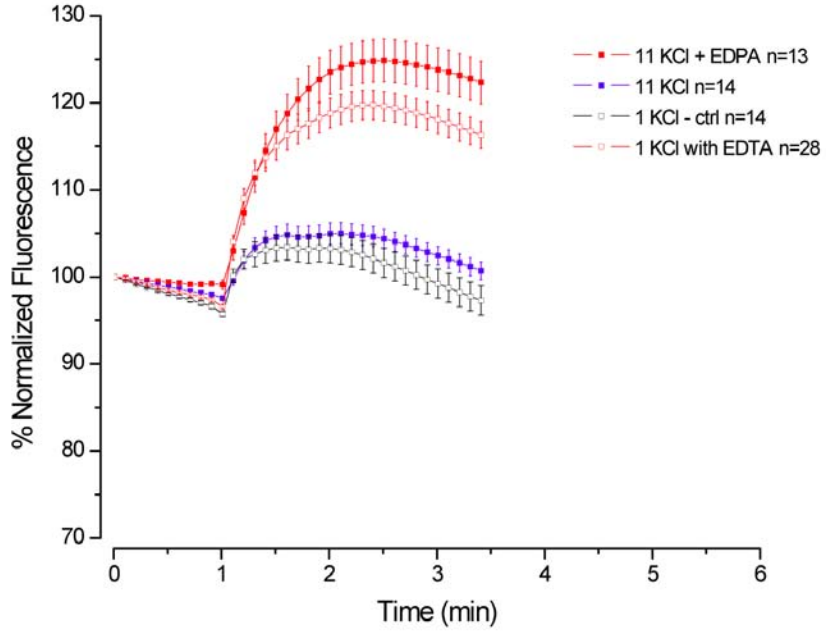

Figure 43. Fluorescence response of ZnAF-2 slices to multiple KCl stimulations

---

Note: Black open symbols represent control slices (stimulated only once with KCl). Blue curve – fluorescence of ZnAF-2 slices that have been stimulated with KCl 10 times with a 5 min recovery time in between and then stimulated again to collect the fluorescence curve. Red closed symbols – fluorescence of ZnAF-2 slices that have been stimulated with KCl in the presence of 1 mM EDPA 10 times with 5 min recovery time in between and then stimulated again to collect the fluorescence curve. Red open symbols – fluorescence of ZnAF-2 slices that were treated with 1 mM EDTA for 50 min and then stimulated with KCl to generate the fluorescence curve. KCl was applied at min 1.

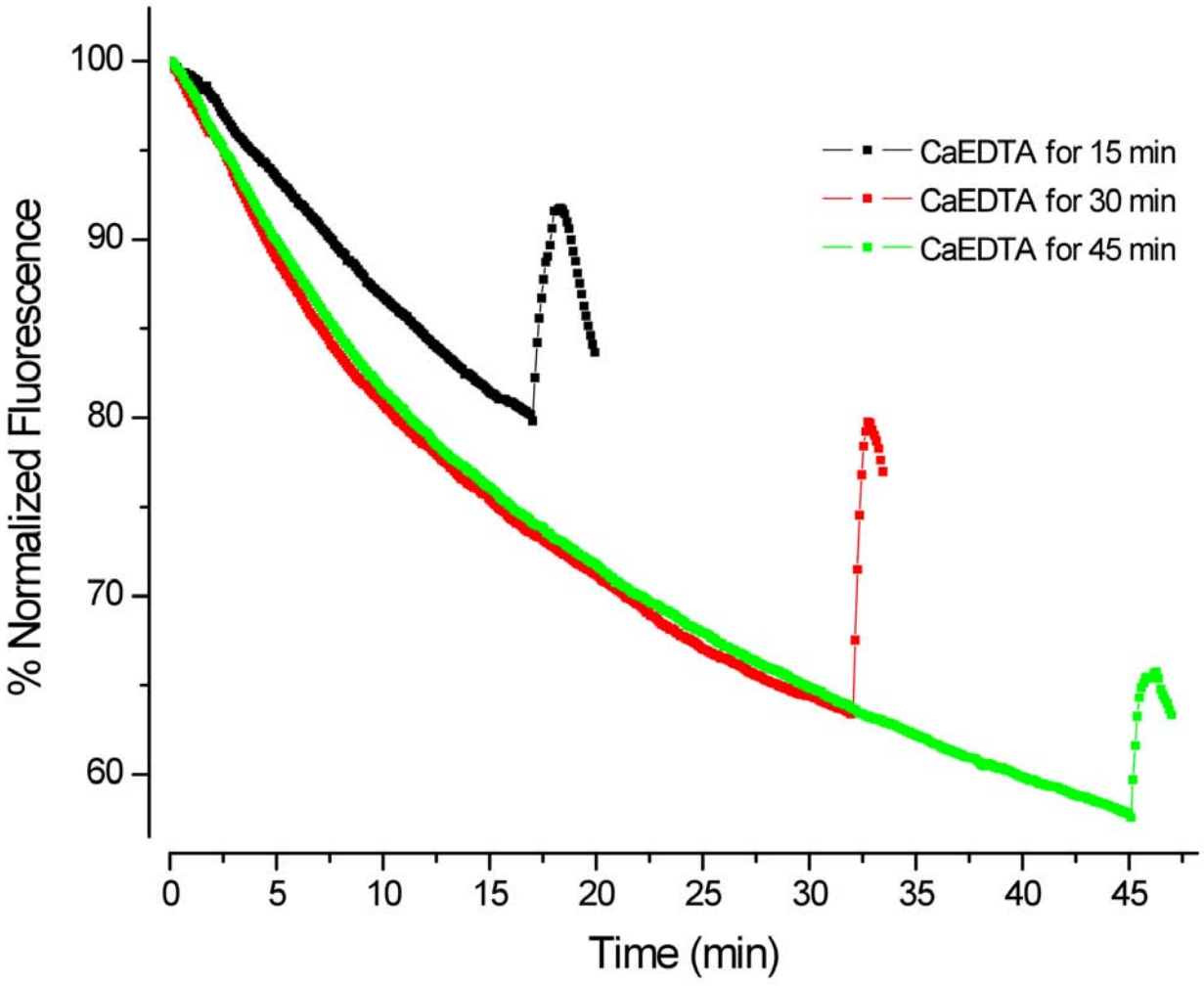

Figure 44. Fluorescence response of ZnAF-2 stimulated slices perfused with CaEDTA for varying times

---

Note: Black curve – fluorescence of ZnAF-2 slices perfused with 1 mM CaEDTA for 15 min and then stimulated with KCl. Red curve – fluorescence of ZnAF-2 slices perfused with 1 mM CaEDTA for 30 min and then stimulated with KCl. Green curve – fluorescence of ZnAF-2 slices perfused with 1 mM CaEDTA slices for 45 min and then stimulated with KCl. CaEDTA was perfused at min 1 and washed off for 2 min before KCl was applied. KCl was applied for only 30 s.

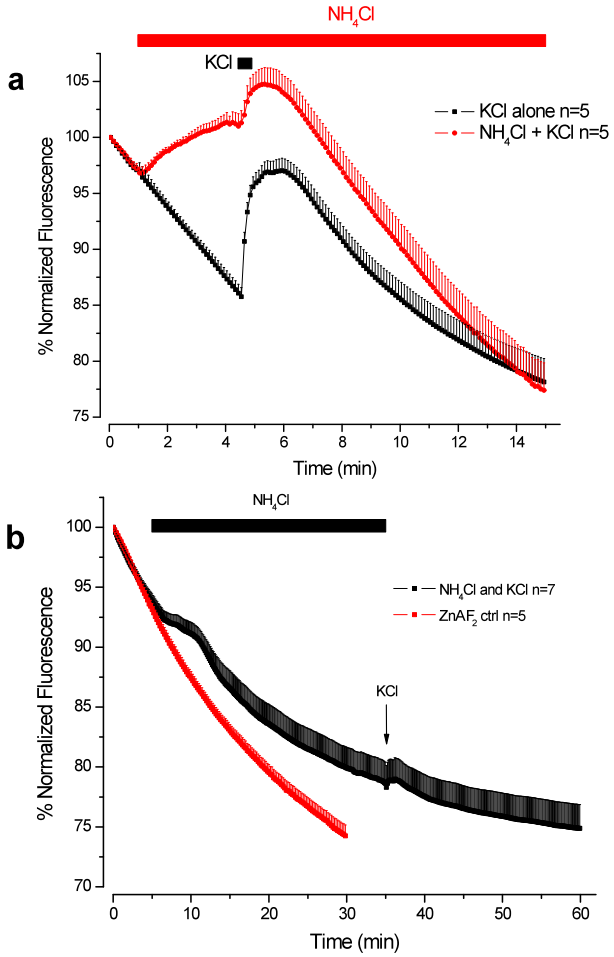

Figure 45. Fluorescence response of ZnAF-2 slices with varying NH_4Cl application time

---

Note: Graph a - pH dependence of ZnAF-2 fluorescence. Arrows indicate the timing of the application. NH_4Cl (black curve) was applied for the duration of the experiment, whereas KCl in conjunction with NH_4Cl was applied at min 5. Red curve is the response of ZnAF-2 loaded slices to 50 mM KCl applied at min 1. In both cases KCl was applied for only 30 s. Graph b - Response of ZnAF-2 loaded slices to KCl stimulation after being treated with NH_4Cl for 30 min. Arrows indicate the timing of the application. KCl was applied for 30 s, while NH_4Cl for the duration of the experiment.

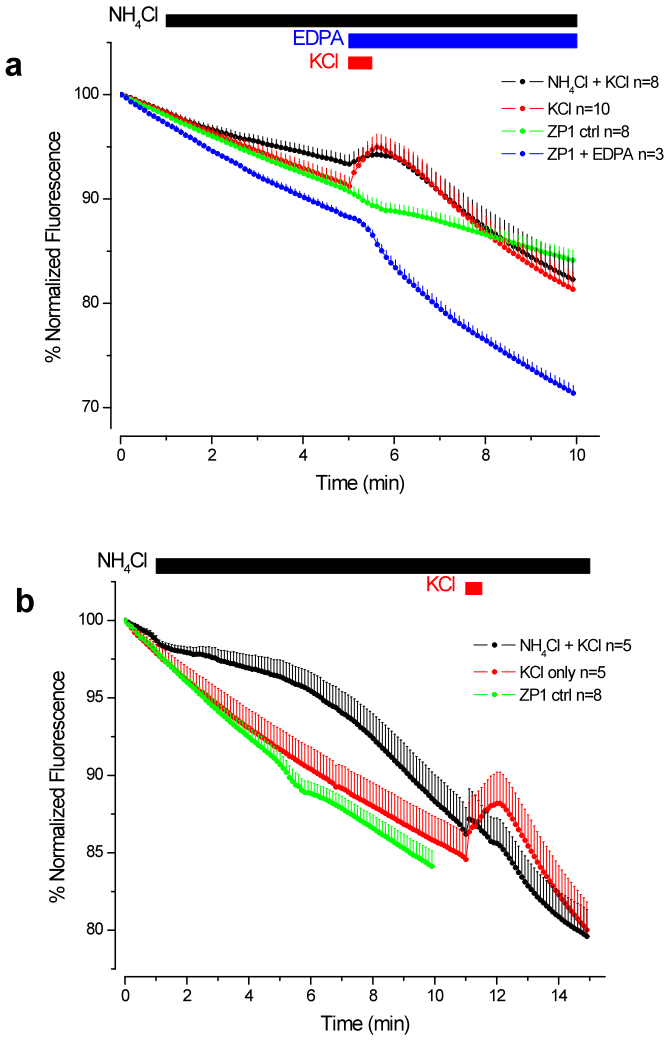

Figure 46. Response of ZP1 loaded slices to KCl stimulation, NH_4Cl and EDPA application

---

Note: Graph a - Red curve represents the response of ZP1 loaded slices to 30 s application of 50 mM KCl. Black curve represents the response of ZP1 loaded slices to 50 mM NH_4Cl treatment and subsequent KCl stimulation. Blue curve represents the response of ZP1 loaded slices to 1 mM EDPA chelation and green curve is the control curve. NH_4Cl was applied at min 1 for the duration of the experiment, whereas EDPA and KCl were applied at min 5. Graph b - Fluorescence response of ZP1 loaded slices to longer NH_4Cl application and subsequent KCl stimulation. Black curve represents fluorescence response of slices treated with 5 mM NH_4Cl for 10 min and then stimulated with 50 mM KCl. Arrows indicate the timing of application. NH_4Cl was applied for the remainder of the experiment. Red curve represents the response of ZP1 loaded slices to 50 mM KCl stimulation. Green curve is control.

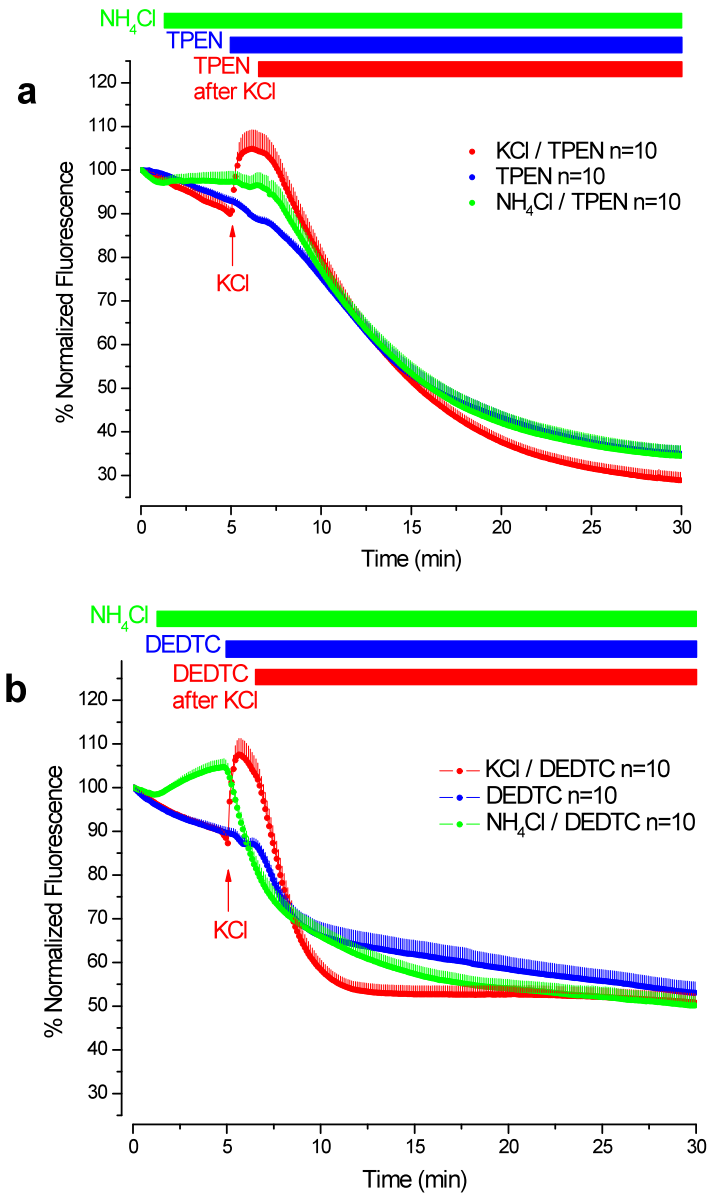

Figure 47. Fluorescence response to membrane permeable chelators: TPEN and DEDTC

Note: Graph a - Fluorescence response of ZnAF-2 loaded slices to TPEN chelation. Red curve is the response of ZnAF-2 slices to 50 mM KCl stimulation followed by 200 μM TPEN addition after 1 min. Green curve is the response of ZnAF-2 slices to 50 mM NH_4Cl treatment and subsequent TPEN addition. Blue curve is the response of ZnAF-2 slices to TPEN application only. Graph b - Response of ZnAF-2 loaded slices to DEDTC chelation. Curves follow the same pattern as for TPEN.

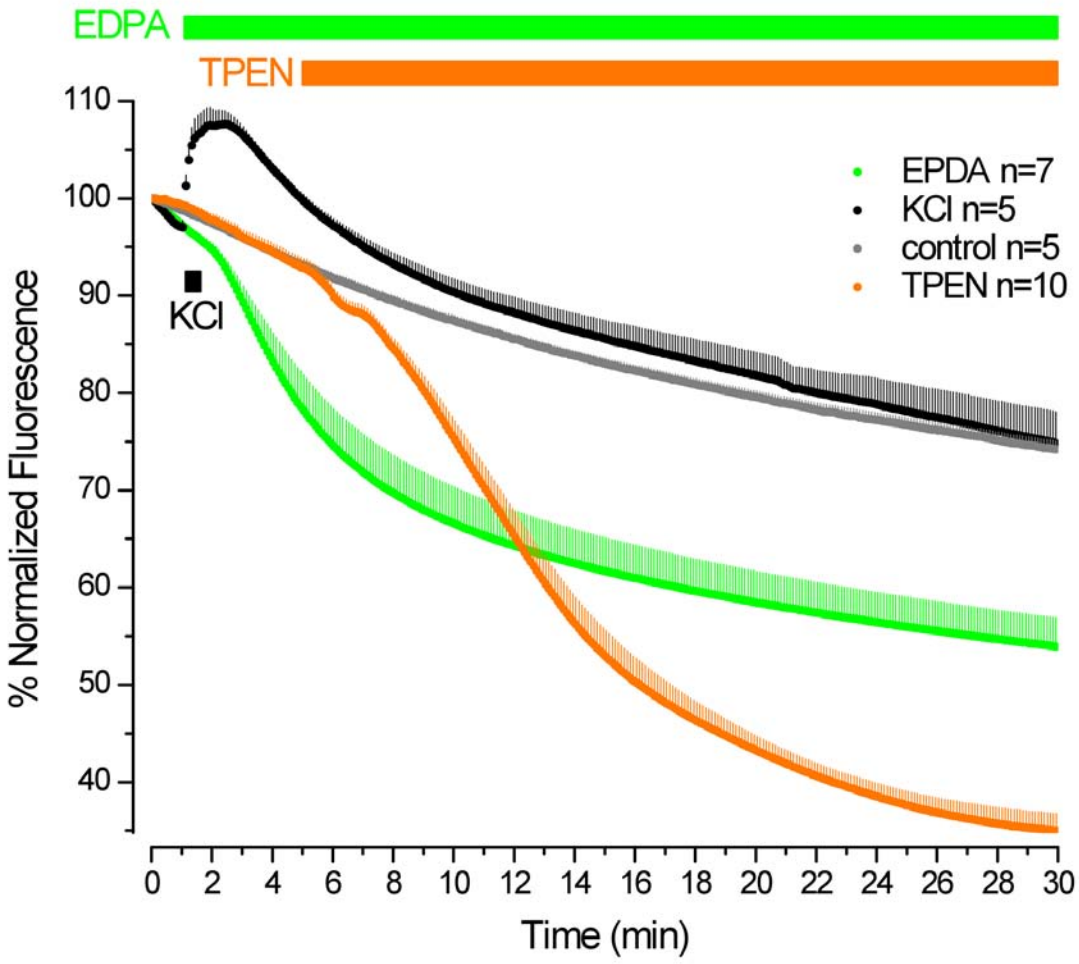

Figure 48. Response of ZnAF-2 loaded slices to membrane permeable and impermeable chelators

---

Note: A comparison between addition of 1 mM EDPA (extracellular chelator) and 200 μM TPEN (intracellular chelator) to unstimulated slices, and KCl stimulated slices. Gray line is control. Arrows indicate the timing of the application. KCl was applied for only 30 s, while TPEN and EDPA for the remainder of the experiment.

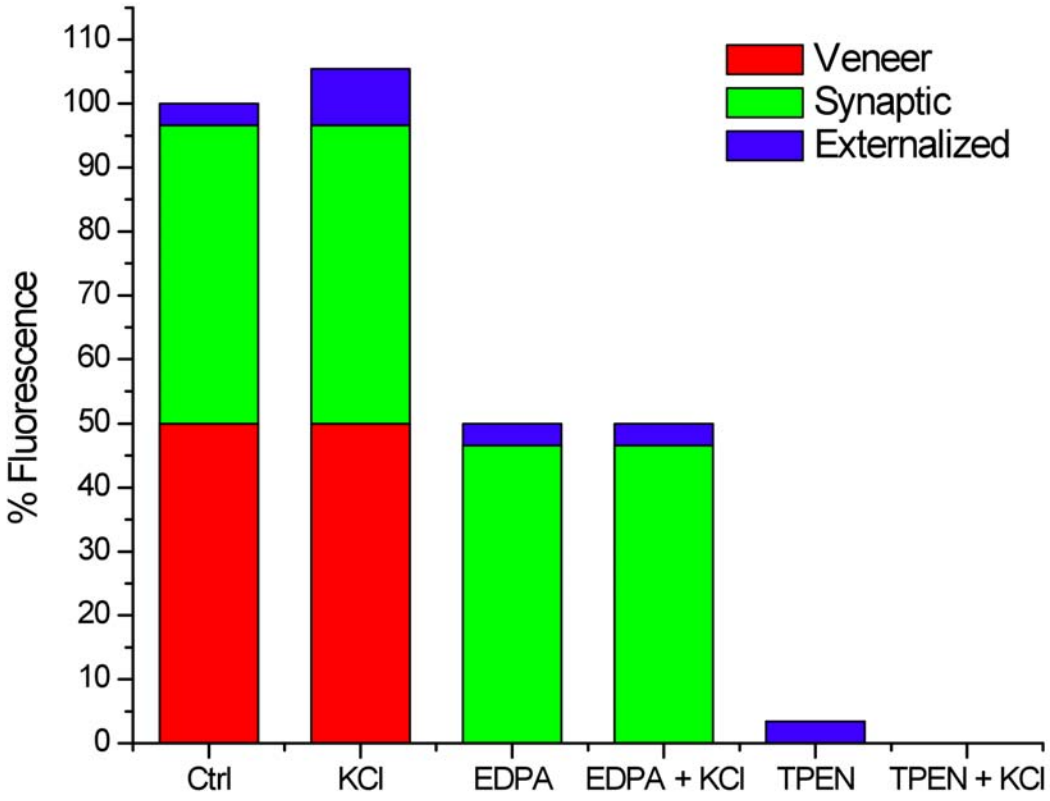

Figure 49. A general breakdown of fluorescence increase upon KCl stimulation

---

Note: The green part represents the fluorescence that comes from synaptic zinc, the red part represents the fluorescence that arises from the zinc veneer and finally the blue part represents the fluorescence that arises from the zinc that is externalized during KCl stimulation and vesicle fusion.

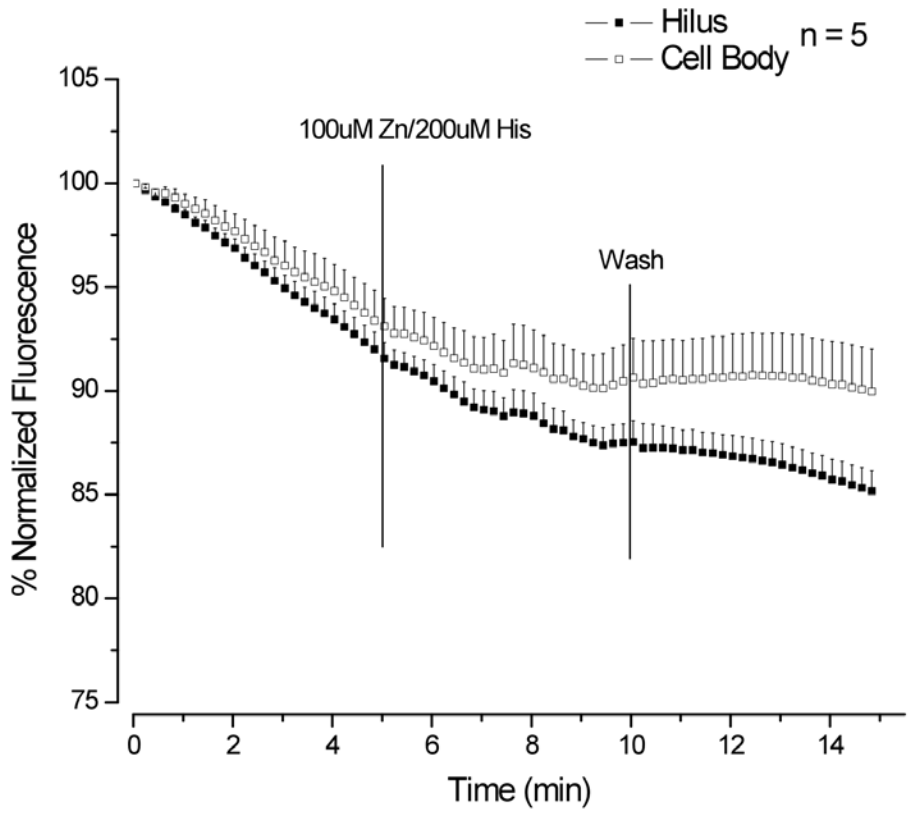

Figure 50. Fluorescence response of ZnAF-2 loaded slices to Zinc/His application

---

Note: The vertical bar represents the application time of Zn/His, which lasts until wash begins. Open squares – cell body fluorescence (cytoplasm); closed squares – hilus fluorescence (synaptic vesicles).

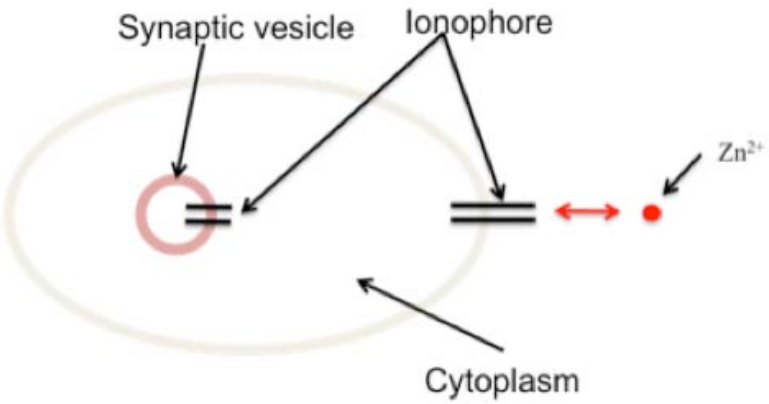

Figure 51. A general diagram of the action of an ionophore

Note: The ionophore can shuttle zinc through either the cell or the synaptic vesicle membrane and allows for Zn to move inside or outside. Not all ionophores can assist zinc in crossing both membranes. Pyrithione, for example allows zinc to cross both membranes, whereas clioquinol allows zinc to cross only the cell membrane.

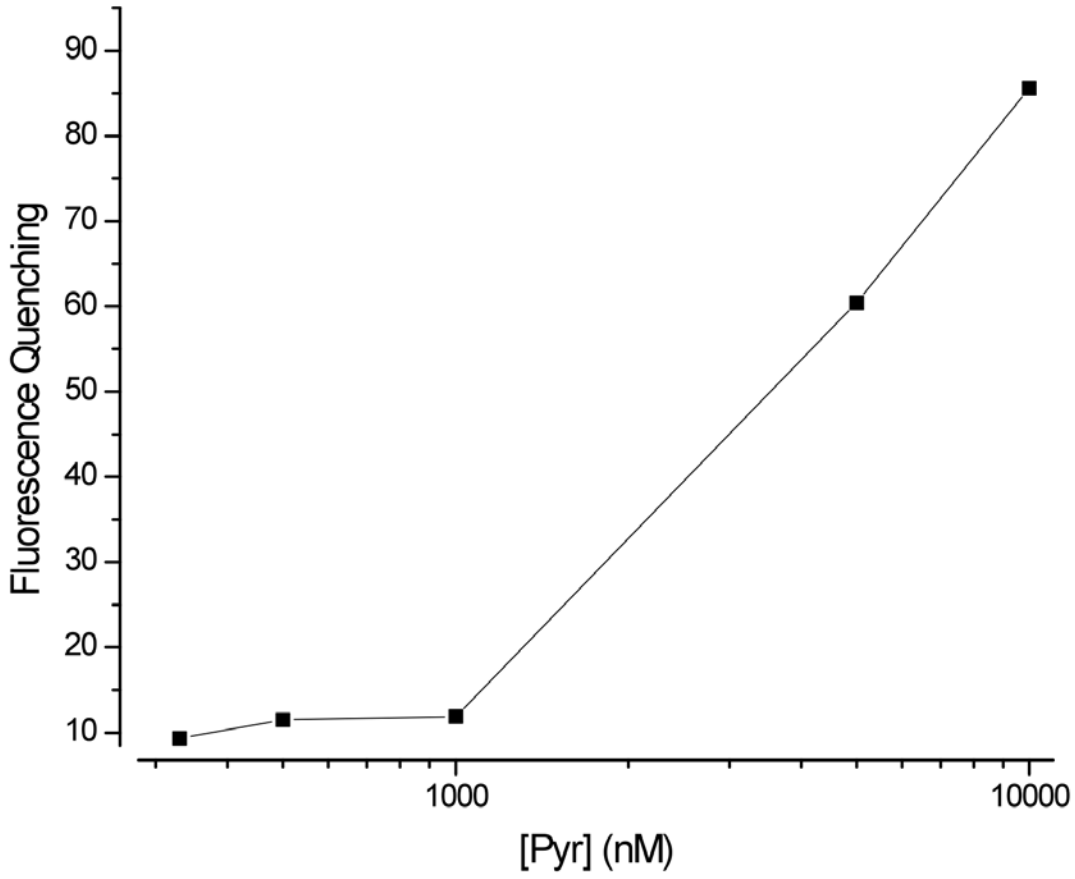

Figure 52. ZnAF-2 quenching vs Pyrithione concentration

Note: Spectrofluorimeter experiments where varying concentrations of pyr were added to 500 nM ZnAF-2 in the presence of 10 μM zinc. The fluorescence is given as the total drop in fluorescence with pyrithione addition.

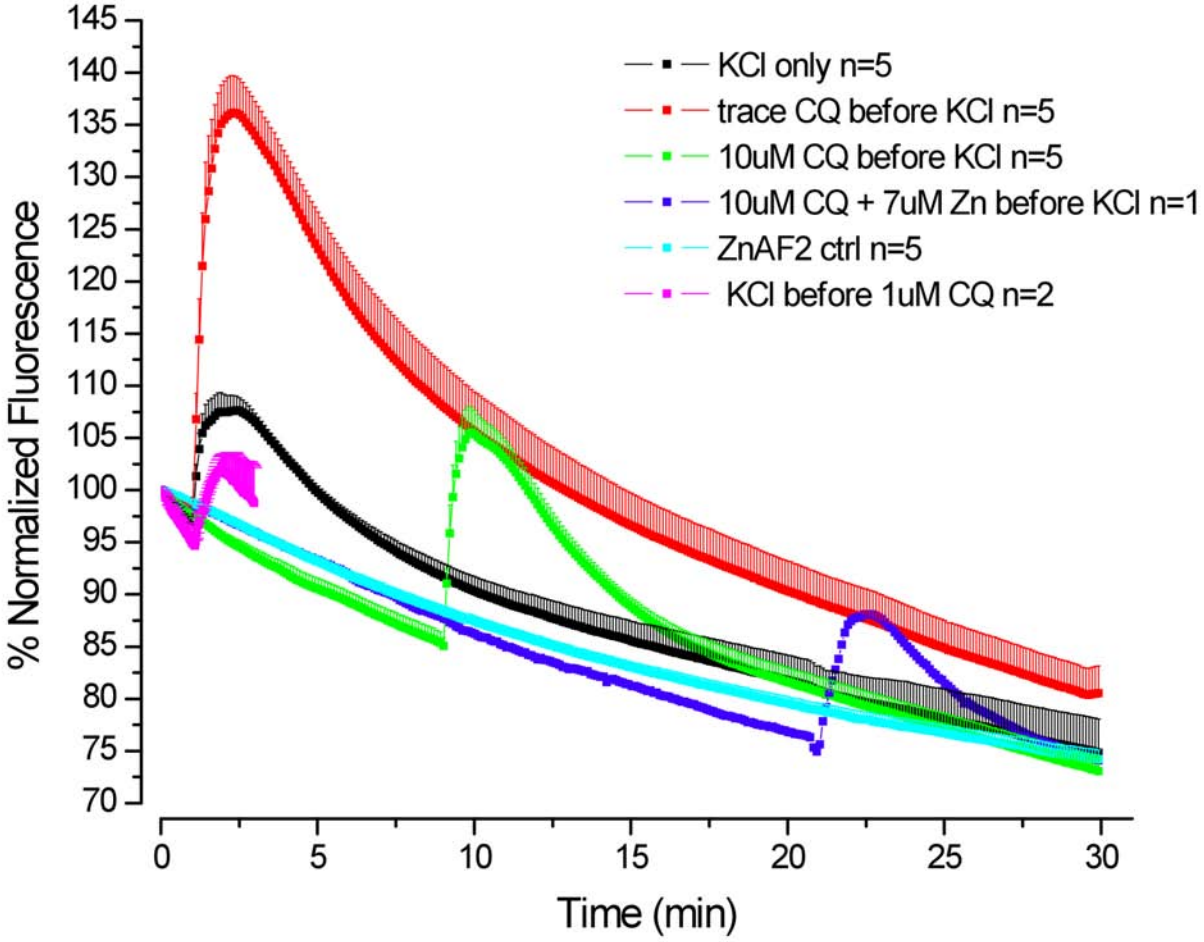

Figure 53. Effect of Clioquinol (CQ) on the fluorescence increase upon KCl stimulation

---

Note: Black curve – KCl stimulated slices only. Red curve – KCl stimulated slices after traces of CQ. Green curve – KCl stimulated slices after 10 μM CQ application for 5 min. Blue curve – 10 μM CQ and 7 μM Zn co-application before KCl stimulation. Aqua curve – ZnAF-2 control and magenta curve – KCl stimulation before 1 μM CQ application.

Table 2. Effect of Multiple KCl stimulations in the presence and absence of chelator on stripping of externalized and/or veneer zinc

	1 KCl stimulations after EDTA n=30	11 KCl stimulations with EDPA n=16	11 KCl stimulations no EDPA n=16	ZnAF-2 control n=45
Average Initial Value (AU)	316	194	291	319
SEM	12	9	17	12

Table 3. Effect of pH change due to NH_4Cl treatment of slices upon zinc stocking of synaptic vesicles

	NH_4Cl then ZnAF-2 (n=22)	ZnAF-2 control (n=13)
Average Initial Value (AU)	429	421
SEM	13	10

CHAPTER VII.*
ROLE OF NERVE GROWTH FACTOR APPLICATION TIME ON PC12 CELL RESPONSE TO KCL INDUCED STIMULATION

Introduction

The study of the underlying molecular mechanisms of differentiation is critical for a better understanding of development related diseases and subsequent regenerative medicine strategies. Neural stem cell-based replacement therapies have been suggested for a wide-range of neurological disorders, such as epilepsy, Parkinson's disease, amyotrophic lateral sclerosis (ALS) and Huntington's disease. Successful therapeutic strategies require a better understanding of the molecular mechanisms that can be used to control cellular phenotype fate as well as spatially dictate growth properties. It is widely known that neural stem cells have the ability to differentiate into mature progeny of neurons, astrocytes, oligodendrocytes and even smooth muscle cells (Erikkson et al., 1998; Ming and Song, 2005; Qian et al., 1997). The human brain manufactures trophic factors in both damaged and undamaged tissues to sustain and strengthen synaptic survival (Erikkson et al., 1998; Fallon et al., 2000; Magavi et al., 2000; Palmer et al., 1999; Qian et al., 1997; Sawamoto et al., 2006; Sun et al., 2003). The formation of neuronal connections is mainly dependent on growth factors and cytokines (Lu et al., 2003) and pre- and post-synaptic differentiations are spatiotemporally coordinated (Akerud et al., 2001; Erikkson et al., 1998; Santiago et al., 2005; Sun et al., 2003). Fibroblast growth factor, collagen IV and β2-laminins are some of the signaling molecules required to transform neurites (neuronal-like extensions) into fully functioning nerve terminals (Fox et al., 2007). Crucial cell-to-cell communication and signal

---

* This work was done under Dr. Donald M. Cannon.

transduction needed for neuronal differentiation and synaptogenesis is achieved through endo- and exocytosis. Signaling molecules (trophic factors) are released in the extracellular space through exocytosis. These molecules are then internalized through endocytosis into neighboring cells, thus triggering cellular changes. In neuronal cells these two processes are tightly regulated and do not occur at random, but only through external stimuli (i.e. ligand binding) (Sagi-Eisenberg, 2007).

The mechanisms of neural differentiation are difficult to observe in complex mammalian systems. Single cell analysis can provide a fundamental perspective by simplifying this complexity as well as providing a glimpse into the individual behavior of each single cell (Cannon Jr. et al., 2000). Pheochromocytoma (PC12) cells have been extensively used as a good single cell neuronal model. If stimulated with elevated K^+ (100 mM) isotonic solution, PC12 cells undergo vesicular exocytosis in a Ca^{2+}-dependent manner and release catecholamines (dopamine) (Greene et al., 1987; Greene and Tischler, 1976). They also differentiate and form neurites when exposed to nerve growth factor (NGF) (Greene et al., 1987; Greene and Tischler, 1976). NGF is a growth factor that promotes neuronal outgrowth and survival, as well as plasticity (Cohen et al., 1978; Nishida et al., 2007). NGF binding to TrkA receptors facilitates neurite formation by promoting p53 binding to DNA (Brynczka et al., 2007; Brynczka and Merrick, 2007).

Optical microscopy has provided a useful analytical tool for single cell analysis. In particular fluorescence microscopy offers chemical specificity and higher sensitivity needed to understand intricate molecular information. Fluorescence microscopes are relatively inexpensive and readily available while the pool of available fluorescent dyes has increased. In this study, a well-known membrane potential dye, FM 1-43, was used to interrogate exocytotic events in differentiated and undifferentiated PC12 cells. FM 1-43 is a styryl dye that was first synthesized by Betz *et al*. in the early 1990's as an improvement on its precursor (Betz et al., 1992; Betz et al., 1996). FM 1-43 has been used extensively to study the process of exo- or endo-trafficking in many neuronal

systems due to three properties (Carrasco et al., 2007; Cochilla et al., 1999; Henkel et al., 1996a; Kasai et al., 2005; Kay et al., 1999; Kishimoto et al., 2005; Liu et al., 2005; Morgenthaler et al., 2003; Prange and Murphy, 1999; Staple et al., 1997; Zhang et al., 2007). It has a tail that consists of a four carbon chain, aiding partition into membranes, it reversibly partitions into the membrane and cannot cross within the cytoplasm due to the positive charge it carries and finally it fluoresces weakly in a polar medium such as water, but its fluorescence quantum yield increases as it partitions into the membrane (Betz et al., 1996; Henkel et al., 1996b). We have developed an advanced FM 1-43 fluorescent microscopy protocol with the necessary sensitivity and resolution to distinguish between functional differences of single PC12 cells at various stages of differentiation. Our method of staining does not invoke bulk stimulation as in most reported studies, but allows for individual cell stimulation. We have utilized ADVASEP-7, a chelating agent for FM 1-43, to remove background interferences from unbound dye (Kay et al., 1999). This has permitted us to view the appearance of brightly lit vesicles and distinguish between exocytotic release patterns in NGF-treated as compared to non-treated PC12 cells. The observed exocytotic differences are primarily associated with the amount and spatial location of release sites and are dependent on the time of NGF treatment (no treatment, 5 day and 14 day NGF treatment). Our experiments support the hypothesis that PC12 cells treated with NGF for a varying amount of time express different phenotypes manifested in differences in exocytosis patterns.

Experimental Methods

Chemicals and isotonic solutions

All chemicals were purchased from Sigma Aldrich unless otherwise specified. Chemicals: RPMI (Gibco), horse serum, fetal bovine serum, penicillin, streptomycin, amphotericin B, nerve growth factor, NaCl, KCl, $MgCl_2 \cdot 6H_2O$, HEPES, glucose, $CaCl_2 \cdot 2H_2O$, collagen (Vitrogen), poly-l-lysine, ethanol, H_2SO_4, 30% H_2O_2.

Isotonic/HEPES solution was prepared with autoclaved water and had the following concentrations: in mM: 150 NaCl; 5 KCl; 1.2 $MgCl_2$•$6H_2O$; 10 HEPES; 5 glucose; 2 $CaCl_2$•$2H_2O$. Isotonic elevated K^+/HEPES solution was prepared in the following concentration: in mM: 55 NaCl; 100 KCl; 1.2 $MgCl_2$•$6H_2O$; 10 HEPES; 5 glucose; 2 $CaCl_2$•$2H_2O$.

Cell Culture

PC12 cells were generously provided by Dr. Andrew G. Ewing's lab, University of Pennsylvania. Cells were maintained in 85% RPMI media supplemented with 10% horse serum, 5% fetal bovine serum, 68 mg/L penicillin, 100 mg/L streptomycin and 10 mL/L amphotericin B. The cells were incubated in T-25 flasks at 37^oC, 7% CO_2 and 100% humidity environment. Cells were continually monitored through a CKX31 Olympus microscope to ensure sterility and were split every 6-7 days after confluency was reached. Undifferentiated PC12 cells were plated and experiments were conducted after at least 2 hours of plating. No cells were plated on the same day as splitting occurred, since it was found that PC12 cells do not release well soon after splitting.

Differentiated cells were first primed with 5 μL NGF (20 ng/mL) for 5 days and then plated on coverslips coated with a cell adhesion layer. Priming PC12 cells with NGF before plating causes them to differentiate faster once plated on a coated surface. Cells were allowed to differentiate for at least 5 days before fluorescence studies were performed.

Coverslip Preparation

Glass coverslips were first Piranha etched in a 1:4 mixture of 30% H_2O_2 and H_2SO_4 to remove any impurities and organic materials from the glass surface. The coverslips were then rinsed twice in isopropanol and dried under an ultra high purity nitrogen stream. The coverslips were then submerged in a collagen/poly-l-lysine mixture for at least an hour. The cell adhesion mixture was prepared from 1:25:50 collagen to

30% EtOH to poly-L-lysine (0.1mg/mL). The coverslips were then allowed to air-dry overnight in a sterile environment. Before plating, the coverslips were submerged in a balanced salt HEPES solution for at least 15 minutes to equilibrate the pH to 7.4.

Fluorescence Setup

Cells attached to coverslips were placed in a 2 μM FM 1-43 solution and were stimulated through a borosilicate stimulation pipette pulled to ~10 μm diameter through a Sutter CO_2 laser puller. Stimulation pipettes were filled with elevated K^+ solution and placed ~ 150 μm from adherent cells using Narishige micromanipulators. Nanoliter volumes of elevated K^+ solution were released through a General Valve picospritzer® III (pressure 5 psi and pulse duration 3 s) calibrated with mineral oil.

Exocytosis control experiments were conducted with 2 mM EDTA in isotonic solution. ADVASEP-7 (β-cyclodextrin derivative a generous gift from Dr. Alan Kay, UI Department of Biology) was added to stimulated cells approximately 5min after the stimulation sequence was collected to enhance FM 1-43 fluorescence.

Fluorescence Hardware

All images were acquired with an Olympus IX71 inverted fluorescence microscope through a FITC channel (exc. 510 / em 525 nm). The microscope is equipped with an ORCA camera. Images were collected at 2x2 binning at 12.5% output intensity. Exposure time was 15 ms and gain was zero. Images were collected as image sequences with a 1 s interval and were analyzed through WASABI (Hamamatsu software) and ImageJ (NIH software).

Safety

Piranha etching is a dangerous procedure and needs to be conducted with the highest precaution and full personal protective wear.

Results and Discussion

Loading of FM 1-43 in undifferentiated (0 day NGF treatment) PC12 cells

PC12 cells are a well-established model neuronal cell line that has shown exocytotic release in both the undifferentiated and differentiated phenotype states (Kishimoto et al., 2005; Liu et al., 2005; Westerink et al., 2000; Zerby and Ewing, 1996). It has previously been electrochemically established that differentiated (NGF- treated) PC12 cells release mostly from varicosities (swelling along neurites) and less from the cell body, (Zerby and Ewing, 1996) while undifferentiated cells release only from the cell body. It is not known however, if there is a difference in release patterns between cells that have been allowed to differentiate at varying times. We have utilized an FM 1-43 fluorescence assay to study differences in exocytotic release patterns in undifferentiated and differentiated cells. In most studies FM 1-43 has first been loaded into the cells/tissue by placing them in elevated K^+ solution, which induces bulk stimulation. The cells/tissue are then re-stimulated and the decrease in fluorescence intensity is observed. We have chosen to monitor the loading of FM 1-43 into PC12 cells, because the separation between photobleaching and de-loading of the dye is analytically more difficult (both appear as a decrease in dye fluorescence). Our FM 1-43 loading set up also affords single cell stimulation as opposed to bulk stimulation, allowing for discrimination of individual cell behavior.

Upon stimulation with 100 mM K^+ isotonic solution undifferentiated PC12 cells display a fully homogeneous cellular fluorescence distribution. The fluorescence image in figure 54a shows that the initial cell fluorescence before cell stimulation is confined only to the outer cell membrane. The fluorescence image in figure 54c displays the same cells after K^+ stimulation and the intracellular fluorescence increase is clearly observed. The resulting fluorescence after stimulation is 2.71 times larger than initial fluorescence

intensity – see filled circles ● curve in figure 55 (intensity values were normalized to first value). This substantial increase corresponds to a large-scale exocytosis occurring in PC12 cells, which can be explained by both large and small dense core vesicle fusion, as previously seen in literature (Westerink et al., 2000). As previously mentioned the loading of FM 1-43 into PC12 cells revealed through the large scale fluorescence intensity increase is unequivocal, as compared to the de-loading of the dye where fluorescence intensity changes are more subtle and entwined with photobleaching effects. To determine whether this fluorescence intensity increase is truly due to Ca^{2+}-dependent vesicular exocytosis through elevated K^+ stimulation and not from other non-exocytic pathways, the dye solution is prepared in 2 mM EDTA and the stimulation experiments are repeated.

Loading of FM 1-43 in undifferentiated PC12 cells in the presence of EDTA

The EDTA/isotonic solution is a classical control for verifying exocytosis, specifically by chelating available Ca^{2+} ions required for vesicle fusion. The open circles in the figure 55 graph represent undifferentiated cell stimulation through elevated K^+ in the presence of 2 mM EDTA. Fluorescence intensity does not increase as in filled circles ● curve; in fact it decreases by 14.85 ±1.0%. This slow decrease is due to photobleaching effects from continuous illumination during data collection (50 images at 1 s interval). In the absence of an extracellular Ca^{2+} source, K^+ stimulation of PC12 cells does not induce vesicular exocytosis, therefore FM 1-43 does not enter the cell and an increase in fluorescence intensity is not observed as in the stimulated cells in the absence of EDTA. In addition, when stimulation is performed with elevated Na^+ isotonic solution instead of K^+, the same results are obtained. These results exclude the possibility that the observed increase in fluorescence intensity is due to any mechanical force exerted on the cell by fluid movement causing a temporary membrane disruption and a different way for FM 1-

43 to enter the cell.

ADVASEP-7 addition to non-stimulated undifferentiated cells

In our fluorescence assays we have utilized ADVASEP-7 (100 nM), a β-cyclodextrin derivative that acts as a chelating agent for FM 1-43 and also increases its fluorescence (for structure see (Kay et al., 1999)). When administered to the extracellular medium, ADVASEP-7 sequesters unbound and outer membrane leaflet bound FM 1-43 and the complex diffuses away, which is manifested as a drop in fluorescence from stained cells. ADVASEP-7 is not membrane permeable, so if the dye is internalized through vesicle re-uptake, it cannot be chelated. ADVASEP-7 is first added to non-stimulated undifferentiated cells to test whether it removes FM 1-43 from the membrane of these cells (see graph in figure 56). The drop in fluorescence intensity for undifferentiated cells is 80.4 ± 7.3% verifying that ADVASEP-7 removes unbound or outer membrane bound FM 1-43, and the interference from background fluorescence.

ADVASEP-7 addition to stimulated undifferentiated cells

As previously stated, the large intracellular fluorescence increase observed for undifferentiated cells is due to K^+ stimulation. EDTA control experiments however cannot fully determine that FM 1-43 is internalized into the cells. To determine that the observed fluorescence intensity increase during stimulation is due to FM 1-43 internalization, ADVASEP-7 is added to stimulated undifferentiated cells, approximately 5 min after the stimulation sequence is collected. The initial fluorescence intensity increase after stimulation for undifferentiated cells is 171.1 ± 42.6%, however the subsequent fluorescence intensity drop due to ADVASEP-7 addition is only 18.2 ± 6.2%. Since fluorescence intensity values do not drop to baseline values, but FM 1-43 fluorescence decreases by only a fraction (0.7%) of total fluorescence (see figure 55), the dye has been internalized through vesicle reuptake. Therefore, the intensity drop after

ADVASEP-7 addition to stimulated cells is due to the chelation of outer membrane bound and extracellular free dye. This conclusion is strongly supported by the graph in figure 55, which shows the stimulation and ADVASEP-7 sequences for undifferentiated cells in the absence (filled circles and filled triangles respectively) and presence of EDTA (open circles and open triangles). The ADVASEP-7 addition to stimulated cells in the presence of EDTA (open triangles) causes a drop in FM 1-43 fluorescence intensity of 89.9 ± 3.6% as opposed to only 18.2 ± 6.2% for stimulated cells in the absence of EDTA.

The addition of ADVASEP-7 to stimulated cells has also enabled us to view where the internalized FM 1-43 accumulates. The graph in figure 57 shows line profiles for a cell before (filled circles), mid-way (open circles) and end of stimulation (open diamonds) as well as after ADVASEP-7 addition (open squares). These line profiles show that FM 1-43 accumulates around the nucleus, which supports previous results that internalized fluorescent beads in Tetrahymena are transported directly to the nucleus (Hosein et al., 2005). The beads trapped in endozomes do not linger in the cytosol, but are moved through a direct route to the nucleus of the cell. This direct transport to the nucleus can shorten the response time of the cell to outer stimuli and trigger immediate signaling events and cellular changes. Our data supports this finding for stimulated PC12 cells, although the finer structure of dye accumulation around the PC12 cell nucleus is more apparent in differentiated cell line profiles (see discussion about stimulated differentiated cells).

Loading of FM 1-43 in NGF-treated PC12 cells

Differentiated cells display very different stimulation patterns than undifferentiated cells. These differences are primarily associated with the amount and spatial location of release sites. The sensitivity needed to observe the differences in release patterns was obtained through the use of our highly resolved fluorescence imaging setup and ADVASEP-7, which enhances intracellular fluorescence by chelating

FM 1-43 from the outer cell membrane (Kay et al., 1999). This setup has allowed us to observe the loading of FM 1-43 into cells with little interference from outer membrane associated dye, translating into lower background interference and providing high spatial resolution and sensitivity. As mentioned, stimulated undifferentiated PC12 cells exhibit a fully homogeneous cellular fluorescence distribution, whereas fluorescence intensity increase in cells that are allowed to differentiate for 5 days is manifested by the appearance of discrete bright spots in both the cell body and neurites (figure 58). Even though the fluorescence intensity increase manifested through these bright spots was even larger than for undifferentiated cells (fluorescence intensity increased as much as 324% for some of the bright spots and as low as 130%), it is not as massive, thus exocytosis is more limited in differentiated cells. This may correspond to exocytosis of only a certain type of vesicle (either large or small dense core vesicles, instead of both). Also, even though our set up provides us with high spatial resolution, it does not allow for predicting if these bright spots are individual vesicles or a junction of multiple vesicles (though most of the larger and brighter spots are obviously made up of more than one vesicle).

Loading of FM 1-43 in differentiated PC12 cells in the presence of EDTA

The stimulation of differentiated PC12 cells in the presence of EDTA is expected to follow the same results as the stimulation of undifferentiated cells in the same conditions since the principle is the same. Indeed, fluorescence intensity after K^+ stimulation in the presence of EDTA for differentiated cells decreases by 25.2 ± 5.6% due to photobleaching similar to undifferentiated cells (see graph in figure 59). EDTA removes the extracellular Ca^{2+} source and inhibits K^+ stimulation of vesicular exocytosis in differentiated PC12 cells, thus FM 1-43 internalization is not observed. The decrease in fluorescence intensity from differentiated cells is statistically the same as the decrease in undifferentiated cells.

ADVASEP-7 addition to non-stimulated differentiated cells

The same ADVASEP-7 addition to non-stimulated undifferentiated cells is performed with differentiated cells (see figure 56). The drop in fluorescence intensity levels after ADVASEP-7 addition to the non-stimulated differentiated cells is 90.7 ± 4.8%, verifying that free floating and outer membrane bound FM 1-43 is chelated. The fluorescence intensity drop for non-stimulated differentiated cells is similar to that for undifferentiated cells.

ADVASEP-7 addition to stimulated differentiated cells

The fluorescence intensity drop after ADVASEP-7 addition to stimulated differentiated cells in the absence of EDTA is calculated *after* the appearance of the bright spots, which become visible only after the removal of membrane bound FM 1-43 and the bulk fluorescence. Therefore the time frame of this sequence is approximately half of the same ADVASEP-7 addition sequence to stimulated undifferentiated cells. The drop in fluorescence for the ADVASEP-7 addition to stimulated differentiated cells in the absence of EDTA is 57.8 ± 28.5% (see figure 59 – open circle). The addition of ADVASEP-7 to stimulated differentiated cells has been crucial to uncovering the appearance of these bright spots. As ADVASEP-7 removes FM 1-43 bound to the membrane, the bright spots begin to appear and their movement within the cell can be observed.

ADVASEP-7 addition to stimulated differentiated cells in the presence of EDTA indicates that stimulated differentiated cells do not internalize the dye, as fluorescence intensity drops by 93.5 ± 6.4% (figure 59 – open squares). Therefore the dye pathway of entry into the cells (be they undifferentiated or differentiated) is through Ca^{2+}-dependent vesicular fusion, since the dye does not become internalized in the presence of EDTA.

ADVASEP-7 removal of FM 1-43 from stimulated differentiated cells provides a clearer picture not only of vesicular release, but also of the dye accumulation in the cell

as mentioned earlier. The line profile in figure 60 shows the fluorescence intensity of a stimulated differentiated cell as a function of the distance across the cell body (through the nucleus). The low region of fluorescence intensity corresponds to the nucleus area. The highest and most concentrated fluorescence intensity is around the nucleus indicating that FM 1-43 is clustered around the nucleus, supporting recent findings. Once again this quick transport of the endozome contents directly to the nucleus could be vital to how a cell responds and adapts to its surrounding environment.

Our most important finding is the difference in release patterns between cells that are allowed to differentiate for varying amounts of time (no treatment, 5 day and 14 day NGF treatment). Undifferentiated cells undergo a massive whole cell exocytotic release manifested in large-scale fluorescence increase. Cells that have been differentiated for 5 days release less than undifferentiated cells, mostly from the cell body and less from neurites. The fluorescence intensity increase is observed as the appearance of discrete bright spots, instead of whole cell fluorescence increase. This indicates that as the cells start to differentiate into a different phenotype, the exocytotic release lessens. This becomes even more evident with cells that are allowed a longer differentiation time (14 days). They release mostly around the cell body and much less in neurites even compared to cells that have differentiated for 5 days (see images in figure 61b and 61c). It is not very apparent from these experiments as to why the cells that have been allowed to differentiate longer release less and why release is spatially dependent. It is clear however that these cells express a different phenotype than undifferentiated cells.

Conclusion

Undifferentiated and differentiated PC12 cell exocytotic release patterns are compared and differences in the amount and spatial location of the release sights are found. Understanding the molecular basis of NGF interaction with PC12 cells to bring about these differences in phenotype expression can lead to increased insight about the

process of differentiation and provide a more accurate manipulation of the mechanism of differentiation itself.

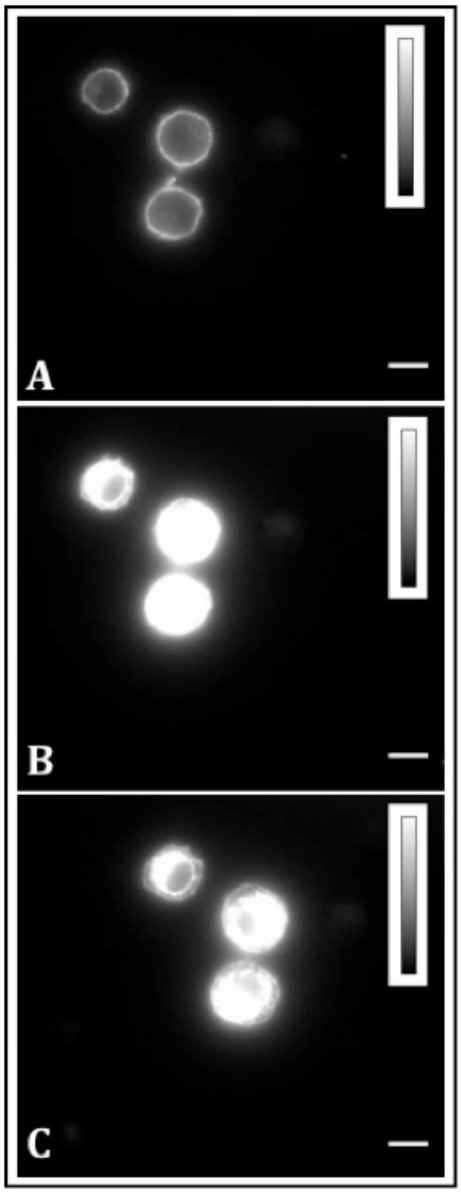

Figure 54. Fluorescence images of undifferentiated PC12 cells bathed in 2 μM FM 1-43/isotonic extracellular solution

---

Note: (A) undifferentiated cells before elevated K^+ stimulation. (B) same undifferentiated cells after elevated K^+ stimulation sequence is collected (50s). (C) same undifferentiated cells after ADVASEP-7 addition to the extracellular medium. Scale bar is 10 μm and intensity scale is 10 to 3900.

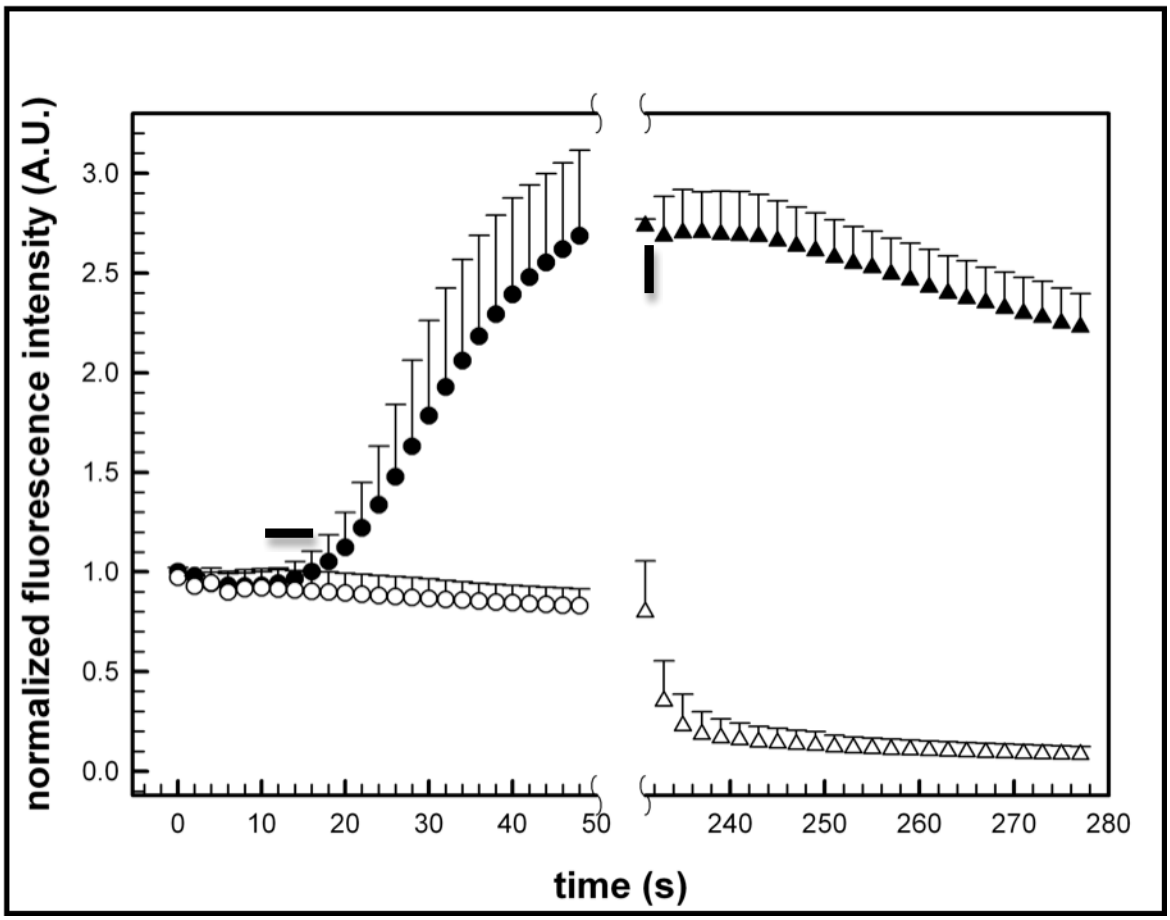

Figure 55. Normalized fluorescence vs. time validating exocytosis via EDTA/Ca^{2+} chelation control experiments in undifferentiated cells

---

Note: Filled circles - normalized FM 1-43 fluorescence intensity as a function of time during and after elevated K^+ stimulation of undifferentiated cells. Filled triangles - normalized FM 1-43 fluorescence intensity as a function of time after ADVASEP-7 addition (5 min after the elevated K^+ stimulation sequence was collected). Open circles - normalized FM 1-43 fluorescence intensity during and after elevated K^+ stimulation of undifferentiated cells in the presence of EDTA. Open triangles - normalized FM 1-43 fluorescence intensity as a function of time after ADVASEP-7 addition to stimulated undifferentiated in EDTA solution. Horizontal bar ─ time of K^+ stimulation, vertical bar ─ ADVASEP-7 addition to stimulated cells (n = 12).

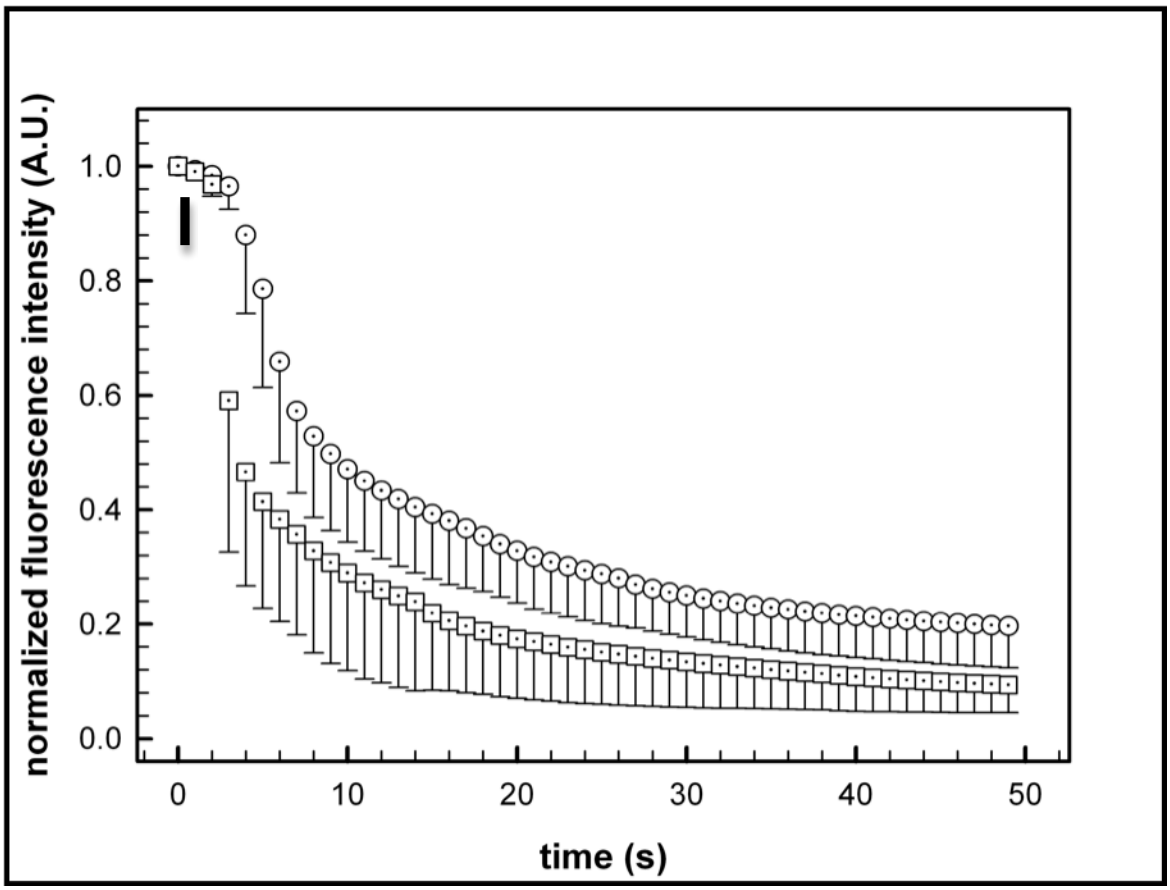

Figure 56. Normalized fluorescence vs. time for ADVASEP-7 addition to non-stimulated undifferentiated and differentiated cells

---

Note: Dotted circles - normalized fluorescence intensity as a function of time after ADVASEP addition to non-stimulated undifferentiated cells. (n = 10) Dotted squares - normalized fluorescence intensity as a function of time after ADVASEP addition to non-stimulated differentiated cells (n = 5). Vertical bar ─ ADVASEP-7 addition.

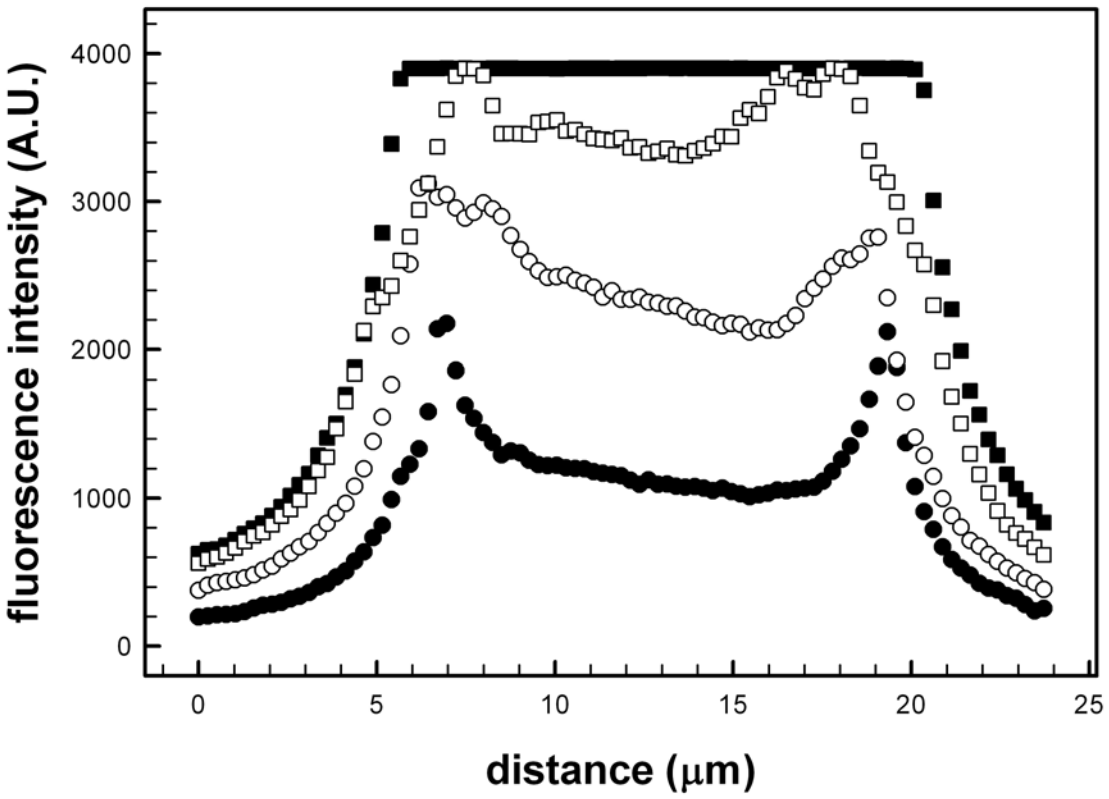

Figure 57. Fluorescence intensity line profiles of cell 3 (bottom cell) in figure 54

Note: Closed circles - fluorescence intensity as a function of distance before elevated K^+ stimulation of an undifferentiated PC12 cell. Open circles - fluorescence intensity as a function of distance mid-way through elevated K^+ stimulation of the same cell. Closed squares - fluorescence intensity as a function of distance at the end of elevated K^+ stimulation. Open scquares - fluorescence intensity as a function of distance after ADVASEP-7 was added to the previously stimulated cell. Line profiles were analyzed through ImageJ.

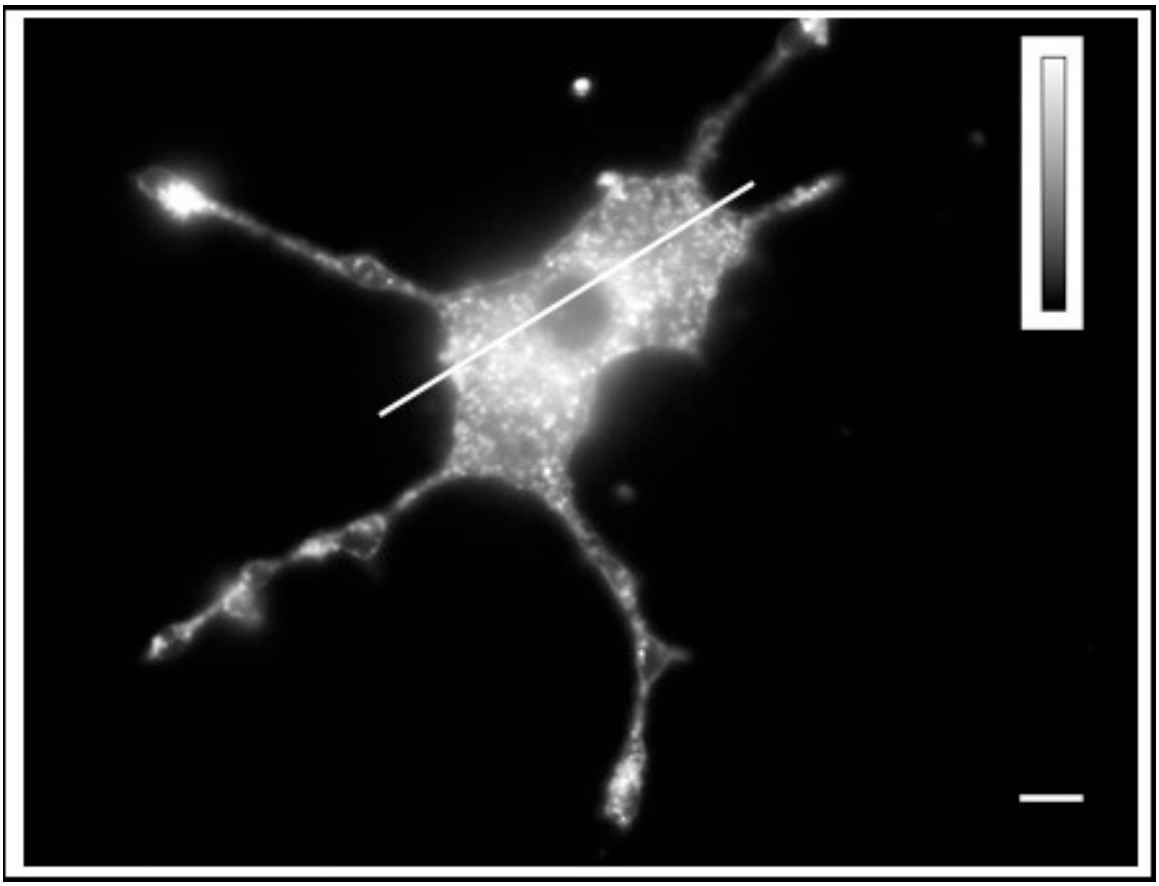

Figure 58. FM 1-43 fluorescence of a cell treated with 20 ng/mL NGF followed by plating for 5 days

---

Note: ADVASEP-7 addition to a stimulated differentiated cell allows the appearance of brightly fluorescent spots in the cell body and neurites. Scale bar is 10 μm and intensity bar is 100 – 2800). Line across cell was used to extract a cell line profile (see figure 60).

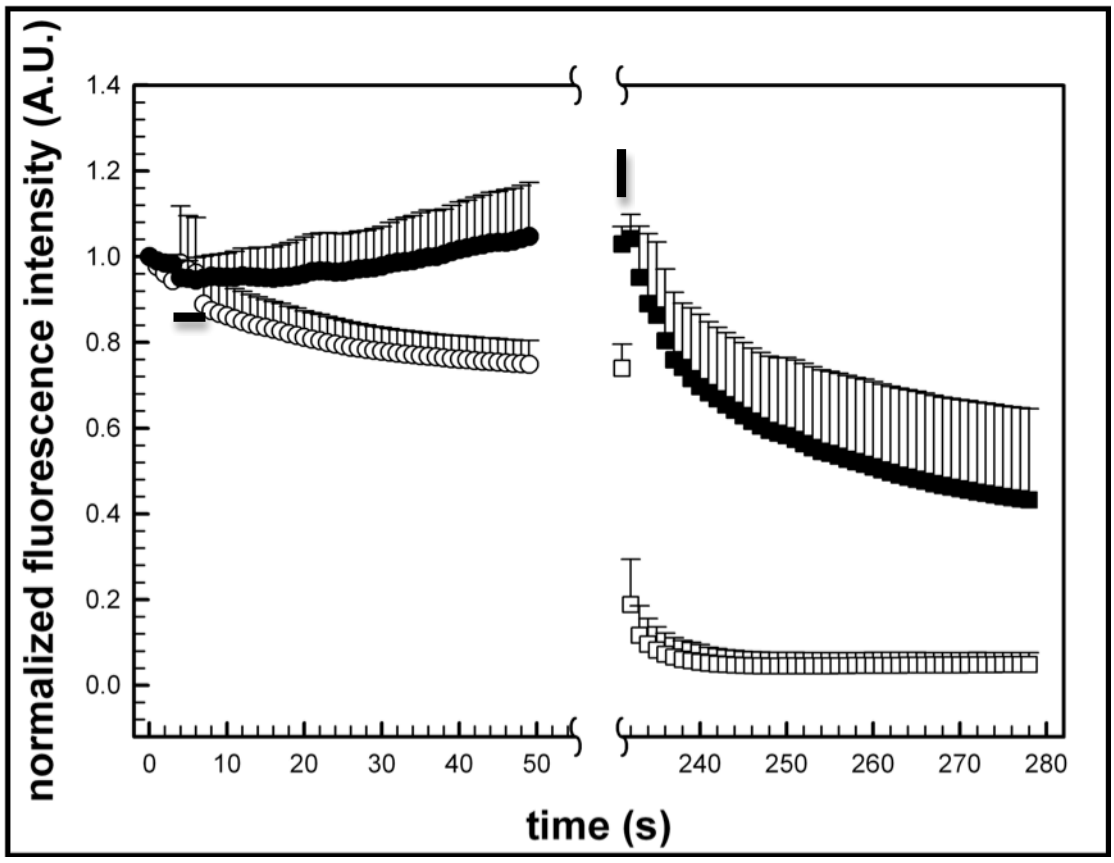

Figure 59. Normalized fluorescence intensity vs. time validating exocytosis via EDTA/Ca^{2+} chelation control experiments in differentiated cells

---

Note: Filled circles - normalized FM 1-43 fluorescence intensity as a function of time during and after elevated K^+ stimulation of differentiated cells. Filled squares - normalized FM 1-43 fluorescence intensity as a function of time after ADVASEP-7 addition (5 min after the elevated K^+ stimulation sequence was collected). Open circles - normalized FM 1-43 fluorescence intensity during and after elevated K^+ stimulation of differentiated cells in the presence of EDTA. Open squares - normalized FM 1-43 fluorescence intensity as a function of time after ADVASEP-7 addition to stimulated differentiated in EDTA solution. Horizontal bar ─ time of K^+ stimulation, vertical bar ─ ADVASEP-7 addition to stimulated cells (n = 5).

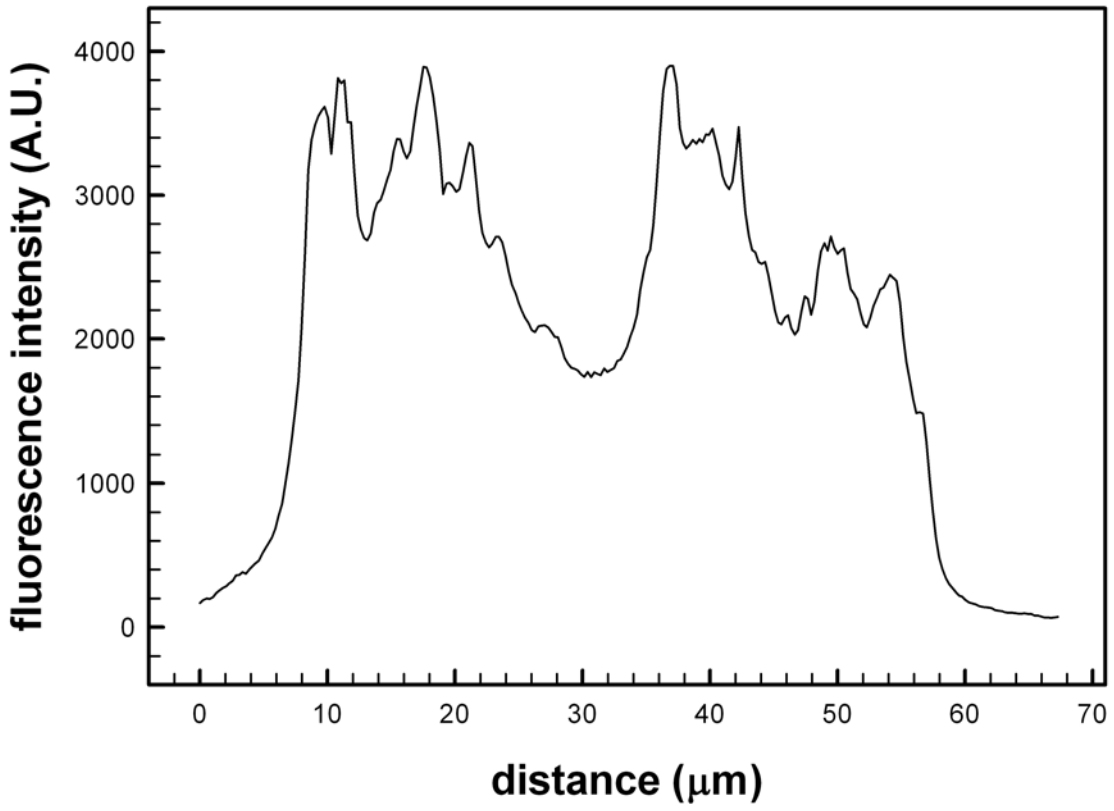

Figure 60. Fluorescence intensity line profile for the differentiated cell in figure 58

Note: The addition of ADVASEP-7 to a stimulated differentiated cell provides the ability to view finer structures due to removal of background fluorescence. Line profile was analyzed through ImageJ.

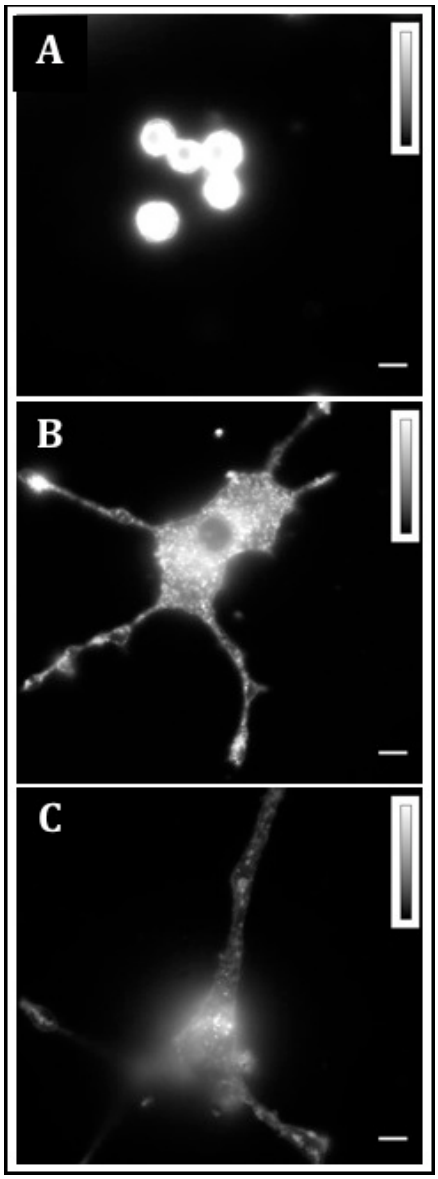

Figure 61. Fluorescence imagess showing spatial differences in exocytosis sites in PC12 cells as a function of their degree of differentiation caused by NGF incubation

---

Note: (A) Non-differentiated, (B) primed for 5 days followed by 5 day plating, and (C) primed for 5 days followed by 2 weeks plating. Scale bars are 10 μm and intensity bars are 5 to 3910.

CHAPTER VIII.

SUMMARY AND FUTURE DIRECTIONS

The main goal of this research was to characterize vesicular zinc behavior during stimulation using zinc-selective fluorescent probes. The current working hypothesis in the field is that zinc is fully released upon cell stimulation and is free to diffuse in the synaptic cleft. After being released in the extracellular space, zinc is then able to bind to receptors on the post-synaptic membrane and modulating the post-synaptic cell response to the neurotransmitter glutamate. This hypothesis is built upon the fact that zinc is found in very high concentrations (greater than 300 μM) in certain synaptic vesicles that contain the neurotransmitter glutamate. This zinc is called chelatable zinc, since it can be visualized via zinc-selective fluorescent probes and histochemical methods. Exogenously applied zinc is also found to modulate many different ion channels and receptors in both the pre- and post-synaptic cells. To better understand the dynamics of zinc release from synaptic vesicles, we utilized zinc-selective fluorescent probes (which become fluorescent only upon zinc binding) to visualize the hypothesized zinc release.

We chose to study the hippocampus, although there are other areas of the brain that contain large concentrations of zinc in the synaptic vesicles, because the hippocampus contains a beautiful separation between the cell body and the synaptic terminal layers. This demarcation of layers allows us to study the synaptic zinc unhindered by fluorescence artifacts that can arise from the cell body layer. We also chose to use fluorescence imaging, because it provides a visualization tool for detecting synaptic zinc. Electrical recordings are not able to provide an image of whether zinc is being released or not. Other methods used to determine zinc release such as atomic absorption spectroscopy also fall short in establishing topographically if zinc is released and where it translocates after its release.

Stimulation of slices loaded with zinc-probes causes a large and persistent increase upon vesicle fusion and does not dissipate with continuous washing as would be expected if zinc were being released. This result suggests that zinc is being "externalized" while it still remains bound to a molecule or protein in the synaptic membrane in the form of a ternary complex. Experiments were also conducted to understand whether the increase in fluorescence is due to pH effects on the fluorescent probes. Part of the increase in fluorescence comes from pH effects, but a change in quantum yield induced by a pH increase is not enough to explain all the increase in fluorescence observed upon stimulation. pH effects on the fluorescent probes also do not explain why the fluorescence does not fall below control slices as would be expected if zinc were being released in the extracellular space.

Experiments conducted with extracellular zinc applications revealed that concentrations of zinc higher than about 6 μM lead to zinc-phosphate precipitate formation. The addition of an amino acid such as histidine facilitates zinc uptake by increasing zinc solubility in the extracellular space. The formation of zinc-phosphate precipitates also suggest that zinc may not be freely released upon stimulation as the local concentration of zinc after release would be large (certainly greater than the threshold we found for precipitate formation) and would cause zinc-phosphate precipitation to occur.

We used fluorescent probes to study zinc buffering and uptake in hippocampal slices. In these slices, the separation between the cell body layer and the synaptic terminal layer is very clear and zinc influxes in the cytoplasm and synaptic vesicles could be followed without interference. We found that exogenously applied zinc in the presence of a zinc ionophore, induces a large and persistent increase in fluorescence signal indicating that zinc is transported to vesicles or cellular compartments. No transient elevations in fluorescence were found, which indicate that zinc is very tightly buffered in the cytoplasm. From our data, there is no clear indication of how zinc passes from the

cytoplasm into vesicles or cellular compartments. It is possible that zinc is immediately bound to metalloproteins such as MT upon crossing the cell membrane.

This work also presents evidence to refute the zinc release hypothesis and provides support for the zinc externalization hypothesis, which states that zinc is externalized as a ternary complex with a synaptic membrane protein or molecule, but is not fully released during synaptic transmission. This conclusion is controversial in the field of synaptic zinc, which holds tightly to the zinc release hypothesis. Externalized zinc presents a challenge to the long held view of zinc release, since it suggests that the role of zinc as neuromodulator needs to be revisited. The fact that zinc is being externalized does not completely refute the idea that zinc is playing a modulatory role during synaptic transmission. Externalized zinc can form a ternary complex with molecules in the synaptic cleft and become internalized, triggering a signaling cascade. We do not exclude the possibility that zinc can move from the pre- to the post-synaptic site, but more slowly than in the unconstrained diffusion model. Nonetheless, work done under the assumption that zinc release hypothesis is true would need to be re-interpreted to allow for the possibility that zinc might just be externalized. How tightly the putative membrane protein hangs onto zinc may be modulated, so in one extreme it may retain it and in the other it may allow zinc to move off relatively freely. More work needs to be done to address the question on whether zinc is sometimes fully released and other times only externalized. Additional work also needs to be done to determine what type of protein or molecule is able to bind zinc inside the synaptic vesicles prohibiting its full release upon vesicle fusion. An additional result that requires further observation is the removal of the zinc veneer and its impact upon synaptic stimulation. It has been known for sometime that the neuronal cell accumulates zinc on the extracellular surface of its membrane, however the role of this zinc is also not well known. Experiments tailored towards understanding the relationship between stripping of zinc veneer and synaptic

release could lead to larger insight into the role of zinc veneer and what the relationship between the zinc veneer and synaptic zinc is.

REFERENCES

(2004). Neuroscience, third edition edn (Sunderland: Sinauer Associates, Massachusetts).

(2007). The hippocampus book (New York: Oxford University Press).

Abebodun, F., and Post, J.F. (1995). Role of intracellular free Ca(II) and Zn(II) in dexamethasone-induced apoptosis and dexamethasone resistance in human leukemic CEM cell lines. J. Cell. Physiol. *163*, 80-86.

Aiken, S.P., Horn, N.M., and Saunders, N.R. (1992). Effects of amino acids on zinc transport in rat erythrocytes. The Journal of Physiology *445*, 69-80.

Akerud, P., Canals, J.M., Snyder, E.Y., and Arenas, E. (2001). Neuroprotection through delivery of glial cell line-derived neurotrophic factor by neural stem cells in a mouse model of Parkinson's disease. J. Neurosci. *21*, 8108-8118.

Allison, J.D. (2003). MINTEQA2 for Windows. (Allison Geoscience Consultants, Inc.).

Assaf, S.Y., and Chung, S.-H. (1984). Release of endogenous Zn from brain tissue during activity. Nature *308*, 734-736.

Barceloux, D.G. (1999). Zinc. J Toxicol Clin Toxicol *37*, 279-292.

Beaulieu, C., R., D., and Cynader, M. (1992). Enrichment of glutamate in zinc-containing terminals of the cat visual cortex. Neuro Report *3*, 861-864.

Begum, N.A., Kobayashi, M., Moriwaki, Y., Matsumoto, M., Toyoshima, K., and Seya, T. (2002). Mycobacterium bovis BCG Cell Wall and Lipopolysaccharide Induce a Novel Gene, BIGM103, Encoding a 7-TM Protein: Identification of a New Protein Family Having Zn-Transporter and Zn-Metalloprotease Signatures. Genomics *80*, 630-645.

Bellocchio, E.E., Reimer, R.J., Fremeau, R.T., Jr., and Edwards, R.H. (2000). Uptake of Glutamate into Synaptic Vesicles by an Inorganic Phosphate Transporter. Science *289*, 957-960.

Bentivoglio, M., and Swanson, L.W. (2001). On the fine structure of the pes Hippocampi major (with plates XIII-XXIII). Brain Research Bulletin *54*, 461-483.

Betz, W.J., Mao, F., and Bewick, G.S. (1992). Activity-dependent fluorescent staining and destaining of living vertebrate motor nerve terminals. J. Neurosci. *12*, 363-375.

Betz, W.J., Mao, F., and Smith, C.B. (1996). Imaging exocytosis and endocytosis. Current Opinion in Neurobiology *6*, 365.

Bird, A., McCall, K., Kramer, M., Blankman, E., Winge, D., and Eide, D. (2003). Zinc fingers can act as Zn(II) sensors to regulate transcriptional activation domain function. EMBO J. *22*, 5137-5146.

Birinyi, A., Parker, D., Antal, M., and Shupliakov, O. (2001). Zinc co-localizes with GABA and glycine in synapsese in the lamprey spinal cord. J Comp Neurol *433*, 208-221.

Bloß, T., Clemens, S., and Nies, D. (2002). Characterization of the ZAT1p zinc transporter from Arabidopsis thaliana in microbial model organisms and reconstituted proteoliposomes. Planta *214*, 783-791.

Bouras, C., Giannakopoulos, P., Good, P.F., Hsu, A., Hof, P.R., and Perl, D.P. (1996). A laser microprobe mass analysis of trace elements in brain mineralizations and capillaries in Fahr's disease. Acta Neuropathol. *92*, 351-357.

Breckenridge, L.J., and Almers, W. (1987). Currents through the fusion pore that forms during exocytosis of a secretory vesicle. Nature *328*, 824-827.

Brynczka, C., Labhart, P., and Merrick, B.A. (2007). NGF-mediated transcriptional targets of p53 in PC12 neuronal differentiation. BMC Genomics *8*, 139.

Brynczka, C., and Merrick, B.A. (2007). Nerve growth factor potentiates p53 DNA binding, but inhibits nitric oxide-induced apoptosis in nuronal PC12 cells. Neurochem. Res. *32*, 1573-1585.

Budde, T., Minta, A., White, J.A., and Kay, A.R. (1997). Imaging free zinc in synaptic terminals in live hippocampal slices. Neuroscience *79*, 347-358.

Burdette, S.C., and Lippard, S.J. (2003). Meeting of the minds: metalloneurochemistry. Proc Natl Acad Sci USA *100*, 3605-3610.

Burdette, S.C., Walkup, G.K., Spingler, B., Tsien, R.Y., and Lippard, S.J. (2001). Fluorescent Sensors for Zn2+ Based on a Fluorescein Platform: Synthesis, Properties and Intracellular Distribution. Journal of the American Chemical Society *123*, 7831-7841.

Burton, R.F. (1975). Ringer solutions and physiological salines (John Wright & Sons).

Cannon Jr., D.M., Winograd, N., and Ewing, A.G. (2000). Quantitative chemical analysis of single cells. Annu. Rev. Biophys. Biomolec. Struct. *29*, 239-263.

Canzoniero, L.M., Manzerra, P., Sheline, C.T., and Choi, D.W. (2003). Membrane-permeant chelators can attenuate Zn2+ -induced cortical neuronal death. Neuropharmacol. *45*, 420-428.

Canzoniero, L.M., and Sensi, S.L. (1997). Measurement of intracellular free zinc in living neurons. Neurobiol Dis *4*, 275-279.

Carrasco, M.A., Castro, P., Sepulveda, F.J., Tapia, J.C., Gatica, K., Davis, M.I., and Aguayo, L.G. (2007). Regulation of glycinergic and GABAergic synaptogenesis by brain-derived neurotrophic factor in developing spinal neurons. Neurosci. *145*, 484.

Cassell, M.D., and Brown, M.W. (1984). The distribution of Timm's stain in the nonsulphide-perfused human hippocampal formation. The Journal of Comparative Neurology *222*, 461-471.

Ceccarelli, B., Hurlbut, W.P., and Mauro, A. (1972). Depletion of vesicles from frog neuromuscular junctionsby prolonged tetanic stimulation. J. Cell Biol. *54*, 30-38.

Ceccarelli, B., Hurlbut, W.P., and Mauro, A. (1973). Turnover of transmitter and synaptic vesicles at the frog neuromuscular junction. J. Cell Biol. *57*, 499-524.

Chao, Y., and Fu, D. (2004). Kinetic Study of the Antiport Mechanism of an Escherichia coli Zinc Transporter, ZitB. Journal of Biological Chemistry *279*, 12043-12050.

Charton, G., Rovira, C., Ben-Ari, Y., and Leviel, V. (1985). Spontaneous and evoked release of endogenous Zn2+ in the hippocampal mossy fiber zone of the rat in situ. Exp Brain Res *58*, 202-205.

Cherny, R.A., Atwood, C.S., Xilinas, M.E., Gray, D.N., Jones, W.D., McLean, C.A., Barnham, K.J., Volitakis, I., Fraser, F.W., Kim, Y.-S.*, et al.* (2001). Treatment with a Copper-Zinc Chelator Markedly and Rapidly Inhibits [beta]-Amyloid Accumulation in Alzheimer's Disease Transgenic Mice. Neuron *30*, 665-676.

Chimienti, F., Devergnas, S.v., Favier, A., and Seve, M. (2004). Identification and Cloning of a Œ≤-Cell‚ÄìSpecific Zinc Transporter, ZnT-8, Localized Into Insulin Secretory Granules. Diabetes *53*, 2330-2337.

Clapp, A.R., Medintz, I.L., and Mattoussi, H. (2006). Forster resonance energy transfer investigations using quantum-dot fluorophores. ChemPhysChem *7*, 47-57.

Cochilla, A.J., Angelson, J.K., and Betz, W.J. (1999). Monitoring secretory membrane with FM1-43 fluorescence. Annu. Rev. Neurosci. *22*, 1-10.

Cohen, L.B., Salzberg, B.M., and Grinvald, A. (1978). Optical methods for monitoring neuronal activity. Annu. Rev. Neurosci. *1*, 171-182.

Cole, T.B., Martyanova, A., and Palmiter, R.D. (2001). Removing zinc from synaptic vesicles does not impair spatial learning, memory, or sensorymotor functions in the mouse. Brain Res *891*, 253-265.

Cole, T.B., Robbins, C.A., Wenzel, H.J., Schwartzkroin, P.A., and Plamiter, R.D. (2000). Seizures and neuronal damage in mice lacking vesicular zinc. Epilepsy Res *39*, 153-169.

Cole, T.B., Wenzel, H.J., Kafer, K.E., Schwartzkroin, P.A., and Palmiter, R.D. (1999). Elimination of zinc from synaptic vesicles in the intact mouse brain by disruption for the ZnT3 gene. Proc Natl Acad Sci USA *96*, 1717-1721.

Collins, J., Bai, L., and Ghishan, F. (2004). The SLC20 family of proteins: dual functions as sodium-phosphate cotransporters and viral receptors. Pflügers Archiv European Journal of Physiology *447*, 647-652.

Colvin, R.A., Fontaine, C.P., Laskowski, M., and Thomas, D. (2003). Zn2+ transporters and Zn2+ homeostasis in neurons. European Journal of Pharmacology *479*, 171-185.

Conrad, E.M., and Ahearn, G.A. (2007). Transepithelial transport of zinc and L-histidine across perfused intestine of American lobster, Homarus americanus. J. Comp. Physiol. *177*, 297-307.

Costello, L.C., and Franklin, R.B. (1998). Novel role of zinc in the regulation of prostate citrate metabolism and its implications in prostate cancer. Prostate *35*, 285-296.

Cousins, R.J., Liuzzi, J.P., and Lichten, L.A. (2006). Mammalian zinc transport, traficking and signals. J Biol Chem *281*, 24085-24089.

Cragg, R.A., Christie, G.R., Phillips, S.n.R., Russi, R.M., K√ºry, S.b., Mathers, J.C., Taylor, P.M., and Ford, D. (2002). A Novel Zinc-regulated Human Zinc Transporter, hZTL1, Is Localized to the Enterocyte Apical Membrane. Journal of Biological Chemistry *277*, 22789-22797.

Danscher, G., Shipley, M.T., and Andersen, P. (1975). Persistent function of mossy fiber synapses after metal chelation with DEDTC. Brain Res. *85*, 522-526.

Danscher, G., and Stoltenberg, M. (2005). Zinc-specific autometallographic in vivo selenium methods: tracing of zinc-enriched (ZEN) terminals, ZEN pathways, and pools of zinc ions in a multitude of other ZEN cells. J Histochem Cytochem *53*, 141-153.

Daumas, S., Halley, H., and Lassalle, J.-M. (2004). Disruption of hippocampal CA3 network: effects on episodic-like memory processing in C57BL/6J mice. Euro. J. Neurosci. *20*, 597-600.

Davson, H., Zlokovic, B., Rakic, L., and Segal, M.B. (1993). An introduction to the blood-brain barrier (Boca Raton, Fl: CRC Press, Inc).

Dineley, K.E., Malaiyandi, L.M., and Reynolds, I.J. (2002). A reevaluation of neuronal zinc measurements: artifacts associated with high intracellular zinc concentrations. Mol. Pharmacol. *62*, 618-627.

Dittmer, P.J., Miranda, J.G., Gorski, J.A., and Palmer, A.E. (2009). Genetically Encoded Sensors to Elucidate Spatial Distribution of Cellular Zinc. Journal of Biological Chemistry *284*, 16289-16297.

Dorozhkin, S.V., and Epple, M. (2002). Biological and Medical Significance of Calcium Phosphates. Angewandte Chemie International Edition *41*, 3130-3146.

Dufner-Beattie, J., Langmade, S.J., Wang, F., Eide, D., and Andrews, G.K. (2003a). Structure, Function, and Regulation of a Subfamily of Mouse Zinc Transporter Genes. Journal of Biological Chemistry *278*, 50142-50150.

Dufner-Beattie, J., Wang, F., Kuo, Y.-M., Gitschier, J., Eide, D., and Andrews, G.K. (2003b). The Acrodermatitis Enteropathica Gene ZIP4 Encodes a Tissue-specific, Zinc-regulated Zinc Transporter in Mice. Journal of Biological Chemistry *278*, 33474-33481.

Duncan, M.W., Marini, A.M., Watters, R., Kopin, I.J., and Markey, S.P. (1992). Zinc, a neurotoxin to cultured neurons, contaminates cycad fluor prepared by traditional Guamanian methods. J Neurosci *12*, 1523-1537.

Dutka, T.L., Cole, L., and Lamb, G.D. (2005). Calcium phosphate precipitation in the sarcoplasmic reticulum reduces action potential-mediated Ca2+ release in mammalian skeletal muscle. Am J Physiol Cell Physiol *289*, C1502-1512.
Dyck, R., Beaulieu, C., and Cynader, M. (1993). Histochemical localization of synaptic zinc in the developing cat visual cortex. J. Comp. Neurosci. *329*, 53-67.

Dyck, R.H. (2009). Zinc and cortical plasticity. Brain Research Review *59*, 347-373.

Eide, D.J. (2004). The SLC39 family of metal ion transporters. Eur. J. Physiol. *447*, 796-800.

Eide, D.J. (2006). Zinc transporters and the cellular trafficking of zinc. Biochimica et Biophysica Acta *1763*, 711-722.

Erecinska, M., and Silver, I.A. (1989). ATP and brain function. J Cereb. Blood Flow Metab. *9*, 2-19.

Erikkson, P.S., Perfilieva, E., Bjork-Erikkson, T., Alborn, A.-M., Nordborg, C., Peterson, D.A., and Gage, F.H. (1998). Neurogenesis in the adult human hippocampus. Nat. Med. *4*, 1313-1317.

Fallon, J., Reid, S., Kinyamu, R., Opale, I., Opale, R., Baratta, J., Korc, M., Endo, T.L., Duong, A., Nguyen, G.*, et al.* (2000). *In vivo* induction of massive proliferation directed migration and differentiation of neural cells in adult mammalian brain. Proc. Natl. Acad. Sci. U.S.A. *97*, 14686-14691.

Fesce, R., Grohovaz, F., Valtorta, F., and Meldolesi, J. (1994). Neurotransmitter release: fusion or [`]kiss-and-run'? Trends in Cell Biology *4*, 1-4.

Fierke, C.A., and Thompson, R.B. (2001). Fluorescence-based biosensing of zinc using carbonic anhydrase. BioMetals *14*, 205-222.

Finney, L.A., and O'Halloran, T.V. (2003). Transition metal speciation in the cell: insights from the chemistry of metal ion receptors. Science *300*, 931-936.

Forbes, I.J., Zalewski, P.D., Hurst, N.P., Giannakis, C., and Whitehouse, M.W. (1989). Zinc increases phorbol ester receptors in intact B-cells, neutrophil polymorphs and platelets. FEBS Lett. *247*, 445-447.

Fox, M.A., Sanes, J.R., Borza, D.-B., Eswarakumar, V.P., Fassler, R., Hudson, B.G., John, S.W.M., Ninomiya, Y., Pedchenko, V., Pfaff, S.L.*, et al.* (2007). Distinct target-derived signals organize formation, maturation and maintenance of motor nerve terminals. Cell *129*, 179.

Frederickson, C.J. (1989). Neurobiology of zinc and zinc-containing neurons. Int Rev Neurobiol *31*, 145-238.

Frederickson, C.J., Danscher, G., J. Storm-Mathisen, J.Z., and Ottersen, O.P. (1990). Chapter 6 Zinc-containing neurons in hippocampus and related CNS structures. In Progress in Brain Research (Elsevier), pp. 71-84.

Frederickson, C.J., Klitenick, M.A., Manton, W.I., and Kirkpatrick, J.B. (1983). Cytoarchitechtonic distribution of zinc in the hippocampus of man and rat. Brain Res *273*, 335-339.

Frederickson, C.J., Koh, J.Y., and Bush, A.I. (2005). The neurobiology of zinc in health and disease. Nat Rev *6*.

Frederickson, C.J., and Moncrieff, D.W. (1994). Zinc-containing neurons. Biol Signals *3*, 127-139.

Frederickson, C.J., Suh, S.W., Silva, D., Frederickson, C.J., and Thompson, R.B. (2000). Importance of Zinc in the Central Nervous System: The Zinc-Containing Neuron. J. Nutr. *130*, 1471S-1483.

Furman, S., Lichtstein, D., and Ilani, A. (1997). Sodium-dependent transport of phosphate in neuronal and related cells. Biochimica et Biophysica Acta (BBA) - Biomembranes *1325*, 34-40.

Gaither, L.A., and Eide, D.J. (2000). Functional Expression of the Human hZIP2 Zinc Transporter. Journal of Biological Chemistry *275*, 5560-5564.

Gaither, L.A., and Eide, D.J. (2001a). Eukaryotic zinc transporters and their regulation. BioMetals *14*, 251-270.

Gaither, L.A., and Eide, D.J. (2001b). The Human ZIP1 Transporter Mediates Zinc Uptake in Human K562 Erythroleukemia Cells. Journal of Biological Chemistry *276*, 22258-22264.

Gee, K.R., Zhou, Z.-L., Qian, W.-J., and Kennedy, R. (2002a). Detection and Imaging of Zinc Secretion from Pancreatic Œ≤-Cells Using a New Fluorescent Zinc Indicator. Journal of the American Chemical Society *124*, 776-778.

Gee, K.R., Zhou, Z.L., Ton-That, D., Sensi, S.L., and Weiss, J.H. (2002b). Measuring zinc in living cells.: A new generation of sensitive and selective fluorescent probes. Cell Calcium *31*, 245-251.

Giachelli, C.M., Jono, S., Shioi, A., Nishizawa, Y., Mori, K., and Morii, H. (2001). Vascular calcification and inorganic phosphate. Am. J. Kidney Dis. *38*, S34-S37.

Gilboe, D.D. (1998). NMR-based identification of intra- and extracellular compartments of the brain Pi peak. J. Neurochem. *71*, 2542-2548.

Glinn, M., Ni, B., and Paul, S.M. (1997). Inorganic phosphate enhances phosphonucleotide concentrations in cultured fetal rat cortical neurons. Brain Research *757*, 85-92.

Glover, C.N., and Hogstrand, C. (2002). Amino acid modulation of in vivo intestinal zinc absorption in freshwater rainbow trout. J Exp Biol *205*, 151-158.

Godfraind, J.M., Krnjevic, K., Maretic, H., and Pumain, R. (1973). Inhibition of cortical neurones by imidazole and some derivatives. Canadian Journal of Physiology and Pharmacology *51*, 790-797.

Green, L.M., and Berg, J.M. (1990). Retroviral nucleocapsid protein-metal ion interactions: folding and sequence variants. Proc. Natl. Acad. Sci. U.S.A. *87*, 6403-6407.

Greene, L.A., Aletta, J.M., Rukenstein, A., and Green, S.H. (1987). PC12 pheochromocytoma cells: culture, nerve growth factor treatment, and experimental exploitation. Methods in Enzymology *147*, 207-217.

Greene, L.A., and Tischler, A.S. (1976). Establishment of a noradrenergic clonal line of rat adrenal pheochromocytoma cells, which respond to nerve growth factor. Proc Natl Acad Sci USA *73*, 2424-2428.

Grynkiewicz, G., Poenie, M., and Tsien, R.Y. (1985). A new generation of Ca^{2+} indicators with greatly improved fluorescence properties. Journal of Biological Chemistry *260*, 3440-3450.

Guffanti, A.A., Wei, Y., Rood, S.V., and Krulwich, T.A. (2002). An antiport mechanism for a member of the cation diffusion facilitator family: divalent cations efflux in exchange for $K^+$and H^+. Molecular Microbiology *45*, 145-153.

Halstead, J.A., Ronaghy, H.A., and Abadi, P. (1972). Zinc deficiency in man-the Shiraz experiment. Am J Med *53*.

Hamill, O.P., Marty, A., Neher, E., Sakmann, B., and Sigworth, F.J. (1981). Improved patch-clamp techniques for high-resolution current recording from cells and cell-free membrane patches. Pflügers Archiv European Journal of Physiology *391*, 85-100.

Harrison, N.L., and Gibbons, S.J. (1994). Zn2+: An endogenous modulator of ligand- and voltage-gated ion channels. Neuropharmacology *33*, 935-952.

Haug, F.-M.S. (1967). Electron microscopical localization of the zinc in hippocampal mossy fibre synapses by a modified sulfide silver procedure. Histochemie *8*, 355-368.

He, L., and Wu, L.-G. (2007). The debate on the kiss-and-run fusion at synapses. Trends in Neurosciences *30*, 447-455.

Henkel, A.W., Lubke, J., and Betz, W.J. (1996a). FM1-43 dye ultrastructural localization in and release from frog motor nerve terminals. Proc. Natl. Acad. Sci. U.S.A. *93*, 1918-1923.

Henkel, A.W., Lubke, J., and Betz, W.J. (1996b). FM1-43 dye ultrastructural localization in and release from frog motor nerve terminals. PNAS *93*, 1918-1923.

Heuser, J.E., and Reese, T.S. (1973). Evidence for recycling of synaptic vesicle membrane during transmitter release at the frog neuromuscular junction. J. Cell Biol. *57*, 315-344.

Hirano, T., Kikuchi, K., Urano, Y., Higuchi, T., and Nagano, T. (2000). Highly Zinc-Selective Fluorescent Sensor Molecules Suitable for Biological Applications. Journal of the American Chemical Society *122*, 12399-12400.

Hosein, R.E., Williams, S.A., and Gavin, R.H. (2005). Directed motility of phagosomes in Tetrahymena thermophila requires actin and Myo1p, a novel unconventional myosin. Cell Motil. Cytoskeleton *61*, 49-60.

Hosie, A., Dunne, E., Harvey, R., and Smart, T. (2003a). Zinc-mediated inhibition of GABA(A) receptors: discrete binding sites underlie subtype specificity. Nat Neurosci *6*, 362-369.

Hosie, A.M., Dunne, E.L., Harvey, R.J., and Smart, T.G. (2003b). Zinc mediated inhibition of GABA(A) receptors: discrete binding sites underlie subtype specificity. Nat Neurosci *6*, 362-369.

Howell, G.A., Welch, M.G., and Frederickson, C.J. (1984). Stimulation-induced uptake and release of zinc in hippocampal slices. Nature *308*, 736-738.

Huang, L., and Gitschier, J. (1997). A novel gene involved in zinc transport is deficient in the lethal milk mouse. Nat Genet *17*, 292 - 297.

Huang, L., Kirschke, C., and Gitschier, J. (2002). Functional characterization of a novel mammalian zinc transporter, ZnT6. J Biol Chem *277*, 26389 - 26385.

Huang, L., Kirschke, C.P., Zhang, Y., and Yu, Y.Y. (2005). The ZIP7 Gene (Slc39a7) Encodes a Zinc Transporter Involved in Zinc Homeostasis of the Golgi Apparatus. Journal of Biological Chemistry *280*, 15456-15463.

Ichinohe, N., and Rockland, K.S. (2005). Distribution of synaptic zinc in the macaque monkey amygdala. J. Comp. Neurol. *489*, 135-147.

Kambe, T., Narita, H., Yamaguchi-Iwai, Y., Hirose, J., Amano, T., Sugiura, N., Sasaki, R., Mori, K., Iwanaga, T., and Nagao, M. (2002). Cloning and characterization of a novel mammalian zinc transporter, ZnT-5, abundantly expressed in pancreatic beta cells. J Biol Chem *271*, 19094 - 19055.

Kantheti, P., Qiao, X., Diaz, M.E., Peden, A.A., Meyer, G.E., Carskadon, S.L., Kapfhamer, D., Sufalko, D., Robinson, M.S., and Noebels, J.L. (1998). Mutation in AP-3 delta in the mocha mouse links endosomal transport to storage deficiency in platelets, melanosomes and synaptic vesicles. Neuron *21*, 111-122.

Kasai, H., Hatakeyama, H., Kishimoto, T., Liu, T.-T., Nemoto, T., and Takahashi, N. (2005). A new quantitative (two photon extracellular polar-tracer imaging-based quantification (TEPIQ)) analysis for diameters of exocytic vesicles and its application to mouse pancreatic islets. J. Physiol. *568*, 891-903.

Kay, A. (2004). Detecting and minimizing zinc contamination in physiological solutions. BMC Physiology *4*, 4.

Kay, A.R. (2003). Evidence for Chelatable Zinc in the Extracellular Space of the Hippocampus, But Little Evidence for Synaptic Release of Zn. J. Neurosci. *23*, 6847-6855.

Kay, A.R. (2006). Imaging synaptic zinc: promises and perils. Trends in Neurosciences *29*, 200-206.

Kay, A.R., Alfonso, A., Alford, S., Cline, H.T., Holgado, A.M., Sakmann, B., Snitsarev, V.A., Stricker, T.P., Takahashi, M., and Wu, L.-G. (1999). Imaging Synaptic Activity in Intact Brain and Slices with FM1-43 in C. elegans, Lamprey, and Rat. Neuron *24*, 809-817.

Kay, A.R., Neyton, J., and Paoletti, P. (2006). A Startling Role for Synaptic Zinc. Neuron *52*, 572-574.

Kay, A.R., and Toth, K. (2006). Influence of Location of a Fluorescent Zinc Probe in Brain Slices on Its Response to Synaptic Activation. J Neurophysiol *95*, 1949-1956.

Kay, A.R., and Toth, K. (2008). Is Zinc a Neuromodulator? Sci. Signal. *1*, re3-.

King, J.C., and Cousins, R.J. (2006). Zinc. In: Modern Nutrition in Health and DIsease (Philadelphia: Lippincott Williams & Wilkins).

Kirschke, C., and Huang, L. (2003a). ZnT7, a novel mammalian zinc transporter, accumulates zinc in the Golgi apparatus. J Biol Chem *278*, 4096-4102.

Kirschke, C.P., and Huang, L. (2003b). ZnT7, a novel mammalian zinc transporter, accumulates zinc in the Golgi apparatus. J. Biol. Chem. *278*, 4096-4102.

Kishimoto, T., Liu, T.-T., Hatakeyama, H., Nemoto, T., Takahashi, N., and Kasai, H. (2005). Sequential compund exocytosis of large dense-core vesicles in PC12 cells studied with TEPIQ (two photon extracellular polar-tracer imaging-based quantification) analysis. J. Physiol. *568*, 905-915.

Kleineke, J.W., and Brand, I.A. (1997). Rapid changes in intracellular Zn2+ in rat hepatocytes. J. Pharmacol. Toxicol. Methods *38*, 181-187.

Korichneva, I., Hoyos, B., Chua, R., Levi, E., and Hammerling, U. (2002). Zinc release from protein kinase C as the common event during activation by lipid second messenger or reactive oxygen. J Biol Chem *277*, 44327-44331.

Kramer, U., Cotter-Howells, J.D., Charnock, J.M., Baker, A.J.M., and Smith, J.A.C. (1996). Free histidine as a metal chelator in plants that accumulate nickel. Nature *379*, 635-638.

Krebs, H.A., and Henseleit, K. (1932). Untersuchungen über die Harnsoffbildung im Tierkörper. Hoppe-Seyler's Zeitschrift fur physiologische Chemie *210*, 33-46.

Krezel, A., and Maret, W. (2007). The nanomolar and picomolar zinc binding properties of metallothionein. J. Am. Chem. Soc. *129*, 10911-10921.

Krężel, A., and Maret, W. (2006). Zinc-buffering capacity of a eukaryotic cell at physiological pZn. Journal of Biological Inorganic Chemistry *11*, 1049-1062.

Lambert, N.A., Levitin, M., and Harrison, N.L. (1992). Induction of giant depolarizing potentials by zinc in area CA1 of the rat hippocampus does not result from the block of GABAB receptors. Neurosci Lett *135*, 215-218.

Lander, E.S., Linton, L.M., Birren, B., Nusbaum, C., Zody, M.C., Baldwin, J., Devon, K., Dewar, K., Doyle, M., FitzHugh, W.*, et al.* (2001). Initial sequencing and analysis of the human genome. Nature *409*, 860-921.

Lassalle, J.-M., Bataille, T., and Halley, H. (2000). Reversible inactivation of the hippocampal mossy fiber synapses in mice impairs spatial learning, but neither consolidation nor memory retrieval, in the Morris navigation task. Neurobiol. Learn. Mem. *73*, 243-257.

Lee, J.-Y., Cole, T.B., Palmiter, R.D., and Koh, J.-Y. (2000). Accumulation of zinc in degenerating hippocampal neurons on ZnT3-null mice after seizures: evidence against synaptic vesicle origin. J. Neurosci. *20:RC79*, 1-5.

Lee, J.-Y., Cole, T.B., Palmiter, R.D., Suh, S.W., and Koh, J.-Y. (2002). Contribution by synaptic zinc to the gender-disparate plaque formation in human Swedish mutant APP transgenic mice. Proc. Natl. Acad. Sci. U.S.A. *99*, 7705-7710.

Li, C.-L., and McIlwain, H. (1957). Maintenance of resting membrane potentials in slices of mammalian cerebral cortex and other tissues in vitro. The Journal of Physiology *139*, 178-190.

Li, Y., Hough, C., Frederickson, C., and Sarvey, J. (2001a). Induction of mossy fiber --> Ca3 long-term potentiation requires translocation of synaptically released Zn2+. J Neurosci *21*, 8015 - 8025.

Li, Y., Hough, C., Suh, S., Sarvey, J., and Frederickson, C. (2001b). Rapid translocation of Zn(2+) from presynaptic terminals into postsynaptic hippocampal neurons after physiological stimulation. J Neurophysiol *86*, 2597 - 2604.

Liu, T.-T., Kishimoto, T., Hatakeyama, H., Nemoto, T., Takahashi, N., and Kasai, H. (2005). Exocytosis and endocytosis of small vesicles in PC12 cells studied withTEPIQ (two-photon extracellular polar-tracer imaging-based quantification) analysis. J. Physiol., 3.

Liuzzi, J., Blanchard, R., and Cousins, R. (2001). Differential regulation of zinc transporter 1, 2, and 4 mRNA expression by dietary zinc in rats. J Nutr *131*, 46 - 52.

Liuzzi, J.P., Lichten, L.A., Rivera, S., Blanchard, R.K., Aydemir, T.B., Knutson, M.D., Ganz, T., and Cousins, R.J. (2005). Interleukin-6 regulates the zinc transporter Zip14 in liver and contributes to the hypozincemia of the acute-phase response. Proc. Nat. Acad. Sci. U.S.A. *102*, 6843-6848.

Lopantsev, V., Wenzel, H.J., Cole, T.B., Palmiter, R.D., and Schwartzkroin, P.A. (2003). Lack of vesicular zinc in mossy fibers does not affect synaptic excitability of CA3 pyramidal cells in zinc transporter 3 knockout mice. Neuroscience *116*, 237-248.

Lu, P., Jones, L.L., Snyder, E.Y., and Tuszynski, M.H. (2003). Neural stem cells constitutively secrete neurotrophic factors and promote extensive host axonal growth after spinal cord injury. Exp Neurol *181*, 115-129.

Lu, Y.-M., Taverna, F.A., Tu, R., Ackerley, C.A., Wang, Y.-T., and Roder, J. (2000). Endogenous Zn2+ is required for the induction of long-term potentiation at rat hippocampal mossy fiber-CA3 synapses. Synapse *38*, 187-197.

MacDiarmid, C.W., Gaither, L.A., and Eide, D. (2000). Zinc transporters that regulate vacuolar zinc storage in Saccharomyces cerevisiae. EMBO J *19*, 2845-2855.

MacDonald, R.S. (2000). The role of zinc in growth and cell proliferation. J Nutr *130*, 1500S-1508S.

Magavi, S.S., Leavitt, B.R., and Macklis, J.D. (2000). Induction of neurogenesis in the neocortex of adult mice. Nature *405*, 951-955.

Mahy, N., Prats, A., Riveros, A., Andres, N., and F., B. (1999). Basal ganglia calcification induced by excitotoxicity: an experimental model characterised by electron microscopy and X-ray microanalysis. Acta Neuropathologica *98*, 217-225.

Maret, W. (2003). Cellular zinc and redox states converge in the metallothionein/thionein pair. J Nutr *133*, 1460S-1462S.

Maret, W. (2009). Molecular aspects of human cellular zinc homeostasis: redox control of zinc potentials and zinc signals. BioMetals *22*, 149-157.

Margoshes, M., and Vallee, B.L. (1957). A cadmium protein from equine kidney cortex. J. Am. Chem. Soc. *79*, 4813-4814.

Martel, J., and Young, J.D.-E. (2008). Purported nanobacteria in human blood as calcium carbonate nanoparticles. Proceedings of the National Academy of Sciences *105*, 5549-5554.

Martell, A.E., and Hancock, R.D. (1996). Metal complexes in aqueous solution: Modern inorganic chemistry (New York, NY: Plenum Press).

Maske, H. (1955). Über den topochemischen Nachweis von Zink im Ammonshorn verschiedener Säugestiere. Naturwissenschaften *42*, 424.

Massry, S.G., Hajjar, S.M., Koureta, P., Fadda, G.Z., and Smogorzewski, M. (1991). Phosphate depletion increases cytosolic calcium of brain synaptosomes. Am J Physiol Renal Physiol *260*, F12-18.

Mazzarello, P. (1999). The Hidden Structure: A Scientific Biography of Camillo Golgi (Oxford University Press).

Michael, S.F., Kilfoil, V.J., Schmidt, M.H., Amann, B.T., and Berg, J.M. (1992). Metal binding and folding properties of a minimalist Cys2His2 zinc finger peptide. Proc. Natl. Acad. Sci. U.S.A. *89*, 4796-4800.

Miles, R. (1990). Synaptic excitation of inhibitory cells by single CA3 hippocampal pyramidal cells of the guinea-pig in vitro. The Journal of Physiology *428*, 61-77.

Ming, G.L., and Song, H.L. (2005). Adult neurogenesis in the mammalian central nervous system. Annu. Rev. Neurosci. *28*, 223-250.

Molnar, P., and Nadler, J.V. (2001a). Lack of Effect of Mossy Fiber-Released Zinc on Granule Cell GABAA Receptors in the Pilocarpine Model of Epilepsy. J Neurophysiol *85*, 1932-1940.
Molnar, P., and Nadler, J.V. (2001b). Synaptically-released zinc inhibits N-methyl-d-aspartate receptor activation at recurrent mossy fiber synapses. Brain Res. *910*, 205-207.

Morgenthaler, F.D., Knott, G.W., Floyd Sarria, J.C., Wang, X., Staple, J.K., Catsicas, S., and Hirling, H. (2003). Morphological and molecular heterogeneity in release sites of single neurons. European Journal of Neuroscience *17*, 1365-1374.

Mulroney, S.E., Woda, C.B., Halaihel, N., Louie, B., McDonnell, K., Schulkin, J., Haramati, A., and Levi, M. (2004). Central control of renal sodium-phosphate (NaPi-2) transporters. Am J Physiol Renal Physiol *286*, F647-652.

Murer, H., Forster, I., and Biber, J. (2004). The sodium phosphate cotransporter family SLC34. Pflügers Archiv European Journal of Physiology *447*, 763-767.

Murgia, C., Vespignani, I., Cerase, J., Nobili, F., and Perozzi, G. (1999). Cloning, expression, and vesicular localization of zinc transporter Dri 27/ZnT4 in intestinal tissue and cells. Am J. Physiol *277*, G1231-G1239.

Nakashima, A.S., and Dyck, R.H. (2009). Zinc and cortical plasticity. Brain Research Reviews *59*, 347-373.

Nishida, T., Arii, T., Takaoka, A., Yoshimura, R., and Endo, Y. (2007). Three-dimensional, computer-tomographic analysis of membrane proteins (TrKA, caveolin, clathrin) in PC12 cells. Acta Histochem. Cytochem. *40*, 93-99.

Nitzan, Y., Sekler, I., Frederickson, C., Coulter, D., Balaji, R., Liang, S.-L., Margulis, A., Hershfinkel, M., and Silverman, W. (2003). Clioquinol effects on tissue chelatable zinc in mice. Journal of Molecular Medicine *81*, 637-644.

O'Donnell, M., Chance, R.K., and Bashaw, G.J. (2009). Axon Growth and Guidance: Receptor Regulation and Signal Transduction. Annual Review of Neuroscience *32*, 383-412.

O'Keefe, J., and Nadel, L. (1978). The hippocampus as a cognitive map (Oxford University Press).

Oteiza, P.I., and Mackenzie, G.G. (2005). Zinc, oxidant-triggered cell signaling and human health. Mol Aspects Med *26*, 245-255.

Outten, C.E., and O'Halloran, T.V. (2001). Femtomolar Sensitivity of Metalloregulatory Proteins Controlling Zinc Homeostasis. Science *292*, 2488-2492.

Palmer, T.D., Markakis, E.A., Willhoite, A.R., Safar, F., and Gage, F.H. (1999). Fibroblast growth factor-2 activates latent neurogenic program in neural stem cells from diverse regions of the adult CNS. J. Neurosci *19*, 8487-8497.

Palmiter, R., and Findley, S. (1995a). Cloning and functional characterization of a mammalian zinc transporter that confers resistance to zinc. Embo J *14*, 639 - 649.

Palmiter, R., and Huang, L. (2004). Efflux and compartmentalization of zinc by members of the SLC30 family of solute carriers. Pflügers Archiv European Journal of Physiology *447*, 744-751.

Palmiter, R.D. (1998). Perspective: the elusive function of metallothioneins. Proc Natl Acad Sci USA *95*, 8428-8430.

Palmiter, R.D., Cole, T.B., Quaife, C.J., and Findley, S.D. (1996). ZnT-3, a putative transporter of zinc into synaptic vesicles. Proc Natl Acad Sci USA *93*, 14934-14939.

Palmiter, R.D., and Findley, S.D. (1995b). Cloning and functional characterization of a mammalian zinc transporter that confers resistance to zinc. EMBO J. *14*, 639-649.

Paoletti, P., Vergnano, A.M., Barbour, B., and Casado, M. (2009a). Zinc at glutamatergic synapses. Neurosci. *158*, 126-136.

Paoletti, P., Vergnano, A.M., Barbour, B., and Casado, M. (2009b). Zinc at glutamatergic synapses. Neuroscience *158*, 126-136.

Perez-Clausell, J. (1996). Distribution of terminal fields stained for zinc in the neocortex of the rat. J. Chem. Neuroanat. *11*, 99-111.

Peters, S., Koh, J., and Choi, D.W. (1987). Zinc selectively blocks the action of N-methyl-D-aspartate on cortical neurons. Science *236*, 589-592.

Pozzan, T., Rizzuto, R., Volpe, P., and Meldolesi, J. (1994). Molecular and cellular physiology of intracellular calcium stores. Physiol. Rev. *74*, 595-636.

Prange, O., and Murphy, T.H. (1999). Analysis of multiquantal transmitter release from single cultured cortical neuron terminals. J. Neurophysiol. *81*, 1810-1817.

Prasad, A.S. (1991). Discovery of human zinc deficiency and studies in an experimental human model. Am J Clin Nutr *53*, 403-412.

Prasad, A.S., Schulert, A.R., Miale Jr., A., Farid, Z., and Sandstead, H.H. (1963). Zinc and iron deficiencies in male subjects with dwarfism and hypogonadism but without ancylostomiasis, schistosomiasis or severe anemia. Am J Clin Nutr *12*, 437-444.

Qian Cai, and Sheng, Z.-H. (2009). Molecular Motors and Synaptic Assembly. Neuroscientist *15*, 78-89.

Qian, J., and Noebels, J.L. (2005). Visualization of transmitter release with zinc fluorescence detection at the mouse hippocampal mossy fibre synapse. J. Physiol. *566*, 747-758.

Qian, X., Davis, A.A., Goderie, S.K., and Temple, S. (1997). FGF2 concentration regulates the generation of neurons and glia from multipotent cortical stem cells. Neuron *18*, 81-93.

Rettig, J., and Neher, E. (2002). Emerging Roles of Presynaptic Proteins in Ca++-Triggered Exocytosis. Science *298*, 781-785.

Reyes, J.G. (1995). Zinc transport in mammalian cells. Am. J. Physiol. *270*, C401-C410.

Ringer, S.A. (1883). A further contribution regarding the influence of the different constituents of blood on the contraction of the heart. J. Physiol. *4*, 29-42.

Ripa, S., and R., R. (1995). Zinc and the elderly. Minerva Med. *86*, 37-43.

Rizzoli, S.O., and Betz, W.J. (2005). Synaptic vesicle pool. Nat. Rev. Neurosci. *6*, 57-69.

Rogers, E.E., Eide, D.J., and Guerinot, M.L. (2000). Altered selectivity in an Arabidopsis metal transporter. Proceedings of the National Academy of Sciences of the United States of America *97*, 12356-12360.

Romero-Isart, N., and Vasak, M. (2002). Advances in the structure and chemistry of metallothioneins. J. Inorg. Biochem. *88*, 388-396.

Ruiz, A., Walker, M.C., Fabian-Fine, R., and Kullmann, D.M. (2004). Endogenous zinc inhibits GABAa receptors in a hippocampal pathway. J. Neurophysiol. *91*, 1091-1096.

Rumschik, S.M., Nydegger, I., Zhao, J., and Kay, A.R. (2009). The interplay between inorganic phosphate and amino acids determines zinc solubility in brain slices. Journal of Neurochemistry *108*, 1300-1308.

Sagi-Eisenberg, R. (2007). The mast cell: where endocytosis and regulated exocytosis meet. Immunol. Rev. *217*, 292-303.

Sah, P., Hestrin, S., and Nicoll, R.A. (1989). Tonic activation of NMDA receptors by ambient glutamate enhances excitability of neurons. Science *246*, 815-818.

Sandstead, H.H. (1984). Neurobiology of zinc. In: Neurobiology of zinc. (New York: Alan R. Liss).

Sankaranarayanan, S., De Angelis, S., Rothman, J.E., and Ryan, T.A. (2000). The use of pHluorins for optical measurements of presynaptic activity. Biophys J *79*, 2199-2208.

Santiago, M.F., Liour, S.S., Mendez-Otero, R., and Yu, R.K. (2005). Glial-guided neuronal migration in P19 embryonal carcinoma stem cell aggregates. J. Neurosci. Res. *81*, 9-20.

Sawamoto, K., Wichterle, H., Gonzalez-Perez, O., Cholfin, J.A., Yamada, M., Spassky, N., Murica, N.S., Garcia-Verdugo, J.M., Marin, O., Rubenstein, J.L.R.*, et al.* (2006). New neurons follow the flow of cerebrospinal fluid in the adult brain. Science *311*, 629-632.

Sensi, S.L., Canzoniero, L.M., Yu, S.P., Ying, H.S., Koh, J.Y., Kerchner, G.A., and Choi, D.W. (1997). Measurement of intracellular free zinc in living cortical neurons: routes of entry. J. Neurosci. *17*, 9554-9564.

Seve, M., Chimienti, F., Devergnas, S., and Favier, A. (2004). In silico identification and expression of SLC30 family genes: An expressed sequence tag data mining strategy for the characterization of zinc transporters' tissue expression. BMC Genomics *5*, 32.

Sim, D.L.C., and Chow, V.T.K. (1999). The Novel Human HUEL (C4orf1) Gene Maps to Chromosome 4p12-p13 and Encodes a Nuclear Protein Containing the Nuclear Receptor Interaction Motif. Genomics *59*, 224-233.

Simons, T.J. (1991). Intracellular free zinc and zinc buffering in human red blood cells. J. Membr. Biol. *123*, 63-71.

Simonyan, K., Tovar-Moll, F., Ostuni, J., Hallett, M., Kalasinsky, V.F., Lewin-Smith, M.R., Rushing, E.J., Vortmeyer, A.O., and Ludlow, C.L. (2008). Focal white matter changes in spasmodic dysphonia: a combined diffusion tensor imaging and neuropathological study. Brain *131*, 447-459.

Sivarama Sastry, K., Viswanathan, L., Ramaiah, A., and Sarma, P.S. (1960). Studies on the binding of 65Zn by equine erythrocytes in vitro. Biochem. J. *10*, 432-442.

Skoog, D.A., West, D.M., Holler, F.J., and Crouch, S.R. (2000). Analytical chemistry: An introduction, 7th edition edn (Thompson Learning Inc.).

Slomianka, L. (1992). Neurons of origin of zinc-containing pathways and the distribution of zinc-containing boutons in the hippocampal region of the rat. Neuroscience *48*, 325-352.

Smart, T.G., and Constanti, A. (1990). Differential effect of zinc on the vertebrate GABAA-receptor complex. Br J Pharmacol *99*, 643-654.

Smart, T.G., Hosie, A.M., and Miller, P.S. (2004). Zn2+ Ions: Modulators of Excitatory and Inhibitory Synaptic Activity. Neuroscientist *10*, 432-442.

Smart, T.G., Xie, X., and Krishek, B.J. (1994). Modulation of inhibitory and excitatory amino acid receptor ion channels by zinc. Prog Neurobiol *42*, 393-441.

Smith, C.V., Jones, D.P., Guenthner, T.M., Lash, L.H., and Lauterburg, B.H. (1996). Compartmentation of Glutathione: Implications for the Study of Toxicity and Disease. Toxicology and Applied Pharmacology *140*, 1-12.

Staple, J.K., Osen-Sand, A., Benfenati, F., Pich, E.M., and Catsicas, S. (1997). Molecular and Functional Diversity at Synapses of Individual Neurons In Vitro. European Journal of Neuroscience *9*, 721-731.

Suhy, D.A., Simon, K.D., Linzer, D.I., and O'Halloran, T.V. (1999). Metallothionein is part of a zinc-scavenging mechanism for cell survival under conditions of extreme zinc deprivation. J. Biol. Chem. *274*, 9183-9192.

Sun, Y.E., Martinowich, K., and Ge, W. (2003). Making and repairing the mammalian brain-signaling toward neurogenesis and gliogenesis. Semin. Cell. Dev. Biol. *14*, 161-168.

Suzuki, T., Ishihara, K., Migaki, H., Ishihara, K., Nagao, M., Yamaguchi-Iwai, Y., and Kambe, T. (2005). Two Different Zinc Transport Complexes of Cation Diffusion Facilitator Proteins Localized in the Secretory Pathway Operate to Activate Alkaline Phosphatases in Vertebrate Cells. Journal of Biological Chemistry *280*, 30956-30962.

Takamori, S., Rhee, J.S., Rosenmund, C., and Jahn, R. (2000). Identification of a vesicular glutamate transporter that defines a glutamatergic phenotype in neurons. Nature *407*, 189-194.

Takeda, A. (2000). Movement of zinc and its functional significance in the brain. Brain Res Rev *34*, 137-148.

Tarohda, T., Yamamoto, M., and Amamo, R. (2004). Regional distribution of manganese, iron, copper, and zinc in the rat brain during development. Analytical and Bioanalytical Chemistry *380*, 240-246.

Taylor, K.M. (2000). LIV-1 Breast Cancer Protein Belongs to New Family of Histidine-Rich Membrane Proteins with Potential to Control Intracellular Zn2+ Homeostasis. IUBMB Life *49*, 249-253.

Taylor, K.M., Morgan, H.E., Johnson, A., and Nicholson, R.I. (2005). Structure-function analysis of a novel member of the LIV-1 subfamily of zinc transporters, ZIP14. FEBS Letters *579*, 427-432.

Taylor, K.M., and Nicholson, R.I. (2003). The LZT proteins; the LIV-1 subfamily of zinc transporters. Biochimica et Biophysica Acta (BBA) - Biomembranes *1611*, 16-30.

Thomas, D., Tovey, S.C., Collins, T.J., Bootman, M.D., Berridge, M.J., and Lipp, P. (2000). A comparison of fluorescent Ca2+indicator properties and their use in measuring elementary and global Ca2+signals. Cell Calcium *28*, 213-223.

Thompson, R.B., Peterson, D., Mahoney, W., Cramer, M., Maliwal, B.P., Suh, S.W., Frederickson, C., Fierke, C., and Herman, P. (2002). Fluorescent zinc indicators for neuorbiology. J Neurosci Methods *118*, 63-75.

Thornton, H.B., Nel, D., Thornton, D., van Honk, J., Baker, G.A., and Stein, D.J. (2008). The Neuropsychiatry and Neuropsychology Of Lipoid Proteinosis. J Neuropsychiatry Clin Neurosci *20*, 86-92.

Timm, F. (1958). Zur Histochemie des Ammonshorngebietes. Cell and Tissue Research *48*, 548-555.

Tsujikawa, K., Imai, K., and Katutani, M. (1991). Localization of metallothionein in nuclei of growing primary cultured adult rat hepatocytes. FEBS Lett *283*, 239-242.

Tupler, R., Perini, G., and Green, M.R. (2001). Expressing the human genome. Nature *409*, 832-833.

Ueno, S., Tsukamoto, M., Hirano, T., Kikuchi, K., Yamada, M.K., Nishiyama, N., Nagano, T., Matsuki, N., and Ikegaya, Y. (2002). Mossy fiber Zn2+ spillover modulates heterosynaptic N-methyl-D-aspartate receptor activity in hippocampal CA3 circuits. J. Cell. Biol. *158*, 215-220.

Vallee, B.L., and Falchuk, K.H. (1993). The biochemical basis of zinc physiology. Physiol Rev *73*, 79-118.

Van Zile, M.L., J., C.N., Scott, R.A., and Giedroc, D.P. (2000). The zinc metalloregulatory protein Synechococcus PCC7942 SmtB binds a single zinc ion per monomer with high affinity in a tetrahedral coordination geometry. Biochemistry *39*, 11818-11829.

Varea, E., Ponsoda, X., Molowny, A., Danscher, G., and Lopez-Garcia, C. (2001). Imaging synaptic zinc release in living nervous tissue. J. Neurosci. Methods *110*, 57-63.

Venter, J.C., Adams, M.D., Myers, E.W., Li, P.W., Mural, R.J., Sutton, G.G., Smith, H.O., Yandell, M., Evans, C.A., Holt, R.A.*, et al.* (2001). The sequence of the human genome. Science *291*, 1304-1351.

Vinkenborg, J.L., Nicolson, T.J., Bellomo, E.A., Koay, M.S., Rutter, G.A., and Merkx, M. (2009). Genetically encoded FRET sensors to monitor intracellular Zn2+ homeostasis. Nature Methods *6*, 737-740.

Vogt, K., Mellor, J., Tong, G., and Nicoll, R. (2000). The actions of synaptically released zinc at hippocampal mossy fiber synapses. Neuron *26*, 187-196.

Wang, F., Kim, B.-E., Petris, M.J., and Eide, D.J. (2004). The Mammalian Zip5 Protein Is a Zinc Transporter That Localizes to the Basolateral Surface of Polarized Cells. Journal of Biological Chemistry *279*, 51433-51441.

Wang, Z., Danscher, G., Kim, Y.K., Dahlstrom, A., and Mook Jo, S. (2002). Inhibitory zinc-enriched terminals in the mouse cerebellum: double-immunohistochemistry for zinc transporter 3 and glutamate decarboxylase. Neurosci Lett *321*, 37-40.

Wang, Z., Li, J.Y., Dahlstrom, A., and Danscher, G. (2001). Zinc-enriched GABAergic terminals in mouse spinal cord. Brain Res *921*, 165-172.

Wapnir, R.A., Khani, D.E., Bayne, M.A., and Lifshitz, F. (1983). Absorption of Zinc by the Rat Ileum: Effects of Histidine and Other Low-Molecular-Weight Ligands. J. Nutr. *113*, 1346-1354.

Wenzel, H., Cole, T., Born, D., Schwartzkroin, P., and Palmiter, R. (1997a). Ultrastructural localization of zinc transporter-3 (ZnT-3) to synaptic vesicle membranes within mossy fiber boutons in the hippocampus of mouse and monkey. Proc Natl Acad Sci U S A *94*, 12676 - 12681.

Wenzel, H.J., Cole, T.B., Born, D.E., Schwartzkroin, P.A., and Palmiter, R.D. (1997b). Ultrastructural localization of zinc transporter-3 (ZnT-3) to synaptic vesicle membranes within mossy fiber boutons in the hippocampus of mouse and monkey. Proc Natl Acad Sci USA *94*, 12676-12681.

Westbrook, G.L., and Mayer, M.L. (1987). Micromolar concentrations of Zn2+ antagonize NMDA and GABA responses of hippocampal neurons. Nature *328*, 640-643.

Westerink, R.H.S., de Groot, A., and Vijverberg, H.P.M. (2000). Heterogeneity of catecholamine-containing vesicles in PC12 cells. Biochem. Biophys. Res. Comm. *270*, 625.

Wishart, D.S., Lewis, M.J., Morrissey, J.A., Flegel, M.D., Jeroncic, K., Xiong, Y., Cheng, D., Eisner, R., Gautam, B., Tzur, D.*, et al.* (2008). The human cerebrospinal fluid metabolome. Journal of Chromatography B *871*, 164-173.

Xie, X., and Smart, T.G. (1991). A physiological role for endogenous zinc in rat hippocampal synaptic neurotransmission. Nature *349*.

Ye, B., Maret, W., and Vallee, B.L. (2001). Zinc metallothionein imported into liver mitochondria modulates respiration. Proc. Natl. Acad. Sci. *98*, 2317-2322.

Ye, J.H., Zhang, J., Xiao, C., and Kong, J.-Q. (2006). Patch-clamp studies in the CNS illustrate a simple new method for obtaining viable neurons in rat brain slices: Glycerol replacement of NaCl protects CNS neurons. Journal of Neuroscience Methods *158*, 251-259.

Zerby, S.E., and Ewing, A.G. (1996). Electrochemical monitoring of individual exocytotic events from the varicosities of differentiated PC12 cells. Brain. Res. *712*, 1.

Zhang, X., Chen, Y., Wang, C., and Huang, L.Y.M. (2007). Neuronal somatic ATP release triggers neuron-satellite glial cell communication in dorsal root ganglia. Prc. Natl. Acad. Sci. U.S.A. *104*, 9864-9869.

Zhao, J., Bertoglio, B.A., Devinney Jr, M.J., Dineley, K.E., and Kay, A.R. (2009). The interaction of biological and noxious transition metals with the zinc probes FluoZin-3 and Newport Green. Analytical Biochemistry *384*, 34-41.

Zhao, J., Bertoglio, B.A., Gee, K.R., and Kay, A.R. (2008). The zinc indicator FluoZin-3 is not perturbed significantly by physiological levels of calcium or magnesium. Cell Calcium *44*, 422-426.

Zimmerberg, J., Curran, M., Cohen, F.S., and Brodwick, M. (1987). Simultaneous electrical and optical measurements show that membrane fusion precedes secretory granule swelling during exocytosis of beige mouse mast cells. Proc Nat Acad Sci U S A *84*, 1585-1589.